universität wien

DIPLOMARBEIT

Titel der Diplomarbeit

„ Investigating the role of Staufen2 in the regulation of localized RNA “

Verfasserin

Daniela Lenek

angestrebter akademischer Grad

Magistra der Naturwissenschaften (Mag.rer.nat.)

Wien, 2011

Studienkennzahl lt. Studienblatt:	A 441
Studienrichtung lt. Studienblatt:	Diplomstudium Genetik-Mikrobiologie
Betreuerin / Betreuer:	o.Univ.-Prof. Dr. Michael Kiebler

Table of Contents

Abstract

Many cellular processes require specific RNAs to be transported to distinct compartments where they may be translated or stored until activation. These RNAs are packaged into RNPs (ribonucleoproteins), which then travel into dendrites near synapses. Defects in this process have been associated with severe neurological disorders including X-linked mental retardation. One well-known example of a localized RNA in neurons is the *β-actin* transcript, which localizes to the leading edge of growth cones and neurites resulting in morphological rearrangements of the cytoskeleton, which occur during neuronal development and synaptic plasticity. Two *trans*-acting factors have been implicated in this process: (i) ZBP1 (zipcode-binding protein 1) that binds to a 54-nt localization element in the *β-actin* 3´-UTR (the so-called "zipcode") and that represses its translation during transport; and (ii) the double-stranded RNA-binding protein Staufen2 (Stau2), which was suggested to be necessary for the localization of *β-actin* to dendrites and for the formation of dendritic spines in mature neurons. In contrast to ZBP1, however, a defined molecular action of Stau2 on its target has yet to be described.

The aim of my thesis was to characterize the role of Stau2 in the regulation of β-actin in developing neurons. To achieve this, β-actin levels were quantified after Stau2 knockdown in developing primary hippocampal neurons. Whilst mRNA levels were slightly reduced, β-actin protein levels were unchanged. To examine more directly whether Stau2 controls β-actin translation, as described for ZBP1, luciferase assays were performed. Knockdown of Stau2 had no effect in this assay, whereas overexpression of either Stau2 or ZBP1 increased the activity of luciferase when fused to the β-actin zipcode and part of the coding region. As this assay does not discriminate between enhanced translation and stability, RNA decay assays were carried out. The amounts of residual *β-actin* mRNA at different time points after inhibition of RNA synthesis were quantified using quantitative real-time PCR. The decay of *β-actin* mRNA was accelerated in neurons upon Stau2 knockdown. In contrast, overexpression of Stau2 only had a minor stabilizing effect.

Taken together, my findings indicate that the RNA-binding protein Stau2 increases the stability of *β-actin* transcripts in developing neurons without affecting its translation. As

overall levels of β-actin were not changed, it is conceivable that Stau2 transiently promotes stabilization during transport, in a similar manner as ZBP1 acts on *β-actin* during localization of the transcript to inhibit premature translation. Whether *β-actin* mRNA binds Stau2 directly, possibly dependent on a sequence within the coding region, and whether it interacts with ZBP1 in the same RNPs could be an interesting topic for future investigations.
To fully understand the functions of Stau2-RNPs, it will be necessary to clarify the identity of RNA targets and protein interactions of Stau2 and to describe the actions of Stau2 during transport or at the synapse and growth cone in detail.

I Introduction

1.1 Different mechanisms of regulation of localized mRNAs

With every new experience and thought, connections are formed between the nerve cells that are the substance of our mind. An estimated 10^{14} to 10^{15} synapses are believed to exist in the human brain, a number which is difficult to visualize, even exceeding the entirety of stars in our galaxy (Kandel, 2000). The plasticity of these connections is the foundation of all higher brain functions, such as learning and memory. It is widely accepted that synaptic remodeling is dependent on protein synthesis, which has shown to be vital for long-term memory formation (Barzilai et al. 1989, Kelleher et al. 2004; Brightwell et al., 2007; Klann and Sweatt, 2008) Before polyribsosomes were discovered at the base of spines in the early 80´s, proteins were thought to be produced uniquely in the cell body compartment and then had to be transported to distant sites in the neuron (Martin and Zukin, 2006). Since then, studies have investigated the role of local protein synthesis "on site" in morphological rearrangements, a model which has several advantages. First, the localization of transcripts provides a way to spatially restrict gene expression within the cytoplasm, so that changes in protein synthesis could occur independently at individual activated synapses of a neuron. Secondly, if local stimuli can regulate translation directly, higher temporal resolution can be obtained. This "short-cut" circumvents the lengthy process of delivering the signal to the nucleus to initiate transcription, export of mRNA and cytoplasmic translation followed by targeting of the protein to the site of stimulation. On top of that localized transcripts can be translated multiple times, which is much more economic than the transport of many copies of a protein, especially as the processes of a neuron can extend very far from their cell bodies (Martin and Ephrussi, 2009). These also include axons, as local synthesis does not only occur in dendritic regions. During neuronal development, the axonal growth cone has to react to attractive and aversive cues to find their distant target regions. *β-actin* mRNA in Xenopus growth cones was shown to rapidly localize in response to an attractive stimulus gradient (Leung et al., 2006).

Classes of mRNAs localized in neurons include for example cytoskeletal proteins (e.g. MAP2, Arc), kinases (CaMKIIα, PKCζ), and Calcium-binding proteins (dendrin) or neurotransmitter

receptors. A variety of post-transcriptional mechanisms can regulate these mRNAs either during transport or local protein synthesis, which range from stabilizing or destabilizing factors altering the half-lives of the transcripts to mechanisms for repression or activation of translation. A few of these regulatory mechanisms which have been described in neurons shall be presented here.

1.1.1 Trans-acting factors influencing RNA stability in mammalian neurons

Posttranscriptional mechanisms act on message RNAs at various stages, including splicing, mRNA editing, transport, stability and translation. The stability of an mRNA determines the time it will be available for translation before it gets degraded by ribonucleases. While mRNAs for house-keeping genes usually have long half-lives, some mRNAs decay quickly to ensure low steady-state levels and concise temporal expression. Modest increases in the half-lives of transcripts can result in considerable augmentation of expression levels. Such changes of stability can be conferred by *trans*-acting factors, i.e. RNA-binding proteins (RBPs), which bind to recognition motifs of the mRNA sequence. These motifs, or *cis*-acting elements, are often situated in the 3'-UTR of transcripts. A well-studied example of such a 3'-UTR sequence is the ARE (adenylate-uridylate rich element), which is found in multiple gene families, such as immediate early genes, oncogenes and cytokines (Chen and Shyu, 1995). AREs are able to stabilize transcripts by binding of Hu proteins (homologue of *Drosophila* ELAV; Keene, 1999), while binding of other factors triggers their degradation. Binding of either AUF1 or KSRP (K homology splicing regulatory protein), which is expressed in neurons, induces the exosome mediated degradation pathway by recruiting the exosome to targeted transcripts (Chen et al., 2001). Another decay pathway involves exonucleases in cytoplasmic processing bodies (P-bodies), foci of local degradation which are also present in neurons and dendrites. P-bodies are dynamic multiprotein complexes including RBPs, decapping enzymes and the 5'-3' exonuclease Xrn1p, but no ribosomes (Anderson and Kedersha, 2006). Degradation in P-bodies can also be mediated by microRNAs (Eulalio et al., 2007).

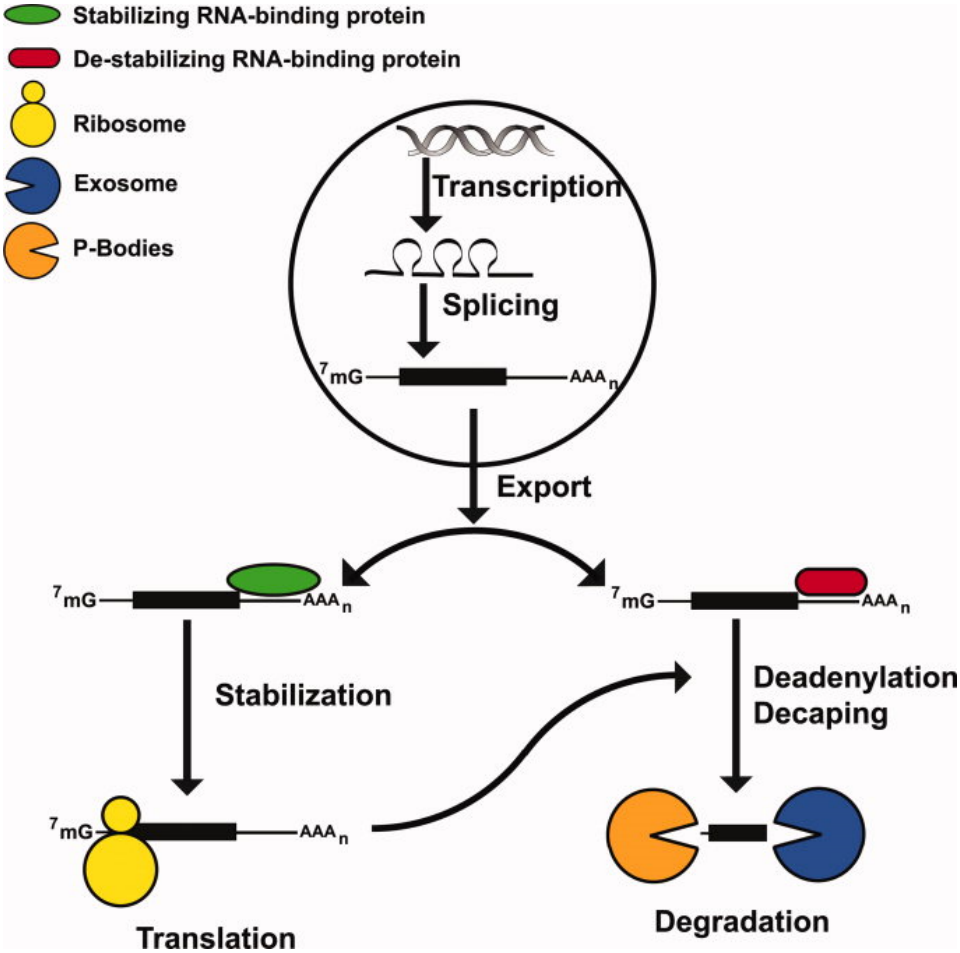

Fig 1.1. Simplified model of mRNA stabilization and decay. After being exported into the cytoplasm, mRNAs can be either stabilized and translated on polyribosomes or destabilized and degraded, depending on the *trans*-acting factors they bind. mRNA decay is initiated by deadenylation and decapping, followed by 3'- 5' degradation of the exosome or 5'- 3' decay of exonucleases in P-bodies (taken from Bolognani and Ferrone-Bizzozero, 2008).

Regulation via mRNA stability is important for several classes of neuronally expressed genes including neurotransmitter receptors, signaling molecules and proteins implicated in neuronal development, such as GAP-43. The stability of *GAP-43* mRNA is controlled by HuD protein which binds the ARE in its 3'-UTR. Altering HuD levels in neurons was shown to cause both changed *GAP-43* mRNA levels as well as significant changes in neurite outgrowth (Anderson et al., 2000). The relevance of mRNA-stabilizing and -destabilizing proteins in neurons was demonstrated in different studies, showing for example that Hu protein levels are increased after learning and memory tasks (Quattrone et al., 2001), or that *trans*-acting factors like AUF1 are themselves regulated by neuronal activity, simulated by addition of NMDA to granule cell cultures (Jurado et al., 2006).

1.1.1.1 The EJC factor eIF4AIII and translation-dependant decay

eIF4AIII is a DEAD-box protein and a core component of the exon junction complex (EJC). It is loaded onto mRNAs by pre-mRNA splicing and is associated with dendritic mRNAs and neuronal RNA granules. The EJC- eIFAIII, Y14, MAGOH, and Barentsz being its core constituents- is deposited upstream of exon-exon junctions in the nucleus and serves as a binding platform for other factors. The loaded mRNAs travel to the cytoplasm, where EJCs in ORFs can positively influence ribosome recruitment, while those downstream of an ORF can trigger nonsense-mediated decay (NMD) (Giorgi et al., 2007)**.** This evolutionarily conserved mRNA surveillance mechanism targets mRNAs harboring premature termination codons (PTCs) for degradation to prevent accumulation of truncated proteins with potentially harmful gain-of-function or loss-of-function. But NMD does not only downregulate aberrant RNAs, it also modulates expression of natural NMD targets (e.g. mRNAs with introns in the 3'-UTR), initiated by interaction of the NMD factor Upf1 and ribosomes stalled at the termination codon after the pioneer round of translation (Chang et al., 2007). One of the targets of eIF4AIII is *Arc* mRNA, which is produced after synaptic activation and delivered to dendrites and possesses 2 introns in its 3'-UTR. *Arc* mRNA and protein levels increase after BDNF stimulation or eIF4AIII knockdown in neurons, which also leads to an increase of synaptic strength (Giorgi et al., 2007).

Substrates of this translation-dependant decay remain stable as long as they are translationally silent and can thus accumulate at distal dendritic sites, until an external signal relieves this repression. After the first round of translation, NMD quickly stops protein synthesis which guarantees a highly timed response, making this mechanism key regulator for a precise control of protein expression in neurons. The Upf (up-frameshift) proteins are trans-acting factors at the core of the NMD machinery and are recruited to mRNAs by the EJC. Eukaryotic suppressors with morphogenetic defects in genitalia (SMG) proteins mediate the phosphorylation status of Upf1, an RNA helicase, and recruit it to P-bodies, where degradation occurs.

1.1.1.2 Staufen1

Other factors can also elicit translation-dependent decay through Upf1 interaction, for example Stau1 (Staufen1). Stau1 can initiate degradation of targets after binding to sites more than 25 nucleotides downstream of a termination codon and recruitment of Upf1. A well-known target of Staufen-mediated decay is *Arf1* mRNA (ADP ribosylation factor 1), which binds Stau1 with a 19bp stem-loop in its 3'UTR (Kim et al., 2007). SMD-targets which contain Alu elements in their 3´UTR were suggested to form double-stranded binding sites for Stau1 by base-pairing with cytoplasmic, long non-coding RNA (lncRNA), also carrying an Alu element (Gong and Maquat, 2011). In contrast to NMD, SMD does not require targets to have undergone splicing, and while NMD also has a broader function in the general quality control of transcripts, Staufen-mediated decay is thought to conditionally regulate the expression of specific genes.

1.1.1.3 FMRP

Many RBPs that control stability also play a role in the regulation of translation, possibly to couple these two processes. One of them is the Fragile X mental retardation protein (FMRP), a protein which is transported into dendrites and found in association with polyribosomes. The name-giving disease, the fragile X syndrome, is caused by aberrant expansion of the CGG-triplet in the 5'-UTR of the FMR1 gene, which leads to a loss of FMRP expression. In the absence of FMRP, dysregulated local protein synthesis leads to a disturbance of synaptic plasticity. FMRP regulates local translation of specific mRNAs at the synapse in response to activation of metabotropic glutamate receptors (Bassell and Warren, 2008). Its targets include *CaMKIIα, MAP1b, Arc* and *Rac1* mRNA.

When FMRP interacts with the cytoplasmic FMRP interacting protein 1 (CYFIP1), which in turn binds the cap-binding factor eIF4E, translational activity is repressed. Upon synaptic stimulation, this complex dissociates and protein synthesis can be initiated (Napoli et al., 2008). Yet neuronal activity is also able to entail stabilizing effects of FMRP. FMRP was shown to protect *PSD-95* mRNA, a scaffolding protein of the postsynaptic density, from degradation in the hippocampus (De Rubeis and Bagni, 2009). Its stabilizing activity could be regulated by various aspects, such as subcellular context or interacting proteins.

1.1.2 Translation control in neurons

Synaptic activity stimulates the transport of mRNAs into dendrites and local mRNA translation. If mRNAs were simultaneously translated during transport, newly made proteins would not specifically tag activated synapses, but would be distributed all over the dendrite. Thus the synthesis of the encoded protein must be repressed until the mRNA arrives at its site of action. The major target of translation control is the initiation step, which is the rate-limiting step in the process.

The translation of specific mRNAs is regulated by trans-acting factors binding their 5'- or 3'-UTR. Translational regulators can be controlled by kinases or phosphatases, which are activated by Ca^{2+} influx. The PI3K/Akt/mTOR and the MAPK/Erk signaling pathways were shown to be involved in stimulating local translation at the synapse, thereby regulating synthesis-dependant LTP (Panja et al., 2009). Especially developing synapses lacking scaffold proteins, such as PSDs that trap and anchor other proteins, need local synthesis to rapidly control the concentration of specific proteins (Zha et al., 2009).

The translational regulation of localized mRNA does, however, not only play a role in dendrites and synapse function. The extreme distances between soma and axonal growth cones combined with the relatively slow rate of protein transport make local protein synthesis indispensable for axon outgrowth and development. Yet mature axons seem to be devoid of the translational machinery. In developing axons several mRNAs were found, for example *β-actin, β-tubulin, cofilin, ADF*, amongst others. While it is not yet clear that translational inhibition would inhibit axon elongation, a rapid growth cone response to external cues in the environment seems to depend on fast local translation, for example the rapid synthesis of RhoA. This is a critical upstream regulator of the cytoskeleton, which is necessary for the collapsing effect in response to the guidance cue Sema3A. Local translation could also amplify signal transduction pathways by strongly increasing rate-limiting proteins. Asymmetric β-actin translation at precise sites within growth cones appears to define the directionality of netrin1-induced, Ca^{2+}-dependant growth cone turning. Microtubule-dependant transport of β-actin may be insufficient in this case, as the edges of growth cones are actin-rich but hardly contain microtubules. Studies of fibroblast migration suggested a similar mechanism (Hengst and Jaffrey, 2007).

1.1.2.1 ZBP1

A well studied example of a regulator of local translation in neurons is ZBP1 (zipcode-binding protein 1), sometimes also termed IMP1 or IGFIIBP1 (IGF-II mRNA binding protein 1). ZBP1 belongs to the highly conserved VICKZ family of RNA-binding proteins that recognize cis-acting elements in various RNAs (Yisraeli, 2005). It was discovered by affinity purification with the "zipcode" sequence of *β-actin* mRNA and subsequently cloned (Ross et al., 1997). This so-called zipcode is a 54-nt element in the 3'-UTR of the *β-actin* mRNA that is sufficient for correct localization of the transcript.

ZBP1 is an mRNA-binding protein containing 4 KH- and 1 RRM-RNA binding domains, as well as a nuclear export and import sequence (Oleynikov and Singer, 2003). During nuclear priming, the protein associates with its target RNA cotranscriptionally. Initially the nascent transcripts in the nucleus are bound by ZBP2, which facilitates the subsequent binding of the shuttling ZBP1 (Pan et al., 2007). ZBP1-granules show rapid anterograde and retrograde dendritic transport along microtubules and dynamic movements into dendritic spines. By binding *cis*-acting sequences, ZBP1 may act as an adapter between mRNAs and the transport machinery. In the case of *β-actin* mRNA, transcripts can be exported into the cytoplasm independently of ZBP1, which is, however, crucial for their localization to dendrites. This trafficking is activity-dependent and can be stimulated by KCl depolarization (Tiruchinapalli et al., 2003).

Throughout the transport, ZBP1 prevents translation initiation in the cytoplasm, possibly by inhibiting the formation of the 80S ribosomal complex on its target mRNA. When the transcript has reached its destination, translation repression is relieved by the non-receptor tyrosine kinase Src, the activity of which is restricted to the cell periphery. ZBP1 contains an SH3-binding motif, which is a docking site for this enzyme. Src phosphorylates ZBP1 at Tyrosine 369, required for RNA binding, thereby releasing the trans-acting factor from the complex (**Fig. 1.2**; Hüttelmaier et al., 2005). Reduced dendritic levels of ZBP1 impair neurite outgrowth and result in a failed response to BDNF treatment, which otherwise increases the density of dendritic filopodia and synapses (Eom et al., 2003).

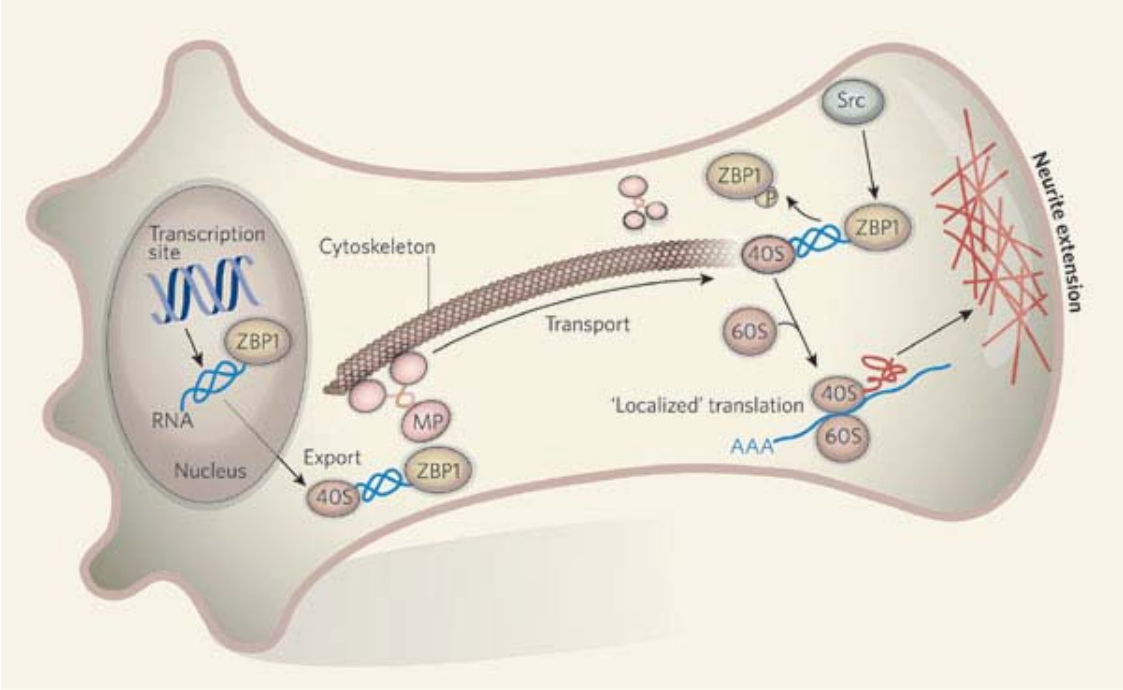

Fig 1.2 Localization and silencing of *β-actin* mRNA in neurons. Hüttelmaier et al. suggest that ZBP1 protein binds *β-actin* mRNA in the nucleus and is exported into the cytoplasm, where it is delivered into neurites in a complex associated with ribosomal subunits and motor proteins. The latter transport the ZBP1 granules along microtubules to their destination in the periphery, where the ZBP1-mediated repression of its target is relieved. Src kinase phosphorylates ZBP1, which gets released from *β-actin* mRNA and allows ribosomal subunits to assemble and initiate local protein synthesis (taken from Dahm and Kiebler, 2005).

Yet suppressing translation of target mRNAs is not the only known regulatory function of ZBP1, it also plays a role in mRNA stabilization in some cases. Under stress conditions, mRNAs are retained in stress granules to prevent premature decay in P-bodies. While targeting of mRNAs to stress granules happens in a nonspecific manner, specific protein–mRNA interactions are involved in stabilizing mRNAs. During the ISR (integrated stress response), ZBP1-knockdown leads to a selective destabilization of target transcripts, and ZBP-1 overexpression increases mRNA stability (Stöhr et al., 2006). RNA-binding proteins like ZBP1 are essential for translational adaptation during cellular stress by modulating mRNA turnover.

A different type of mRNA stabilization mediated by ZBP1 requires interaction with a CRD (coding region determinant), a sequence in the open reading frame of specific mRNAs, such

as *c-myc*. ZBP1 promotes CRD-mediated stabilization of *c-myc* mRNA, associated with several other proteins in an RNA–dependent fashion. This complex formation at the CRD seemingly suppresses the transfer of the mRNA to the polysomal fraction, thereby preventing translation-coupled decay (Weidensdorfer et al., 2009).

1.1.2.2 CPEB and Staufen1

Another protein that facilitates translationally silenced mRNA transport to dendrites is cytoplasmic polyA binding protein (CPEB) (Richter, 2007; Bestman and Cline, 2008). Polyadenylation is controlled by binding of CPEB to a cytoplasmic polyadenylation element (CPE), a *cis* element in the 3'-UTRs of specific mRNAs. CPE has been shown to be sufficient to direct a reporter RNA into dendrites of hippocampal rat neurons in a microtubule-dependent fashion. In neurons derived from CPEB knockout mice, the dendritic transport of a CPE-containing reporter RNA is reduced (Huang et al., 2003). A well-studied example is the CPE-containing *CaMKIIα* mRNA, which is polyadenylated and translated upon synaptic stimulation.

CPEB-containing particles also contain the molecular motors dynein and kinesin as well as Maskin, a CPEB-associated factor that mediates cap-dependent translational repression of CPE-containing mRNA. Maskin interacts with both CPEB and the cap-binding factor eIF4E, and thus suppresses eIF4E–eIF4G interaction, which is necessary to position the 40s ribosomal subunit on the mRNA to initiate translation. It dissociates upon polyadenylation, thereby stimulating translation (Cao and Richter, 2002). Polyadenylation is initiated when Aurora phosphorylates CPEB. Phosphorylation induces CPEB to interact and possibly stabilize CPSF (cleavage and polyadenylation specificity factor), which is believed to be necessary for the recruitment of poly(A) polymerase (Mendez et al., 2000).

The RBP Stau1 has been mentioned above as factor that elicits degradation when bound downstream of a natural termination codon by recruiting Upf1 to specific 3'-UTRs. Additionally, Stau1 is able to enhance translation of a subpopulation of transcripts containing structured 5'-UTRs. Fusing a structured HIV1-TAR element to the 5'-end of a luciferase reporter mRNA resulted in upregulation of reporter activity in mammalian cells that were co-transfected with Stau1, while unstructured 5'-ends did not have this effect. The interaction between transcripts and ribosomes mediated by Stau1 is thought to

facilitate translation intiation (Dugré-Brisson, 2005). Downregulation of Stau1 by siRNA led to a decrease of dendritic mRNAs. Mutant mice expressing a truncated Stau1 protein lacking a crucial RNA-binding domain displayed deficits in the dendritic transport of Stau1-containing RNPs. While behavioural deficits in these mice were limited to locomotor activity, the development of synapses was notably impaired (Vessey et al., 2008).

1.1.2.3 Other mechanisms for translational silencing

Another possibility of post-transcriptional regulation of gene expression is the regulation by small non-coding RNAs, which can act either by cleavage of target transcripts or by reducing translational efficiency, depending on the degree of sequence complementarity. Silencing of translation by microRNAs usually has a rather moderate effect on expression levels and functions via competition for binding of the cap structure. Fine-tuning of expression by miRNAs often relies on combinatorial actions: one miRNA can inhibit up to 10 different mRNAs, and one mRNA can be targeted by different miRNAs.

An example of a brain-specific miRNA is miR-134 which is found in synaptic compartments (Schratt et al., 2009). The level of miR-134 in neurons peaks at postnatal day 13, at a time when synaptic maturation occurs. It has a partially complementary conserved target sequence in the 3'-UTR of *LimK1* (Lim domain-containing protein kinase 1) mRNA. LimK1 regulates actin filament dynamics through inhibition of ADF (actin binding/depolymerizing factor) and cofilin, thus stabilizing the actin cytoskeleton and controlling dendritic spine size. Dendritic spines of LimK1 KO mice have an abnormal structure, a phenotype also seen upon miR-134 overexpression. miR-134 decreased the activity of a luciferase reporter containing the *LimK1* 3'-UTR, reducing the translation of this reporter fused to myr-GFP locally in dendrites (Schratt et al., 2006). The repression of LimK1 translation can be relieved by treatment with BDNF, which is known to promote dendritic spine growth.

1.2 RNA transport and localization

RNA localization is an evolutionary old mechanism employed by different organisms, for example budding yeast, where *ASH1* mRNA localizes to the daughter cells and thereby specifies different mating types between mother and daughter cell (Paquin and Chartrand, 2008). RNA localization is also important for the establishment of the body axes and patterning in *Drosophila* and Xenopus oocytes as well as for cell fate determination in the asymmetric division of neuroblasts in the *Drosophila* embryo. Moreover, the localization of mRNAs is involved in various processes in mammals, for instance the regulation of the actin cytoskeleton in migrating fibroblasts (Condeelis and Singer, 2005), the formation of myelin sheaths by oligodendrocytes or the development of neurons (Dahm et al., 2007). Several neurological diseases are associated with defective subcellular RNA localization, such as X-linked mental retardation, spinocerebellar ataxia and spinal muscular atrophy. In many cases, abnormal neuronal development is caused by mutations affecting the RNA transport machinery, such as the triplet repeat expansions in the FMR1 (fragile X mental retardation 1) gene, which cause loss of function of the RBP FMRP. Some of its target mRNAs encode proteins that are essential for dendritic spine formation (Dahm and Macchi, 2007).

There are essentially three main mechanisms by which RNA localization can be achieved: locally trapping mRNAs that are diffusing through the cytoplasm, selective stabilization of transcripts at certain cellular compartments, while they are degraded everywhere else, and active and directed transport of mRNAs (Martin and Ephrussi, 2009). The latter seems to be the predominant mechanism of localization, as it presents a method of rapid translocation of large particles over long distances. RNA transport follows a multistep pathway (**Fig. 1.3**) that starts in the nucleus. Nuclear events, such as alternative splicing or polyadenylation, can generate isoforms with different targeting specificities. The “cellular address” of an mRNA is usually defined by *cis*-acting elements (also called localization elements), consisting of nucleotides sequences or secondary structures, which are often found in the 3’-UTR and bind to specific *trans*-acting proteins. After being exported to the cytoplasm, additional proteins may assemble on the mRNA. Studies suggest that there are multiple species of RNA granules containing distinct populations of RNA and proteins. The newly formed ribonucleoprotein particles (RBPs) are then transported along microtubules with the aid of kinesin motors. Trafficking of RNA granules in dendrites is dependent on the anterograde

motor protein Kinesin heavy chain or KIF5 (Kanai, 2004). Translation of the transcripts needs to be repressed during this process. In the case of dendrites, RNPs are thought to be anchored at the base of spines, until synaptic activation induces their localization into the synaptic compartment by actin-based myosin motor proteins. Repression is subsequently relieved and ribosomes can initiate protein synthesis.

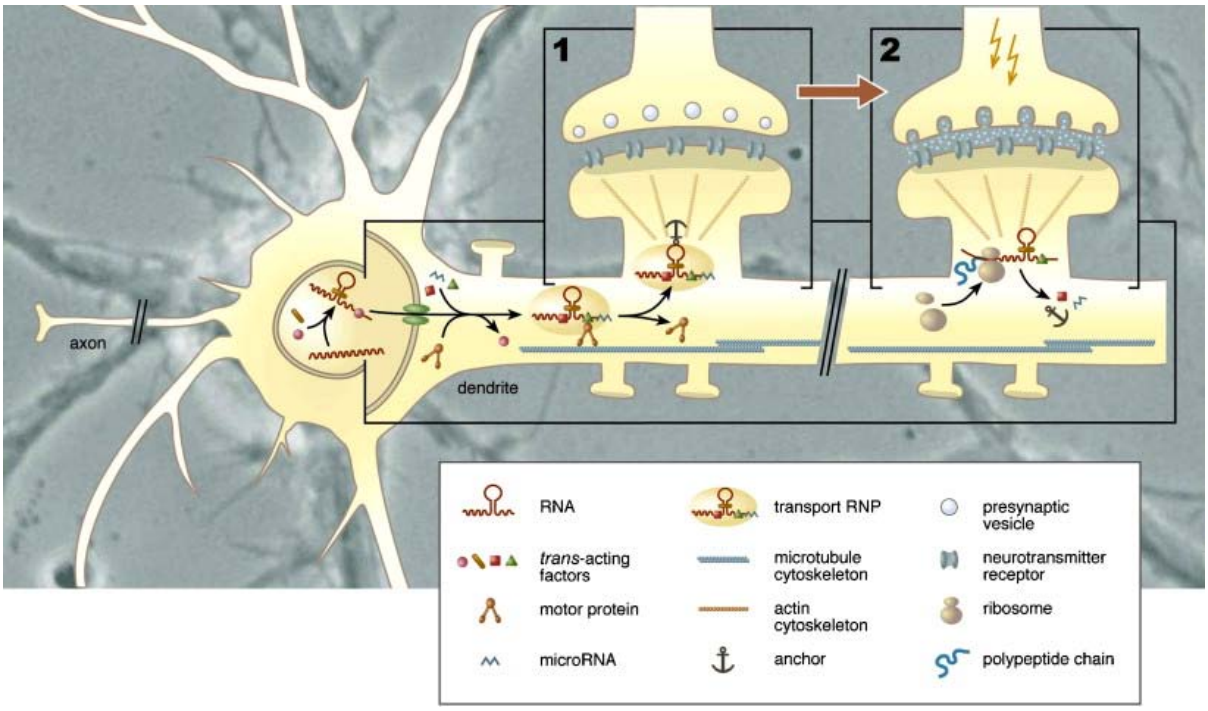

Figure 1.3 – The multistep pathway of RNA localization in neurons. RBPs associate with specific RNAs in the nucleus and are exported to the cytoplasm, where additional proteins can bind to the mRNA. RNA and *trans*-acting factors are packaged into RBPs, kinesin and dynein motor proteins then move them along microtubules. Translation of the localized transcripts remains silenced during transport. When the RNPs have reached their destination in the dendrite (1), they are thought to be anchored at specific sites, such as the base of dendritic spines. Upon synaptic activation (2), translational repression is relieved which allows the ribosome to assemble and initiate local protein synthesis (from Dahm et al. 2007).

The regulation of local protein synthesis is also thought to be dependent on actin dynamics, due to the fact that ribosomes are often found in association with F-actin (filamentous actin) in neurons and that many initiation and elongation factors are actin-binding proteins. The actin cytoskeleton on the other hand is modulated itself by local translation of various RNAs,

such *Arc, RhoA, LimK1* or *β-actin* mRNA. Thus in a model of reciprocal interaction, dendritic mRNA translation leads to actin polymerization, which enhances local protein synthesis through the activation of the translation machinery (Eom et al., 2003; Pastalkova et al., 2006).

According to the theory of the posttranscriptional operon (Keene and Tenenbaum, 2002), different RBPs regulate subsets of mRNAs in a combinatorial manner and posttranscriptional regulation is determined by a code of multiple *cis* sequences in the untranslated regions of mRNAs. Comparable to polycistronic prokaryotic operons, monocistronic mRNA could mimic coordinated regulation of expression by interacting with distinct *trans*-acting proteins, which may act on subsets of mRNAs as a group or even regulate their own mRNAs.

1.3 β-actin mRNA, an important localized transcript in neurons

β-actin mRNA is a well studied example for transcripts that are localized and postranscriptionally regulated. Actin proteins need to be produced quickly and locally to establish cellular asymmetry. They polymerize into long filaments, pushing the cell's membrane outwards, for example at the leading edge of migrating fibroblasts (Kislauskis et al., 1997) or in neuronal growth cones and dendritic filopodia (Bassell et al., 1998). The β-actin isoform is particularly enriched in such dynamic structures, where cytoskeletal rearrangements take place. An explanation for the fact that this is the preferred isoform in remodeling processes could be its higher affinity to several actin binding proteins, which promote de novo nucleation, polymerization, uncapping or severing of filaments (Bassell et al., 1998).

For the rapid sorting of these cytoskeletal components within cellular processes, the *β-actin* transcripts are transported as RNPs. As mentioned above, ZBP1 was shown to be involved in the localization of *β-actin* mRNA by binding to the 54-nt "zipcode" sequence in the *β-actin* 3'-UTR (Hüttelmaier et al., 2005). It was shown that the formation of ZBP1 - *β-actin* mRNA complexes is necessary for its localization to growth cones, where local increases of β-actin concentration stimulate forward movement. Actin-dependent growth cone mobility could be enhanced in cultured chick neurons by administration of neurotrophin NT-3 and

impaired by *β-actin* 3'-UTR antisense oligos (Zhang et al., 2001). In the growth cones of Xenopus neurons, the localization of ZBP1 - β-actin granules depends on BDNF and Ca^{2+} signalling. Ca^{2+} may act on the balance of dephosphorylation and phosphorylation of targets to direct growth cone steering, and β-actin synthesis in growth cones is regulated by the asymmetric activity of Src kinases (Yao et al., 2006).

Yet actin dynamics also play a major role in dendritic spine morphology, and actin modulates dendritic spines by tethering of PSD (postsynaptic density) - scaffold proteins to postsynaptic sites. Aberrant dendritic spine morphology has been related to disturbances in neuronal function such as dementia, thereby indicating a possible role in learning and memory (Sekino et al., 2007). ZBP1 knockdown in hippocampal cultures reduced the dendritic levels of *β-actin* mRNA and inhibited the growth of dendritic filopodia in response to BDNF treatment. Overexpression of β-actin-EGFP constructs increased the densitiy of filopodia and filopodial synapses, while the density of mature dendritic spines remained unaffected (Eom et al., 2003). Furthermore, F-actin (filamentous actin), consisting of β- and γ-actin, within the synaptic compartment is important in activity-dependent blockage of dendritic spine motility (Goetze et al., 2006).

1.4 How is Staufen2 involved in the regulation of transported RNAs?

Apart from ZBP1, another RBP was also implicated in *β-actin* mRNA localization, namely Staufen2. Like ZBP1, Stau2 (Staufen2) belongs to a family of evolutionarily conserved RBPs. Staufen was first described in *Drosophila*, where it is responsible for the localization of *oskar* mRNA to the posterior pole of oocytes and *bicoid* mRNA to the anterior pole, thus defining the body axis of the organism (Ephrussi et al., 1991). By localizing *prospero* mRNA in *Drosophila* neuroblasts, Staufen helps to obtain asymmetric divisions into neuroblasts and ganglion mother cells (Broadus et al., 1998). In *Xenopus*, Staufen was found to be involved in establishing polarity by transporting *Vg1* mRNA to the vegetal pole of the oocyte (Yoon et al., 2004). The elements required for the formation of Staufen-containing RNA granules were first analyzed using the 3'-UTR of *bicoid* mRNA. An extensive stem-loop structure of the RNA was found to be necessary, but not sufficient, to bind Staufen, suggesting that there are additional targeting mechanisms. Staufen has 5 conserved double-stranded RNA-

binding domains (dsRBDs), one of which is lost in mammalian Staufen (St Johnston et al., 1992). These dsRBD-motifs recognize stem-loops non-specifically, yet the correct positioning of secondary structures of dsRNA and their interacting RNA-binding domains could potentially add a degree of specificity.

There are two mammalian homologues of Staufen: Stau1, which is ubiquitously expressed and was mentioned above in the context of the Staufen-mediated decay pathway, and Stau2. Stau2 expression is largely restricted to the brain. It contains 4 dsRBDs, of which dsRBD3 is the major determinant for RNA binding, as well as a tubulin-binding domain, which may function as a link between the cytoskeleton and the RNA component (Wickham et al., 1999). 4 different isoforms of Stau2 are generated by alternative splicing, which range in size from 52-62kD. Only the two largest isoforms, Stau2^{62} and Stau2^{59} are imported into the nucleus and exported to the cytoplasm via exportin-5 and -1, respectively (Brownawell and Macara, 2002; Macchi et al., 2004; Kiebler et al., 2005, Miki and Yoneda, 2004). Thus, Stau2 could act as an adaptor protein for nuclear RNA export. Exportin-5 is also known as an export factor of miRNAs, suggesting a putative role of Stau2^{62} and Stau2^{59} in microRNA trafficking, yet distinct functions for the isoforms could not be distinguished so far.

Mammalian Staufen colocalizes with the rough endoplasmatic reticulum and co-sediments with polysomes (Kiebler et al., 1999; Marion et al., 1999), which could indicate a possible role for Staufen proteins in translational control (Roegiers and Jan, 2000).

Stau2-containing RNP complexes move along microtubules, using kinesin as a motor protein for their transport into dendrites, which appears to be modulated by neuronal activity (Jeong et al., 2007). They include, for example, poly(A)-mRNA, elongation factor 1α, ribosomal subunits, etc., yet the exact composition of these complexes seems to be variable (Kiebler and DesGroseillers, 2000; Kiebler and Bassell, 2006).

Stau2 has been found in proximity of dendritic spines, marked by PSD-95, and its downregulation led to significant decreases of protrusions and PSD-95-clusters, as well as to reduced postsynaptic glutamate-receptor efficiency and mEPSC amplitudes. Likewise, Stau2-downregulation affected F-actin levels in dendrites and diminished localized *β-actin* mRNA punctae in dendrites, while total actin levels remained unaltered. Stau2 was shown to be required for the formation and morphogenesis of dendritic spines in cultured hippocampal neurons (Goetze et al., 2006).

1.5 *Working hypothesis*

Definite RNA cargos of Stau2 remain to be confirmed, although Stau2 was recently suggested to be responsible for the dendritic localization of *Map1b* mRNA in hippocampal neurons (Lebeau et al., 2011). Yet the observed functional connection between Stau2 and the actin cytoskeleton proposes that Stau2 may interact with *β-actin* mRNA, influencing its stability, transport or translation. As reported by Goetze et al. (2006), downregulation of Stau2 in cultured mature hippocampal neurons (15 DIV) caused a reorganization of the actin cytoskeleton, which was shown by phalloidin stainings. *In situ* hybridization assays revealed that Stau2 knockdown also led to a reduction of *β-actin* RNA levels in both cell body and dendrites. Another consequence of Stau2 downregulation was a loss of mature dendritic spines, which start to form at 10 DIV in cultured hippocampal neurons, while the number of extended filopodia was increased.

The expression of mammalian Stau2, which is brain-specific and changes over time, is detectable at all stages throughout neuronal development. In mature hippocampal neurons it was found only in the cell body and dendritic shaft, but -according to unpublished studies in the Kiebler lab- Stau2 is present in all neurites including the growing axon of young neurons. At stage 3 (2 DIV), Stau2 is detected in the axon and localizes within the F-actin rich periphery of the growth cone. Stau2 localization to growth cones is dependent on an intact actin cytoskeleton and is reduced after treatment with cytochalasin D, which disrupts the actin cytoskeleton. Since it is established that Stau2 affects *β-actin* mRNA levels and the localization of *β-actin* containing RNPs in mature neurons, the question arose whether Stau2 would also be involved in the regulation of *β-actin* mRNA during development. Thus, the aim of my project was to further investigate the influence of Stau2 on the actin cytoskeleton in young hippocampal neurons and to unravel the molecular mechanisms underlying the regulation of its targets, focusing on *β-actin* mRNA.

The putative interaction of Stau2 and *β-actin* mRNA may include effects on transcript stability, as for example seen in the Stau1 decay pathway, or the regulation of local translation, such as the temporary repression of β-actin synthesis by ZBP1. Although both ZBP1 and Stau2 could potentially be involved in the translation control and stabilization of mRNA, it remains to be discovered whether they play distinct or redundant roles. The

approach used in this study was to explore the possible effects on β-actin after downregulation of ZBP1 or Stau2. When successful downregulation with either siRNA oligonucleotides or short hairpin plasmids had been established, *β-actin* mRNA levels were examined by quantitative real-time PCR, while corresponding protein levels were analyzed by Western blot or immunostaining. To answer the question, whether Stau2 stabilizes *β-actin* transcripts and/ or enhances their translation, RNA decay assays and luciferase assays were carried out. Luciferase reporters fused to part of the *β-actin* coding region displayed a slight increase of expression levels following Stau2 overexpression, whilst Stau2 downregulation had minor opposite effects. As this could be explained by either enhanced translation or stability, RNA levels were measured after blocking RNA synthesis. Degradation of *β-actin* mRNA turned out to be augmented in hippocampal neurons with downregulated Stau2 levels. Taken together, I think that the experiments presented in this diploma thesis shed new light on the role of Stau2 in developing neurons and the molecular mechanisms of Stau2 in the regulation of localized RNAs.

II Materials & Methods

2.1 Materials

2.1.1 Kits

Wizard® SV Gel and PCR Clean-Up System - Promega
EndoFree Plasmid Purification Kit - Qiagen
Deoxyribonuclease I - Sigma
First Strand cDNA Synthesis Kit - Fermentas
iQ™ SYBR® Green Supermix - Bio-Rad
GenElute Plasmid MiniPrep Kit – Sigma
Dual-Luciferase® Reporter System – Promega
Rat Neuron Nucleofector® Kit – Lonza
Basic Neuron SCN Nucleofector® Kit - Lonza

2.1.2 Reagents

Acrylamide mix, 30% – Roth
ActinomycinD, 95% - Sigma
Agarose – Roth
Ammonium peroxodisulfate (APS) - Roth
Ampicillin – Sigma
Bio-Rad Protein Assay - Bio-Rad
Blocking Solution – Roche
Bovine serum albumin (BSA) Calbiochem
Chloroform – Fluka
Detector Block, 5x KPL
4',6-Diamidino-2-phenylindole dihydrochlorid (DAPI) - Roth
Diethyl pyrocarbonate (DEPC) – Roth
Dimethyl sulfoxide (DMSO) – Sigma
Ethanol, absolute – Roth
Ethanol, technical – Roth
Ethidium bromide – Roth
Formaldehyde, 37% – Merck
Formaldehyde, 37% – Fluka
Formamide (deionized) – Ambion
FuGENE® HD Transfection Reagent – Roche
Glycerol – Sigma

Guanidine hydrochloride - Sigma
Isopropanol (2-Propanol) – Roth
Isopropanol (2-Propanol) for molecular biology, min 99% - Sigma
Loading Dye Solution, 6x – Fermentas
Mowiol – Hoechst
N,N,N',N'-Tetramethylethylendiamin (TEMED) - Roth
Paraformaldehyde – Merck
Ponceau S – Merck
RiboLock Ribonuclease Inhibitor (40 u/µl) – Fermentas
RNase ZAP – Sigma
Sodium acetate – Merck
Sodium chloride – Merck
Sodium dodecyl sulfate (SDS) 10% –Sigma
Trichloric acid (TCA) – Merck
Tris(hydroxymethyl)aminomethane (Tris) – Roth
Triton X-100 – Sigma
Trizol® Reagent - Invitrogen
Tween 20 – Sigma

2.1.3 Solutions and Media

PBS (pH 7.4)
137 mM NaCl
10 mM Phosphate
2.7 mM KCl

Hank's balanced salt solution (HBSS, pH 7.3)

20 mM HEPES
2mM CaCl2
5.4 mM KCl
1 mM MgCl2
136 mM NaCl2
1 mM Na2HPO4
5.6 mM glucose
ddH2O

20x SSC (pH 7,0)
3 M NaCl
0,3 M Natrium-Citrat

B27-supplemented NMEM (NMEM-B27, pH 7.4)

1x MEM (modified Eagle's medium) from a 10x MEM stock
26 mM NaHCO3
1 mM sodium pyruvate
200 mM L-glutamine, stable
33 mM D-glucose
2% B27 supplement
ddH2O
LB (for 1 l)
10 g Tryptone
5 g Yeast extract
10 g NaCl
ddH2O

Lab blocking solution
PBS
2% fetal calf serum (FCS; PAA Laboratories, Pasching, Austria)
2% BSA (Sigma)
0.2% fish skin gelatine (Sigma)

Annealing Buffer
100 mM NaCl
50 mM HEPES pH 7.4

10x Blotting Buffer
250 mM Tris
1.92 M Glycine

2x Laemmli Buffer (10ml)
2.5ml 0.5M Tris HCl pH 6.8
2ml 100% glycerol
0.4g SDS
3.1g DTT (0.2M)
0.02% bromphenol blue
ddH_2O

10x SDS Running Buffer
0.25 M Tris
1.92 M Glycine
1% SDS

10x TBS
150 mM Tris pH to 7.5
1.5 M NaCl

TBS-T
1x TBS with 0.1% Tween 20

50x TAE (2 L)
484 g Tris
114.2 ml Acetic acid
200 ml EDTA (0.5 M, pH 8.0)
pH to 7.5 to 7.8 with HCl

1.5 mm 10% PA gel:

- *5% Stacking gel (3ml)*

H2O 2.1 ml
30% Acrylamide 500 µl
M Tris (pH 6.8) 380 µl
10% SDS 30 µl
10% APS 30 µl
TEMED 3µl

- *10% Separation gel (10ml)*

H2O 4 ml
30% Acrylamide 3.3 ml
1.5 M Tris (pH 8.8) 2.5 ml
10% SDS 100µl
10% APS 100µl
TEMED 4µl

2.1.4 Enzymes

Taq DNA polymerase (5 u/µl) – Fermentas
DNaseI, RNase-free (1 u/µl) – Fermentas
T4 DNA ligase (3 u/µl) – Promega
T4 DNA ligase (5 u/µl) – Fermentas
M-MuLV Reverse Transcriptase (20u/µl)- Fermentas

2.1.5 Restriction enzymes

BglII (10 u/µl) – Fermentas
HindIII (10 u/µl) - Fermentas
EcoR I (10 u/µl) - Fermentas

XhoI (10 u/µl) - NEB
NotI (10 u/µl) – NEB

2.1.6 Antibodies

Antibodies for Western Blot
Antibody dilutions for Western Blots were made in 1x Detector™ Block

Primary antibodies

Rabbit anti-Staufen2 (rabbit H7, 2007 – generated by D.Karra)	1:500
Rabbit anti-ZBP1 (serum; S.Hüttelmaier)	1:600
Mouse anti-Tubulin (monoclonal, Sigma)	1:5000
Mouse anti-betaActin (monoclonal, Sigma)	1:1000
Mouse anti-GAPDH (monoclonal, Sigma)	1:1500

Secondary antibodies

Donkey anti-rabbit 800 (LI-COR Biosciences, IRDye 800 – green)	1:10.000
Donkey anti-mouse 700 (LI-COR Biosciences, IRDye 700 – red)	1:10.000

Antibodies for Immunostaining
Antibody dilutions were prepared in 10% Lab Blocking Solution in HBSS

Primary antibodies

Rabbit anti-Staufen2 (rabbit H7 or Hi4)	1:500- 1:300
Mouse anti-ZBP1 (S.Hüttelmaier)	1:250

Secondary antibodies

Donkey anti-rabbit 488 (Invitrogen)	1:2000
Goat anti-mouse Cy3 (Dianova)	1:2000

Molecular staining

Phalloidin 546 (Invitrogen)	1:500

2.1.7 Primers

Primers for Realtime-PCR

mRNA		Orientation	Sequence	Designed by
GAPDH	Gap-F-2	forward	attcttccacctttgatgc	Y.Xie
	Gap-R-2	reverse	gtccaccaccctgttgctgta	Y.Xie
Tubulin	Tub-F-2	forward	tgtcttccatcactgcttcc	Y.Xie
	Tub-R-2	reverse	tgttcatggtaggctttctcag	Y.Xie
Staufen2	Stau2-F-2	forward	gaacatctcctgctgctgaag	Y.Xie
	Stau2-R-2	reverse	atccttgctaaatattccagttgt	Y.Xie
Peptidylprolyl-isomerase A (cyclophilin A)	PPIA-for	forward	gtcaaccccaccgtgttctt	S.Hüttelmaier*
	PPIA-rev	reverse	ctgctgtctttggaactttg	
18S rRNA	18S-for	forward	gttggtggagcgatttgtctgg	S.Hüttelmaier*
	18S-rev	reverse	agggcagggacttaatcaacgc	
Vinculin	VCL-for	forward	tcacagtggcagaggtagtg	S.Hüttelmaier*
	VCL-rev	reverse	tgacagtgttcattgagttc	
β-Actin	Actb Short-for	forward	gtccaccttccagcagatgt	A.Konecna
	Actb S -rev	reverse	gaaagggtgtaaaacgcagc	
β-Tubulin	Tubb-for	forward	ggaaagctgaggtgaaagg	A.Konecna
	Tubb-rev	reverse	acaggcaacagtgaagagca	
γ-Tubulin	Tubc-for	forward	gaggtggcttagagctgtct	A.Konecna
	Tubc-rev	reverse	caggacagcaaatgcacagt	
Septin 7	Sept7-for	forward	aagcaaactgggaagctcaa	A.Konecna
	Sept7-rev	reverse	tcaaacggatccaacaaaca	
γ-Actin	Actg-for	forward	cttccagcagatgtggatca	A.Konecna
	Actg-rev	reverse	ccagggaaatcgatacttc	
Zipcode-Binding-Protein1	ZBP1-F- 2	forward	atcatcggcaagaagggccagcaca	K.Wieczorek
	ZBP1-R-2	reverse	gggtctggtctctcggcacga	
	ZBP1-F-3	forward	tcgtgccgagagaccagaccc	S.Hüttelmaier*
	ZBP1-R-3b	reverse	ctgattcccactcattctca	
Firefly luciferase	FFL-for	forward	gagtctatcctgctgcagcac	L. Schoderböck
	FFL-rev	reverse	ctcgtccacgaacaccactc	
Renilla luciferase	RNL-for	forward	gtccggcaagagcgggaatgg	L. Schoderböck
	RNL-rev	reverse	acgtccacgacactctcagcat	

Table 2.1.1 Realtime PCR Primers (all primers were ordered from Sigma)

*Primer sequences from S.Hüttelmaier (unpublished, 2009) were adapted from *homo sapiens* to *rattus norvegicus*

Colony PCR primers

	Orientation	Sequence
pSUPER2101f	forward	acacaggaaacagctatgac
pSUPER-2390rv	reverse	gcgccctggcaggaagatgg

Table 2.1.2 Colony PCR Primers

2.1.8 Plasmids

insert	vector backbone	lab plasmid list nr°
	pEGFP-C2	215
Staufen2-EGFP	pEGFP-C2	169
EGFP-ZBP1	pEGFP-C2	240
	pSuperior.neo+GFP	100
shStau2	pSuperior.neo+GFP	181
misStau2	pSuperior.neo+GFP	182
shStau2	pSuperior.neo+GFP	403
shNon-targeting	pSuperior.neo+GFP	410
shZBP1	pSuperior.neo+GFP	404
psiSTRIKE shIMP1	psiSTRIKE U6 hairpin	469
psiSTRIKE shIMP1 scrambled	psiSTRIKE U6 hairpin	471
	psi-CHECK 2	435
Limk1 3'UTR FL	psi-CHECK 2	437
human β-Actin 3´UTR	psi-CHECK 2	444
human β-Actin zipcode	psi-CHECK 2	445
human β-Actin coding region+ zipcode	psi-CHECK 2	446

Table 2.1.3 Plasmids

pSUPER RNAi System™

VECTOR: pSUPERIOR.neo+GFP
CATALOG#: VEC-IND-0007/0008

Length: 5430 bp

Key Sites
BglII: 3182
HindIII: 3188
EcoRI: 2960
SalI: 3203
XhoI: 3209

Vector Features
f1(+) origin: 135-441
PGK promoter: 2840-2442
Neo ORF: 1684-715
EGFP ORF: 2424-1691
H1 promoter: 2965-3167
Ampicillin resistance ORF: 5302-4445

T3 primer (ATTAACCCTCACTAAAG): 3259-3243
M13 reverse primer (AACAGCTATGACCATG): 3292-3277

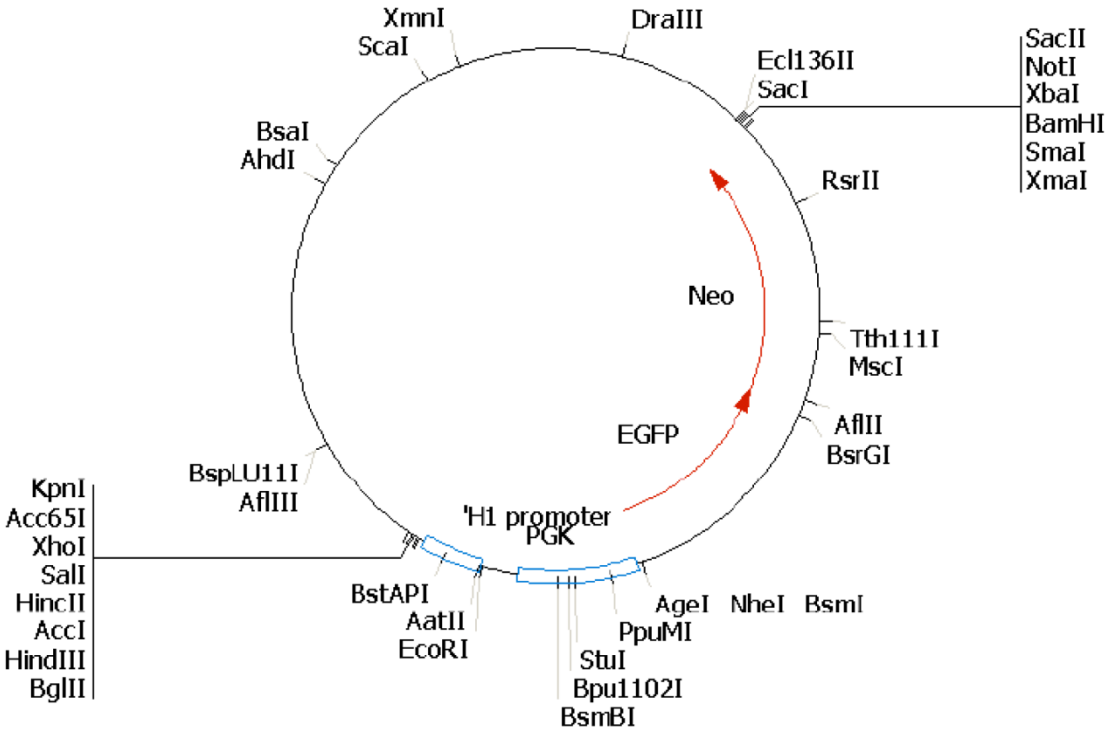

Fig. 2.1.1 pSuperior.neo+GFP map from www.oligoengine.com

2.1.9 Marker

GeneRuler™ 1 kb DNA Ladder (0.5µg/µl) – Fermentas

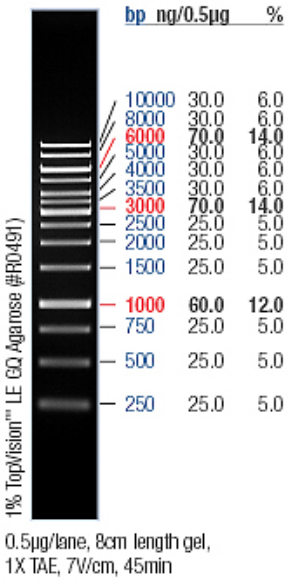

GeneRuler™ 100 bb DNA Ladder (0.5µg/µl)

- Fermentas

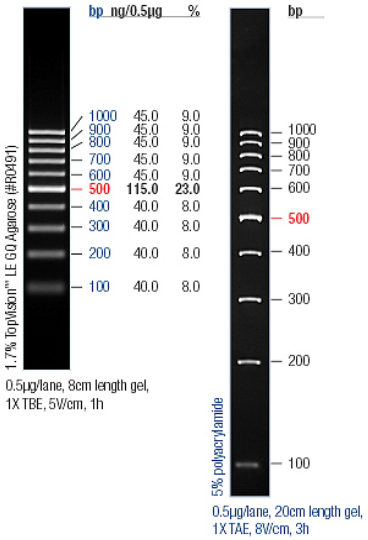

PageRuler™ Prestained Protein Ladder – Fermentas

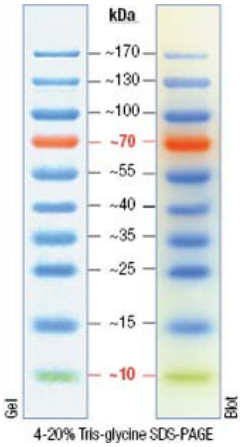

Fig 2.1.2 – http://www.fermentas.com

2.1.10 Equipment

Thermomixer compact, Eppendorf
Vortex VF2 Janke & Kunkel IKA
pH Meter MP 225, Mettler Toledo
Shaker, GFL 3015
Waterbath, GFL

Incubator, shaking, INFORS, Unitron
Incubator, kelvitron t, Heraeus
Balance, KERN ABS
Balance, KERN 440-49N
GeneQuant 100 Spectrophotometer – GE Healthcare
GloMax® 96 Microplate-Luminometer - Promega
Cuvette Suprasil, 10 mm, Hellma
Power Pac 300 power supply for electrophoresis, BIO-RAD
Power Pac HC power supply for electrophoresis, BIO-RAD
Mini-Protean® 3 Cell SDS-PAGE-System, BIO-RAD
Nucleofector® - Lonza
Trans-Blot Cell blotting chamber, BIO-RAD
Odyssey® Infrared Imaging System - LI-COR® Biosciences; software: Odyssey® Application Software 2.1
C1000 Thermal Cycler– BIO-RAD
Peqlab imaging system with UV/IR interference filter type F590 or SYBR® photographic filter
Centrifuge 5417 C Eppendorf
Centrifuge 5417 R Eppendorf
Virifuge 3.OR Heraeus
Rotor Heraeus #8074
Centrifuge AvantiTM J-25, Beckman Coulter
Rotor JLA 10.500, Beckman
Rotor JA 25.50, Beckman
Ultracentrifuge OptimaTM TXL, 120000 rpm, Beckman Rotor TLA 100.3, Beckman with polycarbonate centrifuge tubes, 13x51 cm, Beckman
Molecular Imager® FX (+ Screen Eraser – K), BIO-RAD
MyiQ™ Single Color Real-Time PCR Detection System - BIO-RAD; software: iQ5 Optical System Software (Version 2.0) - BIO-RAD
Leica MZ 16F - Leica; software: Leica Application Suite
Axioplan - Zeiss; software: analySISB - Olympus

Software:
– AnalysisB, Soft Imaging System
– LaserGene version 8.0, DNASTAR
– Metamorph version 7.0, Molecular Devices
– MS Office Excel 2003, Microsoft

2.2 Methods

2.2.1 Cloning

2.2.1.1 Cloning of shRNA Plasmids

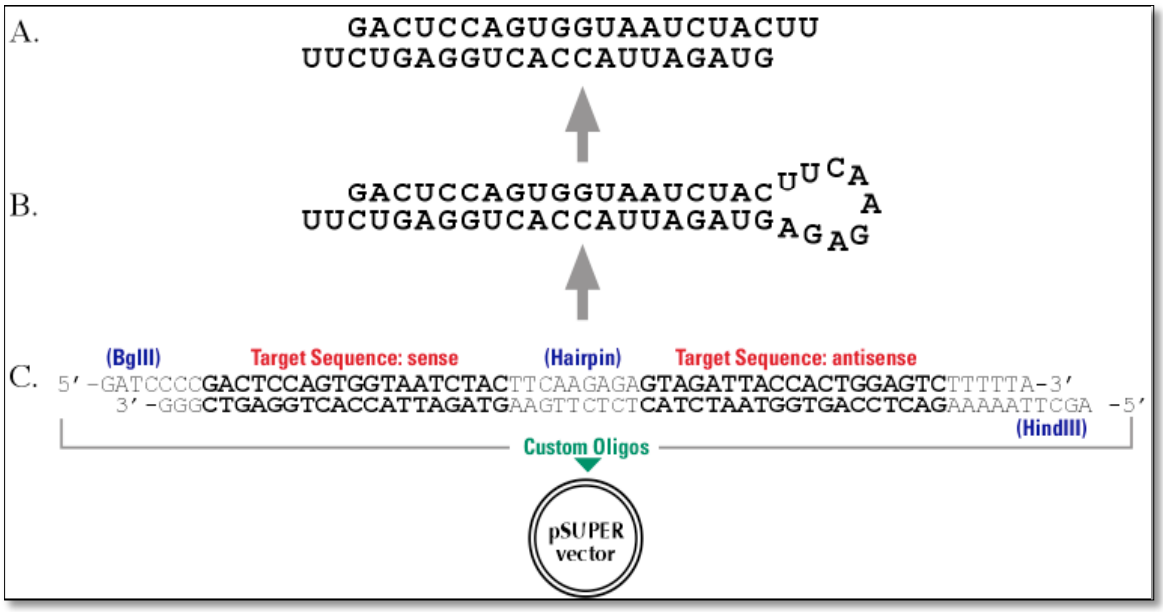

Fig. 2.2.1 (©http://www.oligoengine.com)

To create short hairpin RNA vectors for the specific suppression of gene expression through RNA interference, the pSUPERIOR.neo+gfp vector from the *pSUPER RNAi SystemTM* from OligoEngine (Brummelkamp, T. R. et al. 2002) was used.

In this vector a polymerase-III H1-RNA gene promoter produces siRNA-like transcripts with a start of transcription and a termination signal consisting of a stretch of five thymidines (T5). Subsequent cleavage of the transcript at the termination site after the second U leads to the formation of a mature siRNA with an overhang of two uridine nucleotides at the 3'end.

The oligonucleotides for the silencing of a specific gene contain a unique 19-nt sequence complementary to a sequence within the target mRNA. For cloning into *pSUPERIOR*, two complementary oligos were designed: the forward oligo includes the 19-nt target sequence in both sense and antisense orientation. There is a 9-nt spacer sequence in between, while the ends are flanked by sequences corresponding to sites of the restriction enzymes HindIII and BglII, and the 3' end also contains the T5 sequence (see Fig 2.2.1.). Upon ligation, the overhang sequence of the oligo destroys the BglII site to facilitate the screening of positive clones. The resulting transcript is supposed to fold back on itself to create a 19–base pair stem-loop precursor transcript, which is processed into the mature siRNA duplex, the

antisense strand of which is able to hybridize to the target mRNA to mediate its cleavage. A targeting sequence with a single mismatch should not affect expression of the target gene (Brummelkamp, T. R. et al. 2002) and is therefore suitable as a negative control.

All primer pairs were designed according to the manufacturer's protocol and ordered from Sigma-Aldrich. After annealing of the 60-nt oligos, they were cloned into the linearised pSUPERIOR.neo+gfp vector. While the EGFP expression of this vector served as an indicator of transfection efficiency in mammalian cells, the ampicillin resistance conferred by the plasmid was used for selection of *E. coli* clones after transformation.

Primer annealing

1µl of both the forward and reverse primer, diluted to 3µg/µl in ddH2O, were added to 48 µl Annealing Buffer (100 mM NaCl, 50 mM HEPES pH 7.4) and heated at 90°C for 4 min in the PCR cycler, then cooled down to 37°C in successive steps.

PCR cycler program for primer annealing:

94 °C	4 min
90 °C	4 min
85 °C	4 min
80 °C	4 min
70 °C	4 min
60 °C	4 min
50 °C	4 min
37 °C	10 min
4 °C	forever

The annealed primers were directly used in a ligation reaction or stored at -20°C.

Ligation with pSuperior

To insert the primer sequence into pSUPERIOR, the vector was linearised with HindIII and BglII and ligated with the annealed primer mix with aid of a T4 DNA ligase, which is able to join blunt or sticky ends of dsDNA. 1µl of the vector (0.5µg/µl) and 2µl of the annealed primers were combined with 1µl 10x T4-Ligase Buffer (400 mM Tris-HCl, 100 mM $MgCl_2$, 100 mM DTT, 5 mM ATP; Fermentas), 5µl nuclease-free H_2O and 1µl T4 DNA Ligase (5 u/µl, Fermentas). This mixture was incubated for 2h at RT.

Digestion with *BglII*

As the *BglII* restriction site in the vector is destroyed upon successful cloning of the primer pair, plasmids containing the insert will not be cut by this enzyme any more. Thus a *BglII* digestion step before transformation could be used to reduce the background of false-

positive clones, because the enzyme would only digest self-ligated pSUPERIOR vectors. The ligation reaction was incubated with 1µl *BglII* enzyme (Fermentas) for 30 min at 37°C.

2.2.1.2 Subcloning from pre-existing vectors

Restriction digestion

To transfer a sequence from one vector into another one, the sequence has first to be excised from its plasmid. For example, to clone β-actin sequence fragments from pGEM-T to psiCheck2, they were cut out by a double digestion with the enzymes XhoI and NotI (New England Biolabs). 1.5µl of each enzyme were added to 0.5µl BSA and 5µl 10x Buffer 3 (NEB; a buffer was chosen, in which both restriction enzymes had the highest activity) and filled up with plasmid DNA from a miniprep to a total volume of 50µl, before incubation at 37°C for 2 hours. After that the DNA was separated on an agarose gel to identify and isolate the fragment.

Agarose gel electrophoresis

For the separation of DNA fragments of a few hundred kb or larger, a 1% gel was prepared by dissolving 1g of agarose in 100ml 1x TAE buffer by heating in the microwave. For shorter DNA sequences, 1.5% to 2% gels were prepared accordingly. The solution was cooled down under constant stirring before 50µl of ethidium bromide were added per 100ml. Afterwards the gel was poured and left to polymerize at RT. DNA samples were combined with 6x loading dye (usually 25µl sample + 5µl loading dye) and loaded on the gel together with 10µl of a size marker, such as a 1kb DNA ladder (Fermentas) or a 100bp DNA ladder (Fermentas) for small fragments. The gel was run in 1x TAE buffer at 100 V until bands were sufficiently separated.

Gel elution

Following electrophoresis, the DNA band of the predicted size was cut out and purified using the Wizard® SV Gel and PCR Clean-Up System (Promega) according to the manufacturer's protocol. The bands were excised from the agarose gel with a clean scalpel blade under UV light and transferred to a 1.5ml tube. After weighing the gel slices, 1µl of Membrane Binding Solution were added per 1mg of gel slice, then they were vortexed and and heated at 55°C until the gel had dissolved. The solution was transferred to a Minicolumn in a collection tube, incubated at RT for 1 min to allow DNA binding and centrifuged for 1 min at 16,000g. After washing the membrane twice with Membrane Wash Solution, the DNA was eluted with 50µl nuclease-free water by centrifugation, and either used immediately in a ligation reaction or stored at -20°C.

Ligation

1µl of the vector was combined with 3µl of the purified insert, 5µl 2x T4-Ligase Buffer (Promega) and 1µl T4 DNA Ligase (3 u/µl, Promega), before it was incubated for 2h-3h at RT.

Transformation

100 µl of Top10 E. coli competent cells were thawn on ice and mixed carefully with 2 µl of ligation mix. We used *TOP 10* –chemically competent E.coli (Invitrogen; Genotype: F´ *mcr*A Δ(*mrr-hsd*RMS-*mcr*BC) Φ80*lac*ZΔM15 Δ*lac*X74 *rec*A1*ara*D139 Δ(*ara-leu*)7697 *gal*U *gal*K *rps*L *end*A1 *nup*G). After the mixture was incubated on ice for 30 min, a heat shock was performed in a water bath at 42°C for 1 min, to make possible that the cells take up DNA. Then the cells were again cooled on ice for 2 min before incubation with 700 µl LB medium for 1h at 37°C, shaking at 400 rpm. During this step of bacterial growth, cells can develop resistance against the antibiotic used for selection. Afterwards the cells were pelleted at 4,000 rpm for 5 min, 700 µl of the supernatant were removed and the pellet was resuspended in the remaining 100 µl LB medium. This cell suspension was plated on LB-agar plates containing the suitable antibiotic and incubated at 37°C overnight.

Miniprep

5 ml LB medium containing the suitable antibiotic were inoculated with a transformed colony and incubated overnight at 37°C shaking at 225rpm. The culture was transferred into two 2ml tubes and bacteria were pelleted at 4,000 rpm for 5 min in a microcentrifuge. Then lysis of the cells and the isolation of plasmid DNA were performed using GenElute Plasmid MiniPrep Kit (Sigma) according to the manufacturer's protocol. The DNA was eluted from the columns with 50µl nuclease-free H_2O.

Test-digestion

To verify, that the plasmid DNA from the picked clone contains the insert, the DNA obtained from a miniprep can be used in a test digestion. In the case of *pSuperior*, 1µl of the purified plasmid was cut with 0.75µl of both of the restriction enzymes HindIII and EcoRI in 15.5µl ddH2O and 2µl BamHI-buffer (Fermentas; chosen with the aid of the Fermentas Double Digest™ Engine). The mix was incubated for 2 hours at 37°C and examined by gel electrophoresis. Whilst fragments cut out from negative clones would be 227 bp long, those containing the insert would have 281 bp.

Maxiprep

Positive clones containing desired insert were inoculated in 200 ml LB medium with the appropriate selection antibiotic (100µg/ml) and incubated at 37°C and 225rpm overnight. On the next day, 1ml of the bacterial culture were transferred to a cryotube and combined with 0.5 ml glycerol. This glycerol stock was kept at -80°C as a backup.

Plasmid DNA was prepared from the cultures using the *EndoFree Plasmid Purification Kit (Qiagen).* This method yields high concentrations of endotoxin-free plasmid DNA, which is necessary for the successful transfection of hippocampal neurons (Zeitelhofer, M. et al. 2008). Endotoxins are bacterial components that are highly cytotoxic for neurons. Cells were pelleted by centrifugation at 6,000 g and 4°C for 15 min (Avanti J-25TM Centrifuge - Beckman Coulter, rotor JLA10.500). The following isolation of plasmid DNA was performed as described in the manufacturer's protocol, with the exception that the eluted and precipitated DNA was washed twice with 70% ethanol and centrifuged at 20,000g and 4°C for 5min at the end of the procedure. The washed DNA pellet was dissolved in 180µl endotoxin-free H_2O. The DNA concentration was measured by UV spectrophotometry at a wavelength of 260 nm, and the purity of the sample was also examined by using the 260 nm: 280 nm ratio, which should be above 1.6 for samples free of substantial protein contamination. The isolated DNA was then aliquoted and stored at -20°C.

Colony PCR

Colony PCR was performed to identify transformed clones that contain a plasmid with the desired insert. Therefore single colonies were picked from the original plate with a sterile pipette tip. From each colony a streak was made onto an LB plate with the respective antibiotic and marked by numbers, and then the same tip was used to resuspend the rest of the colony in 25µl of the PCR reaction mix.

Reaction mix:
2.5 µl 10x Taq buffer
1.5 µl 25 mM $MgCl_2$
0.5 µl dNTPs (10 mM for dATP, dCTP, dGTP, dTTP)
0.7 µl 3'-Primer (forward pSuperior)
0.7 µl 5'-Primer (reverse pSuperior)
0.2 µl Taq polymerase (5 u/µl, Fermentas)
18.9 µl ddH_2O
25µl total volume

PCR program:

94°C 60s		1 cycle
94°C 30s	}	30 cycles
47°C 30s		
72°C 60s		
4°C forever		

After the PCR, 5 µl of a 6x Loading Dye (Fermentas) were added to each sample and the total reaction volume was loaded on a 2% agarose gel, together with 12 µl of a 100 bp DNA Ladder (GeneRuler^{TM}, Fermentas) and a positive control, for example the PCR reaction from an empty vector (with pSuperior added instead of a picked colony). After running the gel, pictures of the gel were taken using UV imaging.
In the case of the *pSuperior*-plasmids, several colonies were picked and tested with primers specific for the *pSuperior* vector sequence surrounding the insert (for primer sequences see Table 2.1.1). Amplified fragments from the vectors containing the desired inserts were 60bp longer and therefore running above the empty vectors on a gel. The identified positive clones could then be picked from the plate and were used to inoculate LB for an overnight culture for Minipreps to confirm the result by test digestions.

2.2.2 Cell Biology Methods

Hippocampal Cultures

Hippocampal neurons were derived from E17 (embryonic day 17) embryos from *rattus norvegicus* as described in Zeitelhofer et al. (2007). Dissection of the hippocampi and preparation of hippocampal cells was carried out by Sabine Thomas, Krzysztof Wieczorek, Julia Riefler, Samantha Herbert and Kristina Kosenburger.

Preparation of Cortical Cultures

The whole procedure was carried out under sterile conditions, all solutions and media were pre-warmed to 37°C. The dissected cortices of E17 embryos (without hippocampi) in HBSS were cut up as small as possible with clippers in a petri dish and then transferred into a falcon tube. After centrifugation at 1000rpm for 4 min, the HBSS was removed and pre-warmed trypsin was added. For 10 min the brain tissue was incubated with trypsin in a waterbath at 37°C to disrupt cell-to-cell and cell-to-membrane contacts, before medium (DMEM+horse serum) was added to inactivate the trypsin. Again cells were centrifuged at 1000rpm for 4 min, trypsin was sucked off and 6ml DMEM+HS were added. To dissociate the cells, the solution was first pipetted with blue tips, and then triturated with “fire polished” Pasteur pipettes for approximately 1 min. The cells were subsequently filtered four times through cell sieves of two different pore sizes (70µm- and 100µm- cell strainers)

and diluted with medium to a volume of 25ml. Cell numbers were determined with the aid of a counting chamber, then cells were ready for plating or transfection.

HeLa cells

HeLa cell cultures (*HeLa cells* obtained from DSMZ Heidelberg) were usually split 1:10 approximately every 3 to 4 days at 80-90% confluence. A flask with 15ml DMEM+FCS was equilibrated in an incubator at 37°C and 5% CO_2 for at least 2 hours, before the cells were split. Confluently grown cells were washed with pre-warmed PBS and incubated with 2ml trypsin for 1 min at 37°C. After the excess trypsin was removed, the attached cells could be released by tapping the flask and were resuspended in 10ml DMEM+FCS, of which 1ml was transferred to the new flask.

Nucleofection

Nucleofection is a method of direct electroporation of expression plasmids into the nucleus of mammalian cells ensuring high transfection rates and good cell viability even in postmitotic cells, such as neurons, which are sensitive to mechanical stress and cytotoxic components and diffcult to transfect. In contrast to other transfection methods suitable for neurons (e.g. CaPO-coprecipitation), nucleofection is efficient enough to yield enough material for biochemical analysis, such as Western blotting or realtime-PCR.
Immediately after the preparation of cortical or hippocampal rat neurons from E17 rat embryos, they were transfected with the Amaxa™ Nucleofector using the O-003 program, as described in Zeitelhofer et al. (2009). Either the Rat Neuron Nucleofector® Kit (Lonza) or the Basic Neuron SCN Nucleofector® Kit (Lonza) for small cells numbers were used. The neurons were then incubated at 37°C and 5% CO_2.

Calcium-Phosphate Transfection of Hippocampal neurons

The transfection of hippocampal neurons with plasmid DNA using CaPO-coprecipitation was carried out as described in Goetze et al. (2004).

Transfection of HeLa cells using FuGENE™- HD Transfection Reagent

One day before lipofection with *FuGENE*™ HD Transfection Reagent (Roche), 75,000 HeLa cells were plated per well in a 24-well-plate with DMEM + FCS. At a confluency of 80-90%, the cells were washed with pre-warmed PBS, then 500µl OPTI-MEM™, a serum-free transfection medium, were added to each well. While cells were in the incubator (37°C, 5% CO_2), a mixture of *FuGENE™* reagent and DNA at a ratio of 5:2 was prepared. 0.5µl reagent were added to 0.2µg DNA (0.1 µg of the luciferase reporter plasmid and 0.1 µg of the overexpression plasmid) and mixed with 25µl OPTI-MEM medium per well. The mixture

was vortexed briefly and incubated for 15 min at RT, before it was added drop-wise into the wells. After 5-6 hours at 37°C the transfection medium was replaced by DMEM + FCS. 24 hours later cells were lysed and used for luciferase assays.

Accell® siRNA

Accell oligos from *Dharmacon* were used for the silencing of target genes by RNA interference. The *Accell* siRNAs are 18-30nt long duplex oligonucleotides, which are coupled to a cholesterol moiety via an alcohol-amine linker region. Thereby these molecules are capable of entering cells without an additional delivery procedure. To confer greater stability to the oligonucleotide complexes, chemical modifications have been added to some or all of its C and U nucleotides as well as to the first two nucleotides of the 5' end, such as 2'-O methyl or 2'-F modifications. The antisense strand contains a 2 nucleotide overhang at the 3' end, and it is complementary to the target gene.
Accell siRNA was resuspended in 1x *Dharmacon* siRNA Resuspension Buffer according to the manufacturer's instructions and stored at -80°C in small aliquots, to avoid repeated freeze-thaw-cycles. *Accell* siRNA was added directly into the cell culture medium (NMEM+B27; the *Accell* delivery medium, which is a serum-free medium especially formulated for siRNA delivery, was not used due to cytotoxic effects on neurons), either at 0DIV (days in vitro) or at 3DIV. Accordingly, 5µl siRNA solution from the 100µM stock were added per 1ml medium, yielding a final concentration of 0.5µM. Cells were incubated at 37°C and 5% CO_2 as usual, after 48 hours the medium was partially exchanged with fresh NMEM+B27. 72 to 96 hours after addition of the oligonucleotides, the cells were harvested and RNA and/or proteins were isolated.

***Accell* oligos**		**Target sequences**
siRNA Staufen2 (Set of 4 siRNAs)	siSTAU2 #13	cuuuuauguucaguugacu
	siSTAU2 #14	ccgucaguuuugagguuau
	siSTAU2 #15	gccauagguuuaaaaggaa
	siSTAU2 #16	cgaguauggucaaggaaug
siRNA ZBP1 (Set of 4 siRNAs)	siZBP1 #13	cuccaaaguucgaaugguu
	siZBP1 #14	uuguuaagaucaucggaca
	siZBP1 #15	uugcggagcacaagaucuc
	siZBP1 #16	ccugaagguuuccuacaua
negative control	Non-targeting siRNA	uaaggcuaugaagagauac
positive control	GAPDH siRNA	
transfection control	FAM-labeled Non-targeting siRNA	uaaggcuaugaagagauac

Table 2.2.1 *Accell* oligos

Immunocytochemistry & Microscopy

HBSS and paraformaldehyde (PFA) were prewarmed to 37°C. Cells on coverslips were briefly rinsed with HBSS and fixed in 4% PFA in HBSS for 15 min. After washing with HBSS, cells were permeabilized using 0.1% Triton X-100 for 5 minutes. After another washing step, the coverslips were blocked by addition of the lab blocking solution for 30 min at RT. Then they were incubated with solutions of one or two antibodies diluted in 10% blocking solution in HBSS. After 1.5 - 2 h at RT or overnight at 4°C, the coverslips were washed in HBSS three times for 5 minutes while shaking. The corresponding secondary antibodies were applied for 45 min at RT in the dark. They were linked to a fluorophore and reacted with primary antibodies which were derived from a different organism, thereby leading to visualization of the bound primary antibody. After washing with HBSS as previously, the coverslips were incubated in DAPI solution for 3 min in the dark for nucleic staining. Finally, the cells were washed in HBSS again, then dipped briefly into ddH_2O and mounted with 7µl Mowiol onto objective slides, cells facing downwards.

The stained cells were subsequently examined using an Axioplan microscope (Zeiss). Pictures of the cells were taken with analySISB software (Olympus) and adapted with Adobe Photoshop.

2.2.3 Quantification of RNA-levels

RNA isolation with TRIzol®

The TRIzol® Reagent is a mono-phasic solution of phenol and guanidine isothiocyanate, which breaks up cells and dissolves cell components, while protecting the RNA. Samples containing TRIzol® Reagent were handled under a chemical fume hood.

The medium was removed and cells were washed briefly with PBS pre-warmed to 37°C, before they were resuspended in 1ml TRIzol® Reagent per dish by pipetting up and down. The suspension was transferred into a sterile, RNase-free Eppendorf tube and incubated for 5 min at RT. After adding 0.2 ml chloroform, the solutions were mixed thoroughly by inversion and incubated at RT for 3 min before being centrifuged at 12,000 g and 4°C for 15 min. After centrifugation the aqueous phase containing the RNA had separated from the organic phase and was transferred into a fresh tube, mixed with 0.5 ml isopropanol and incubated for 10 min at RT. After that the RNA was precipitated by centrifugation at 12,000 g and 4°C for 10 min. The supernatant was discarded and the RNA pellet was washed with 1 ml 75% ethanol. Following centrifugation at 7,400 g and 4°C for 5 min, the RNA pellet was air-dried for 10 min. Afterwards the RNA was resuspended in 15µl DEPC-treated water and shaken in the thermomixer at 50°C and 350rpm for 10 min. Total RNA in DEPC-treated water was stored at -80°C.

The concentration of RNA was determined by UV spectrophotometry at 260 nm. 1:100 dilutions were prepared for the measurement. The purity of the sample from protein contamination was represented by the 260 nm: 280 nm ratio, which was usually above 1.6.

To avoid RNase contamination, gloves were worn at all times and both gloves and working space had been cleaned with ethanol and RNaseZAP® (Sigma®). Only water treated with 0.1% diethylpyrocarbonate (DEPC) as well as RNA grade chemicals were used to prepare solutions. Also, barrier tips and RNase-free tubes (Eppendorf) were used for RNA experiments.

DNAse digestion

To reduce DNA contamination after RNA isolation, samples were treated with *DNase 1* (Fermentas). 0.5 - 1µg of RNA were diluted with DEPC-treated Water to a volume of 8µl. After adding 1µl of 10X DNase I reaction buffer with $MgCl_2$ and 1µl of RNase-free DNase I, the mix was incubated 30-60 min at 37°C. To stop the digestion, 1 µl of 25 mM EDTA was added and samples were incubated for 10 min at 65°C. Then the RNA could be directly used in the cDNA synthesis reaction.

cDNA synthesis

CopyDNA was generated for the analysis of the template mRNA because DNA is much more stable than RNA. Reverse transcription of total RNA into cDNA was performed using Moloney Murine Leukemia Virus Reverse Transcriptase (M-MuLV), an RNA- and DNA-dependent DNA polymerase from the First Strand cDNA Synthesis Kit (Fermentas) possessing ribonuclease H activity specific to RNA in RNA-DNA hybrids.
0.5 - 1 µg total RNA in DEPC-H_2O, in a total volume of 11µl after DNase-treatment, were combined with 0.5µl random hexamer primers and 3.5µl DEPC-H_2O. To denature RNA secondary structure within the template, the mix of RNA and primers was heated at 70°C for 5 min and then chilled on ice for 5 min to let the primer anneal to the RNA.
Afterwards 10µl of a mastermix were added to each template, which consisted of the following reagents:

5 µl 5X M-MuLV RT Reaction Buffer
1.25 µl dNTPs (10 mM for dATP, dCTP, dGTP, dTTP)
1.25 µl RiboLock™ Ribonuclease Inhibitor
1.5µl DEPC-H_2O
1 µl M-MuLV Reverse Transcriptase (20 u/µl; Fermentas)

As a control for potential contamination with genomic DNA, 1.5µl DEPC-H_2O was added instead of reverse transcriptase.

The reaction mix then had a total volume of 25µl and was incubated in the PCR cycler:
- 10 min 25°C
- 50 min at 42°C
- 15 min at 70°C (to inactivate the enzyme)

Quantitative real-time PCR

Real-time PCR was performed for the quantification of specific RNAs, after total RNA had been reverse transcribed into cDNA. As DNA is amplified exponentially in the early and middle cycles of a PCR, this allows for the amount of template to be deduced. During a real-time PCR run, the generation of product is constantly monitored by the detection of fluorescence. Consequently a dye has to be present in the reaction mix, like *SYBR Green*, that intercalates double-stranded DNA and emits fluorescence, the intensity of which being proportional to the quantity of DNA present in the reaction.

The PCR cycler *MyQ iCycler* (BioRad) with *iQ5* Optical System Software 2.0 and the *iQ SYBR Green Supermix* (BioRad) were used for real-time PCR experiments. *2x SYBR Green Supermix* contains 100 mM KCl, 40 mM Tris-HCl (pH 8.4), 0.4 mM of each dNTP (dATP, dCTP, dGTP,and dTTP), iTaq DNA polymerase (50 u/ml), 6 mM $MgCl_2$, SYBR Green I, 20 nM fluorescein, and stabilizers. The fluorescein dye in this mixture is used for internal calibration. The *iTaq DNA* polymerase is a hot-start enzyme which is inactive at RT and has to be activated with an initial 3 min denaturation step at 95°C.

For each primer pair a mastermix was prepared, usually with a final primer concentration of 300 nM and the standard $MgCl_2$ concentration of 3 mM.

1x reaction mix for real-time PCR:

12.5µl	2x iQ SYBR Green Supermix
1.5µl	forward primer (5 µM)
1.5µl	reverse primer (5 µM)
6.5µl	ddH_2O
22µl total	

To this mixture 3 µl of cDNA dilution were added into each well of a 96-well-plate. Triplicates were measured for each sample. The template cDNA was usually diluted 1:10 with nuclease-free H_2O, except for cases where primers were specific for particularly rare or abundant transcripts. For example, for the amplification of the very abundant *18S* rRNA, the template was usually diluted 1:100 to be in a comparable range. For the "no template control" (NTC), 3 µl ddH_2O were added into the well instead of cDNA. Any signal detected from this well would hint at a contamination of reagents with nucleic acids or the formation of primer-dimers. To check for genomic DNA within the template, a "no enzyme

control" (NEC) was applied, where reverse transcriptase had been omitted during cDNA synthesis.

Finally the 96-well plates were sealed with Flat Cap Strips (Bio-Rad) to prevent evaporation.

PCR cycle scheme:
- 95°C for 3 min
- 95°C for 10 sec
- 55°C for 30 sec } 40x

Melting curve:
- 55°C to 95°C (+0.5°C per cycle) for 30 sec/ step - 81x

At the end of the amplification cycles, a melting curve analysis was performed, in which the temperature was raised by 0.5°C every 30s. At the melting point, the DNA strands dissociate and the fluorescence rapidly decreases. The melting temperature (Tm) is characteristic for a DNA double helix and depends on its length and base composition. As all fragments amplified with the same primers should show fluorescence peaks at relatively identical temperatures, melting curve analysis can be applied as a quality control for real-time PCR reactions, to make sure that only one specific product is amplified and detected. Different melting curves from the same sample hint at DNA contamination, primer-dimer artifacts, annealing of primers to non-target DNAs, etc.
Primers for qPCR were designed to meet certain criteria, for example that the amplified region should not exceed 200-300bp. Also, primers should have a length of approximately 20 nucleotides and, if possible, they should span an exon-exon boundary or the primer pair should be separated by an exon-exon boundary, to reduce genomic background (for primer sequences, see table 2.1.1).
To confirm that primers work properly, a standard curve real-time PCR was performed for every primer pair. With the aid of this step efficiency of the PCR reaction, R2 and slope values can be monitored. The conditions of the reaction, usually $MgCl_2$ and/or primer concentration, have to be optimized in a way that the efficiency of the PCR is in a range of 85-100%, the R2 coefficient close to 1 and the slope in a range of –3.1 to –3.6. For standard curve reactions, cDNA from brain lysate or untransfected cells was used from which dilution series were prepared in 10-fold steps, ranging from 1:10 to 1:10.000.

Evaluation of all PCR results was done according to the comparative $\Delta\Delta C_t$ (delta-delta Ct) - method (Schmittgen T. and Livak K., 2008). The cycle threshold (Ct) is a baseline set in the logarithmic range of DNA amplification. This is usually at the beginning of the intensity curve, where the increase of fluorescence is exponential. To calculate the relative amounts of a gene of interest, its Ct-value is normalized to the Ct-value of an internal control and compared between two different samples, for example treated and untreated samples or samples transfected with an overexpression vector and such transfected with the empty vector, etc.

$2^{-\Delta\Delta Ct}$ = [(Ct gene of interest - Ct internal control) sample A – (Ct gene of interest - Ct internal control) sample B]

One of the drawbacks of this quantification method is that it only yields relative results and depends highly on the choice of reference genes. Also, it assumes that primers for unknown and reference gene have identical efficiency.
Normalization of the qPCR data to a single reference gene is not recommendable, as even the expression of so-called housekeeping genes, like GAPDH or Tubulin, is occasionally not completely constant across different conditions, which will skew the results. Therefore, the gene of interest was always analyzed together with a set of several reference genes and evaluated by internal cross-normalization (Weidensdorfer et al., 2009). Therefore $\Delta\Delta C_{t}$-values of the gene were calculated for each control and then averaged, outliers having been removed.

RNA agarose gel electrophoresis

To assess the quality of the isolated RNA, RNA gel electrophoresis on a 1.5% agarose gel was performed. As a precaution against RNase-contamination, RNA gel electrophoresis was carried out using special equipment, as RNase-free pipettes or barrier tips, and at a working space reserved for RNA work.
1.5 g agarose (top-vision, RNase-free) were dissolved in 73ml DEPC-treated water, heated in the microwave and cooled down to approx. 55°C under cold tap water. 10ml 10x MOPS electrophoresis buffer and 17ml 37% formaldehyde were added under a chemical fume hood, before the gel was poured into the tray, which had been soaked in 0.2M NaOH before for 60min.

A sample of 1 µg of RNA diluted in 6 µl DEPC water was denatured by adding a mixture of 12.5µl of formamide, 2.5µl 10x MOPS and 4µl 37% formaldehyde. Then samples were heated at 65°C for 10 min, after that they were chilled on ice and 2.5µl RNA loading dye mix was added.
First the gel was pre-run in 1x MOPS buffer for 10 min at 90V (5 V/cm). Then samples and a 1kb DNA ladder were loaded and electrophoresis was run at 90 V for 4 hours. The RNA-bands were stained with SYBR® gold, diluted 1:1000 in 1x MOPS buffer, for 60min.

2.2.4 RNA decay assay

To examine potential changes in mRNA stability between treated and control cells, RNA decay assays were performed. By incubating living cells with a transcription inhibitor and harvesting them at certain time points after addition, mRNA half-lives can be measured.
RNA synthesis was blocked by Actinomycin D (95% pure, cell culture tested Actinomycin D from Sigma, dissolved in DMSO to a stock concentration of 2mg/ml and stored at -20°C). Actinomycin D is an antibiotic that inhibits cell proliferation by intercalation of the guanosine residues of double-stranded DNA, thus interfering with the binding of DNA-dependant RNA-polymerase. The compound was added directly into the cell culture medium at a concentration of 6µg/ml (5µM). Cells were lysed using TRIzol, first at the time when the transcription inhibitor was added (time point 0), then again 3 hours and 6 hours later. Total RNA was isolated (see 2.2.3) and reverse-transcribed into cDNA, so that the mRNA levels from each of the three samples taken at different time points could be assessed by qPCR. Thus the decay rate of *β-actin* mRNA was compared to those of a set of reference genes, after the putative stabilizing factors had been knocked down or overexpressed. An untreated sample was always included as a control of successful RNA decay.

2.2.5 Protein quantification

Protein isolation with TRIzol®

After the addition of chloroform to the cells suspended in Trizol, proteins were isolated from the organic phase according to the manufacturer's protocol.
The aqueous phase- which could be further used for RNA isolation- was removed, 300µl ethanol were added, mixed by inversion and incubated for 2-3 min at RT to precipitate the DNA from the interphase. DNA was pelleted at 2,000g and 4°C for 5 min. The phenol-ethanol supernatant was transferred into a 2 ml tubes, then 1.5 ml isopropanol were added and the mix was incubated at RT for 10 min. After centrifugation at 12,000 g and 4°C for 10 min, the protein pellet was washed with 2 ml 0.3M guanidine hydrochloride in 95% ethanol for 20 min at RT and centrifuged at 7,600g and 4°C for 5 min. This washing step was repeated twice, then the pellet was vortexed in 2 ml ethanol, incubated again for 20 min and centrifuged as before. The protein pellet was air-dried for approximately 20 min, before resuspending it in 1% SDS. To dissolve the protein completely, it was heated at 50°C for 10-20min. Protein suspensions were stored at -20°C. To obtain higher concentrations, proteins could be subsequently precipitated by use of the TCA-DOC method.

Protein Precipitation (TCA-DOC method)

The protein solution was vortexed with 0.02% DOC (deoxycholate) and incubated for 5 min on ice. After adding 11% TCA (trichloroacetic acid), the mixture was vortexed and incubated for at least 30 min on ice, then centrifuged at 14,000 rpm and 4°C for 20 min. The pellet was washed once with 1ml cold acetone, vortexed and centrifuged at 14,000 rpm and 4°C for 5 min. Again the supernatant was removed and the protein pellet was air-dried at RT and finally resupended in 2x Laemmli.

Measurement of protein concentration – Bradford method

To determine the protein concentration, a Bradford assay was performed, which is based on an absorbance shift in the dye Coomassie from 465 nm to 595 nm, when the Coomassie reagent stabilizes its anionic form by the binding of protein. First the Bradford solution (Bio-RAD Protein Assay reagent) was diluted 1:4 in ddH_2O. Dilution series of BSA ranging from concentrations of 1-8 µg/ml served as a standard. For sample measurements, a certain amount of sample, usually diluted 1:10, was added to 1 ml of the Bradford reagent, until its colour would be in the range of the standards. After 5 min incubation at RT, the absorption at 595 nm was measured. The concentration of protein in a sample could then be calculated using the standards.

Preparation of protein lysates

2x Laemmli was heated to 95°C, of which 250 µl were added to a 6 cm dish (with 750k cells). The cells were scraped with a cell scraper (Greiner bio-one) and transferred into an Eppendorf tube. The lysate was heated to 95°C for 10 min while shaking at 400 rpm. After centrifugation at 14,000 rpm for 10 min at room temperature, the supernatant was collected and stored at -20°C. Before using it for an SDS-PAGE, it was reheated to 95°C for app. 5min at 400rpm. At 750,000 cells per dish, 35 µl of the lysate (from one dish) – the maximum loading volume for a 1.5 mm gel – should contain up to 40 µg protein.

SDS-PAGE

During SDS (Sodium dodecyl sulfate)-polyacrylamide gel electrophoresis, SDS denatures and binds proteins, applying negative charges to them. The proteins will then move towards an anode through the gel pores, thereby being separated according to their molecular weight, the smaller proteins moving faster. 10-50 µg of protein in Laemmli buffer were denaturated at 95°C for 5 min and were subsequently loaded on a 1.5 mm thick, 10% SDS-PA gel, together with 4 µl of PageRuler™ Prestained Protein Ladder (Fermentas). Proteins were separated at 130 V for 90 min.

Western Blot

Proteins separated by a SDS-PAGE were blotted onto a nitrocellulose membrane using the Bio-Rad tank blotting system. For one gel, 2 sponges, 4 filter papers and a nitrocellulose membrane were equilibrated in cold Blotting Buffer. They were assembled into a sandwich, gel and membrane being enveloped by 2 filters and a sponge one either side, avoiding air bubbles. Importantly, the gel has to be at the same side as the cathode and the membrane at the side of the anode, so that the negatively charged proteins will move to the membrane.
While amperage of 250 mA was applied for 90 min, the buffer tank was kept cold on ice under constant stirring. To confirm successful transfer of protein, the membrane was then stained with Ponceau S. Then the membrane could be cut for the following probing of the proteins of interest. To reduce unspecific binding, the membrane was blocked for 30 min at RT in Detector™ Block solution (KPL) +NaN_3 while shaking. Incubation with the respective primary antibodies, diluted in Detector™Block, was carried out either for 2 h at RT or overnight at 4°C, on a shaker. Afterwards the membrane was washed at least twice for 15 min at RT with 1x TBS Buffer containing 0.1% Tween. Then the blot was incubated with the secondary antibody diluted in Detector™ Block for 45 min at RT, shaking in the dark. After washing it as previously, it was scanned using the Odyssey® Infrared Imaging System (LI-COR® Biosciences). Quantifications were performed using the Odyssey® Application Software 2.1.

2.2.6 Luciferase Assay (Promega Dual-Luciferase® Reporter 1000 Assay System)

Luciferase assays were employed to assess putative regulatory properties of a DNA sequence on the transcription and/or translation of a reporter gene. The sequence of interest (for example a 3'-UTR) was cloned into a vector with a luciferase gene, which served as reporter. Luciferases are enzymes that catalyze bioluminescent reactions (see figure below). By metabolizing certain substrates, they generate a luminescent signal which can be measured and correlated with the amount of the reporter present in a sample. Usually the Luciferase activity of a co-transfected reporter serves as an internal control that represents baseline translation and is necessary for the normalization of the experimental reporter activity to eliminate differences due to varying transfection efficiencies or cell viability.

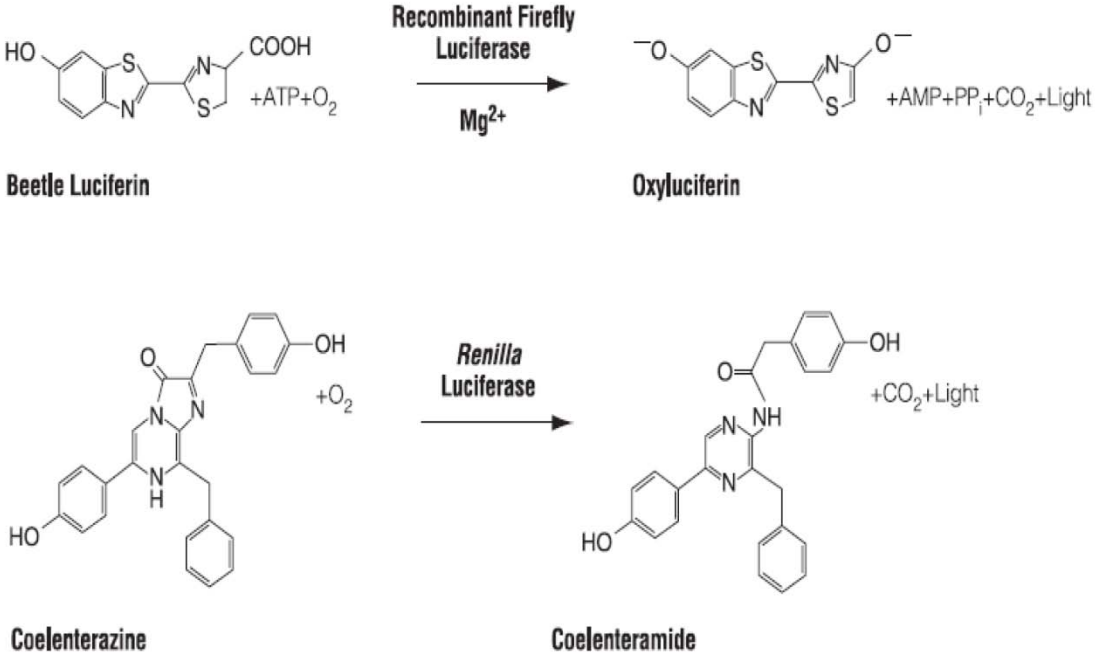

Fig. 2.2.2 ©Promega (Dual-Luciferase® Reporter 1000 Assay System Manual)

For this purpose the *Dual-Luciferase® Reporter System* (Promega) was used, in which the activity of firefly luciferase (*Photinus pyralis*) and of Renilla luciferase (*Renilla reniformis* or sea pansy) are measured successively from a single sample. PsiCHECK™-2 (Promega) served as an expression vector carrying the genes for both luciferases. The main advantage of this system is to avoid triple transfections (of a reporter and a control plasmid together with an effector plasmid), thereby making normalization more reliable. The sequences of interest (for example a 3'-UTR) were cloned into a multiple cloning site at the 3' end of the firefly luciferase expression cassette of psiCHECK™-2 vectors using the XhoI and NotI restriction sites.

Neurons at 0 DIV were transfected with the reporter constructs and either a silencing- or overexpression plasmid at a ratio of 1:4 by nucleoporation and plated into a 24-well-plate (HeLa cells were transfected by *FuGene* lipofection), mostly in triplicates. After either 24 hours (for overexpression) or 96 hours (for knockdown), the culture medium was removed and cells were washed once with pre-warmed PBS. Afterwards they were lysed by incubation with 1x Passive Lysis Buffer (150 µl/well; 5x Lysis Buffer diluted in ddH_2O) for 30 min at RT while shaking. 50 µl of the lysate were transferred into a 96-well-plate. Before starting the assay in the GloMax® 96 Microplate-Luminometer (Promega), an automatic priming sequence was initiated so that both autoinjectors would be filled with the respective reagent, LARII or Stop & Glo®.

The Promega protocol for Dual Luciferase Reactions with Two Injections of the GloMax® 96 Software was run to measure the luminescence intensities. The injection volume was set to 50 µl and the delay between injection and measurement was changed to 2 s, whereas the rest of the program settings were maintained. First firefly luciferase reporter activity was

measured after adding 50 µl of its substrate (Luciferase Assay Reagent II). Afterwards 50 µl Stop & Glo® Reagent were injected into the same tube, quenching the previous reaction and simultaneously initiating the *Renilla* luciferase reaction. The injectors were flushed with ddH_2O and 70% ethanol after every run according to the manufacturer's specifications.

For the quantification of reporter activity after measuring of the luminescence, the intensity of luminescence from the firefly luciferase was always normalized to the Renilla intensity of the same sample. Parallel assays with empty psiCHECK™-2 vectors also served as a control.

III Results

3.1 Investigating a novel siRNA delivery method for the downregulation of Staufen2 and ZBP1 in primary neurons

3.1.1 Establishing successful transfection of primary neurons

A frequently applied method for the transient downregulation of specific proteins in primary cells is the use of short hairpin vectors. They contain palindromes of 19 nucleotides complementary to the sequence to be silenced. The resulting transcript should fold into a hairpin precursor and is supposed to be processed by the endogenous microRNA machinery into functional siRNA. Albeit all obvious merits, there are certain limitations to this method. First, not all proteins are equally accessible to it; some are difficult to downregulate to a measurable extent. Another restriction is imposed by the transfection of these vectors into neurons, because of all transfection methods that had so far been used in our lab, only nucleofection before plating yielded numbers of transfected cells high enough for subsequent analysis by biochemical or molecular methods. Therefore, transfection of more developed neurons with sufficient yields had not been possible. As for one of the proteins I wanted to investigate, namely ZBP1, all previous attempts to downregulate it with short hairpin vectors had been unsuccessful, a novel method was tested, *Accell®* siRNA provided by *Dharmacon®.* These modified, double-stranded oligonucleotides have the ability to enter the cytoplasm of cells without any additional transfection reagent, since they are coupled to a cholesterol moiety via an alcohol-amine linker region (for an example of the *Accell®* oligo structure see **Fig. 3.1c**). Thus this procedure would yield several advantages: first, it is less harmful than nucleofection, which always results in a certain number of destroyed cells; secondly, silencing can be induced in cells of any age.

First the viability of hippocampal neurons was tested, after their neuronal medium (NMEM+B27) was replaced by *Accell®* delivery medium (having an unrevealed formulation) at 3 DIV (days in vitro) either as is or supplemented with B27, a factor necessary for neuronal growth. After an incubation period of 48 hours, visual assessment of these cells showed severely reduced viability in *Accell®* delivery medium both with and without the supplement. Therefore, the possibility of transfection with *Accell®* siRNA without substitution of NMEM

was assessed using a FAM labeled, control *Accell®* siRNA, emitting at 518 nm due to the attached fluorophore. This control siRNA is not supposed to target any RNA, which was confirmed by BLAST search. The standard delivery protocol supplied by the company (**Fig. 3.1a**) was slightly modified to fit the needs of our primary cultures. Subsequently, the oligos were only added to cultures after 3 DIV, so that cells could adhere properly. Also, to minimize waste of expensive reagents, only half of the recommended amount of oligos was used (0.5 µM), since the viability of neurons depends on a relatively large volume of media, and they cannot be grown too densely. Whenever a reduced volume of neuronal medium was used, it was partly exchanged for fresh medium after 48 hours, which is the recommended minimum duration for siRNA uptake according to the company's instructions. Transfection was visualized by fluorescence microscopy 72 hours after the addition of siRNA (**Fig. 3.1b**). To our advantage, transfection efficiencies did not seem to be influenced significantly by a lack of *Accell®* delivery medium, while neuronal survival was much better in NMEM (**Fig. 3.2a**). Alternatively, cells were grown in neuronal medium combined with either 50% or 25% of *Accell®* delivery medium, yet transfection efficiency or cell viability did not appear visibly changed in either case. Therefore, in all following experiments NMEM+B27 was used instead.

To determine the transfection rate, 3 days after treatment with siRNA 379 cells were counted, of which 204 (53.8%) were fluorescent; however, this is most likely an underestimation of the transfection rate with unlabeled oligos due to very stringent counting criteria and interference of the fluorophore with transfection.

As a proof for successful downregulation, quantitative real-time PCR was performed. Hippocampal neurons (2 culture dishes of 0.5 million cells per condition) were grown 3 DIV before the siRNA was added to the neuronal medium. Oligonucleotides targeting the housekeeping gene GAPDH were used as a positive control for efficient knockdown. 48 hours later the medium was exchanged, cells were lysed 72 hours after transfection and total RNA and protein were extracted with *Trizol.* The isolated RNA was reverse transcribed into cDNA and used for quantitative real-time PCR using GAPDH primers and the *MiQ BioRad* SYBR-Green supermix. Results were evaluated using the ΔΔCt -method (Schmittgen & Livak, 2008). Thereby, *GAPDH* mRNA levels in hippocampal neurons could be efficiently reduced by addition of *Accell®* siRNA. The average reduction of *GAPDH* mRNA was 77% in treated

compared to untreated cells (**Fig. 3.2b**). Actual numbers varied considerably between individual experiments, probably due to differences in the numbers of transfected cells, as well as slight variances in reference gene expression, in this case Tubulin.

To obtain a condition more comparable to siRNA-treated cells than simply untransfected neurons, cells were treated with a non-targeting *Accell®* siRNA, which ideally should not cause any changes in mRNA levels. *Stau2* mRNA levels of untransfected neurons and such treated with NT (non-targeting) siRNA were compared by qPCR. Notwithstanding a considerable variation between experiments, on average changes between transfected and untransfected cells were insignificant (**Fig. 3.2c**). Therefore, non-targeting siRNA was further used as a negative control.

A

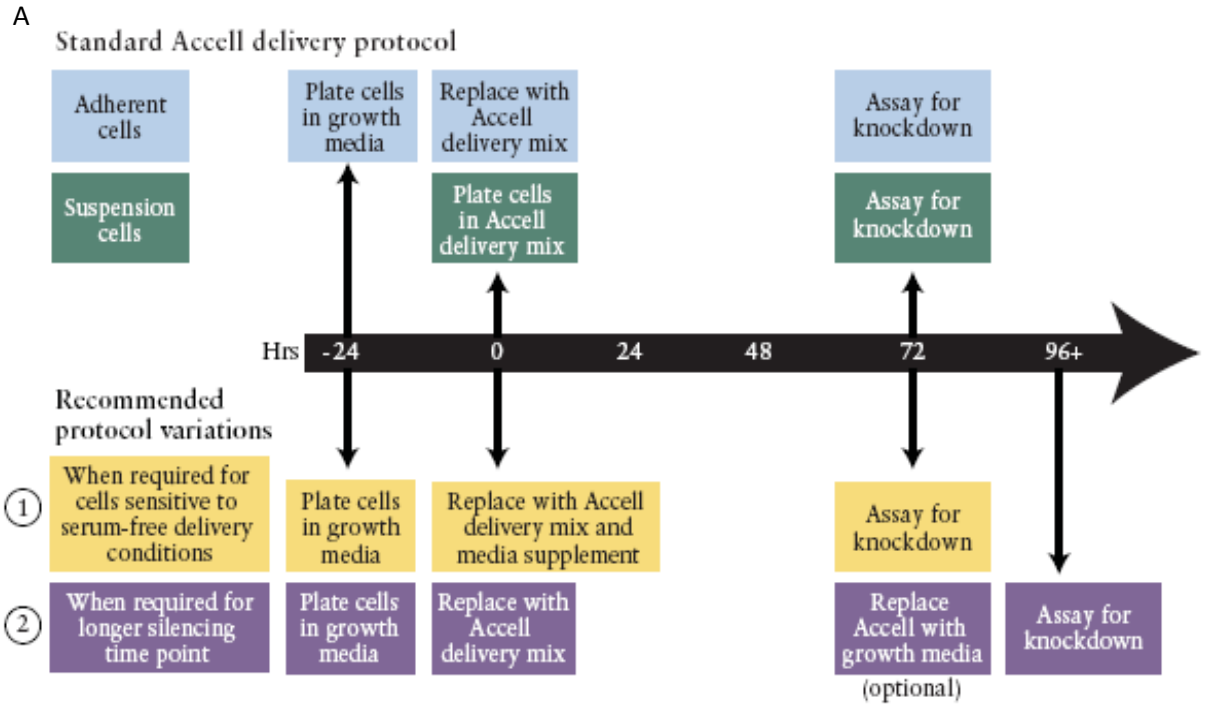

B

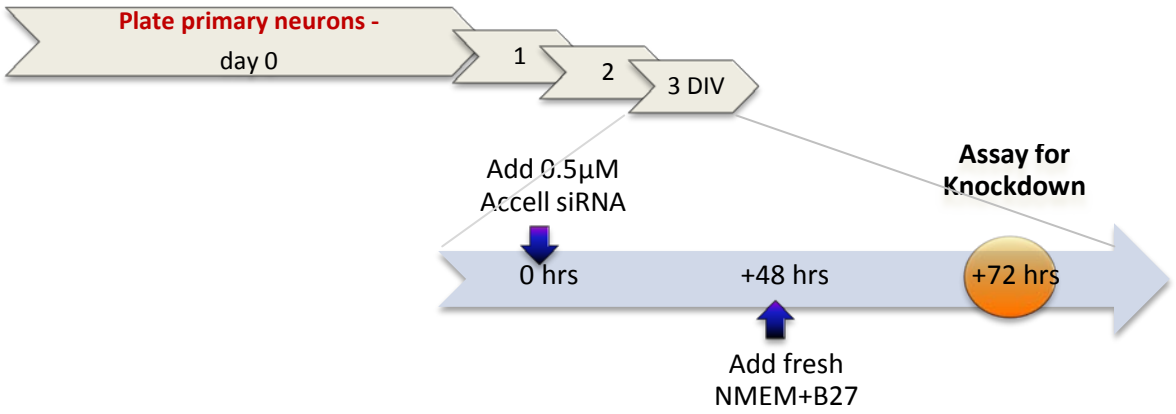

C

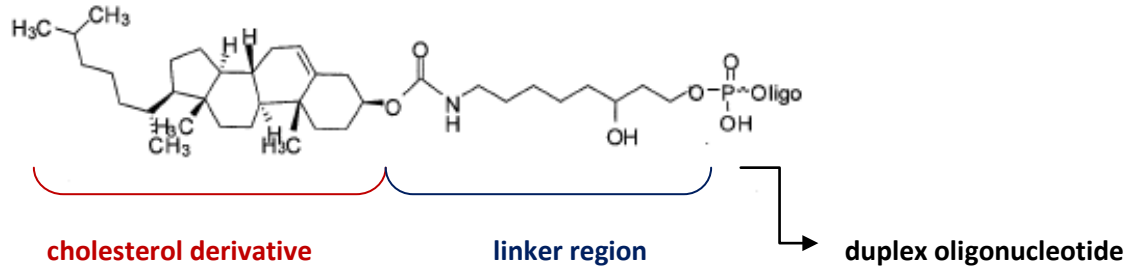

Figure 3.1 - *Accell*® siRNA

Schematic description of (**A**) the standard protocol (© www.dharmacon.com) and (**B**) the modified delivery protocol of *Accell* siRNA. Following the modified protocol, 0.5 µM *Accell* siRNA were added to the neurons in NMEM+B27 medium 3 days after plating, the medium could be exchanged 48 hours later, and cells were used for assays after 72 hours. (**C**) Exemplified structure of an *Accell* oligo.

A

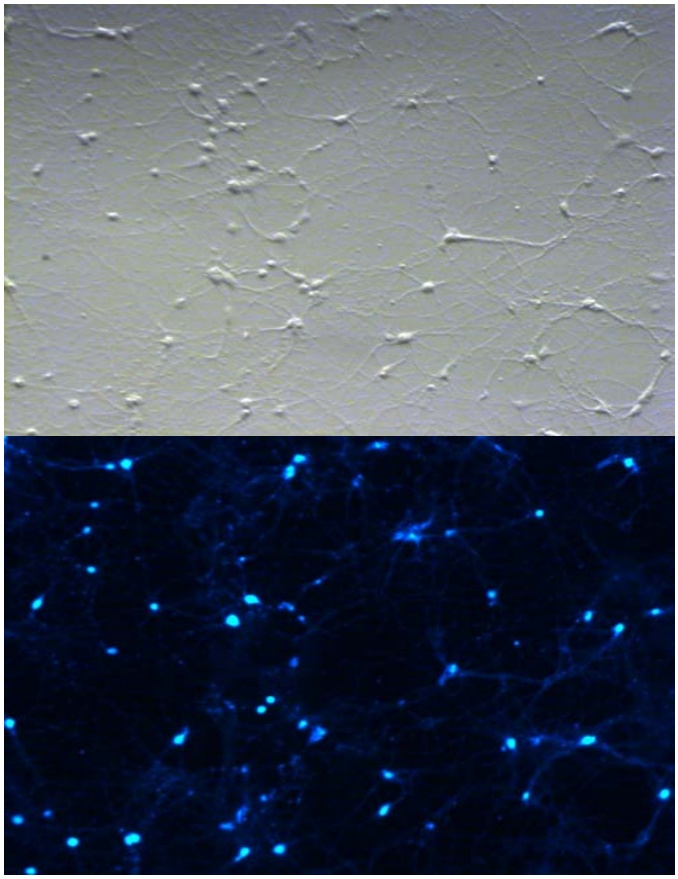

B

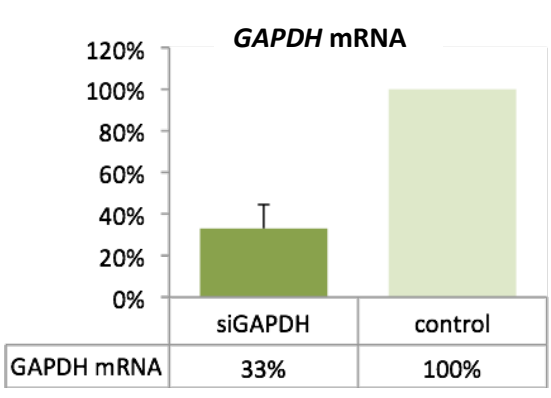

C

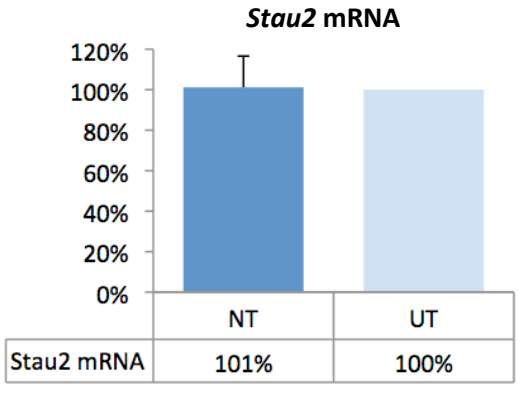

Figure 3.2 – Assessing the efficiency of *Accell*® siRNAs in primary neurons

(**A**) Testing the transfection efficiency of *Accell*® siRNA in hippocampal neurons by transfection with FAM-labeled oligos. Pictures were taken with a Leica MZ 16F.

(**B-C**) Evaluation of the effects of *Accell*® siRNA in neurons by qPCR. (B) Hippocampal neurons were treated with siRNA targeting GAPDH, as a positive control for efficient knockdown. A reduction of *GAPDH* mRNA levels was confirmed by qPCR in 4 individual experiments. (C) A non-targeting siRNA (NT), which is not supposed to induce any effect, was also tested and did not lead to significant changes of *Stau2* mRNA levels compared to untransfected (UT) neurons.

3.1.2 Testing 4 different siRNAs for both Staufen2 and ZBP1

After modifying the protocol so that the *Accell®* siRNA method was effective in primary neurons, sets of 4 different siRNAs were examined targeting either Stau2 or ZBP1. Their sequences, as well as the sequence of the non-targeting siRNA are provided in **Table 3a**. To examine which of those oligonucleotides would decrease *Stau2* or *ZBP1* mRNA levels most efficiently, neurons were transfected with either one of the four siRNAs (labeled #13 to 16 by the company) targeting either Stau2 or ZBP1. Subsequently, amounts of *Stau2* and *ZBP1* mRNA were quantified by qPCR, and transfected cells were compared with untreated cells. Tubulin and GAPDH were used as reference genes, for which real-time primer sequences – as well as all other primers that were used – are given in chapter 2.1.7. Transfection with any of the 4 siRNAs against Stau2 resulted in significant downregulation of *Stau2* mRNA (**Fig. 3.3b**, left chart), whereas siRNA #14 showed to be most effective in two individual experiments, reducing the *Stau2* mRNA in treated cells to 16% of the level in untreated cells. A repetition of the experiment with cells treated with siRNAs against ZBP1 numbered #13-16 gave differing results. This time, not every siRNA worked equally well, with siZBP1 #13 giving the strongest effect, leading to a downregulation of *ZBP1* mRNA to an average of 27% compared to untransfected cells (**Fig. 3.3b**, right diagram). In accordance with these results, the most effective siRNAs were used for further experiments, namely the siRNA targeting Stau2 #14 and the siRNA #13 against ZBP1. Their sequences are highlighted in red in **Table 3a**.

A

Accell oligos		**Target sequences**
siRNA Staufen2	siSTAU2 #13	CUUUUAUGUUCAGUUGACU
(Set of 4 siRNAs)	**siSTAU2 #14**	**CCGUCAGUUUUGAGGUUAU**
	siSTAU2 #15	GCCAUAGGUUUAAAAGGAA
	siSTAU2 #16	CGAGUAUGGUCAAGGAAUG
siRNA ZBP1	**siZBP1 #13**	**CUCCAAAGUUCGAAUGGUU**
(Set of 4 siRNAs)	siZBP1 #14	UUGUUAAGAUCAUCGGACA
	siZBP1 #15	UUGCGGAGCACAAGAUCUC
	siZBP1 #16	CCUGAAGGUUUCCUACAUA
negative control	Non-targeting siRNA	UAAGGCUAUGAAGAGAUAC
positive control	GAPDH siRNA	
transfection control	FAM-labeled non-targeting siRNA	UAAGGCUAUGAAGAGAUAC

B

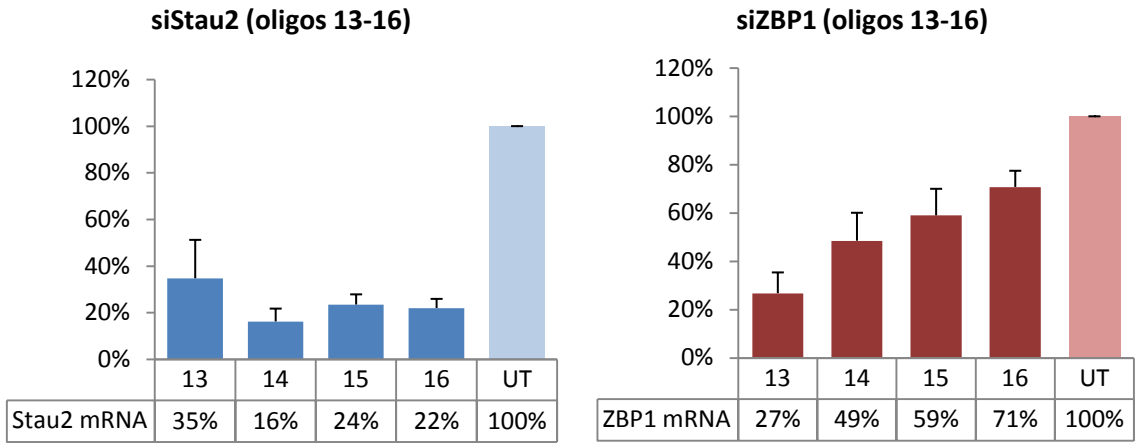

Figure 3.3 - Testing sets of 4 different *Accell*® siRNAs per target

(**A**) Table of Accell oligos directed against Stau2 and ZBP1 and their target sequences. 4 different siRNAs were tested for each gene. Red sequences indicate the oligos that were used for further experiments. The sequence of the non-targeting siRNA is also given, which was used as negative control or transfection control, when coupled to a fluorescent molecule. The sequence of the siRNA targeting GAPDH was not revealed by the company.

(**B**) Evaluation of the knockdown efficiencies of each oligo by qPCR. The reduction of mRNA by four different siRNAs targeting Stau2 and ZBP1, respectively, was compared. The oligos in a set were labeled by the company with the numbers 13 to 16. Two individual experiments were performed, error bars indicate standard deviation. The quantitative ΔΔ-Ct method was employed, and measured RNA levels of transfected cells were set in relation to those of untransfected (UT) cells.

3.2 A comparison between pSuperior plasmids and Accell® siRNA

3.2.1 Assessing the downregulation of mRNA levels by quantitative real-time PCR

Once a protocol for Stau2 knockdown with *Accell®* siRNAs was established, the actual effects of this knockdown, in particular on *β-actin* mRNA, were examined. However, preliminary experiments concerning putative changes of *β-actin* mRNA and protein as well as the overall actin cytoskeleton, which will all be described consecutively, showed certain diversions from previous experiences in the lab. As for all preceding experiments short hairpin vectors had been used for Stau2 knockdown, the question arose, whether different methods of downregulation could be responsible for the conflicting results, possibly due to unwanted side effects. Therefore, a closer investigation of the discrepancy between the effects of *Accell®* siRNA and the *pSuperior* system – a type of short hairpin vector that had been used previously – seemed appropriate.

To exclude that differing target sequences were the reason for different outcomes, irrespective of the method used, *pSuperior* plasmids were cloned containing the exact sequences of the *Accell®* siRNAs against Stau2 (#14) and ZBP1 (# 13), respectively. For the cloning of these sequences into *pSUPERIOR.neo+gfp* vectors (*OligoEngine*), forward and reverse primers (ordered from *Sigma-Aldrich*) containing the 19-nt target sequence were annealed and ligated with the linearized *pSuperior* vector following manufacturer's instructions (for a more detailed description see 2.2.1.1). These newly constructed plasmids subsequently will be called shStau2 and shZBP1, to discern them from the *Accell®* siRNAs, from now on termed siStau2 and siZBP1. Neurons were transfected with these vectors as well as with a previously used *pSuperior* plasmid targeting Stau2 (siStau2-2, Goetze et al., 2006) using Amaxa® nucleofection. After 3 to 4 DIV the cells were lysed and assayed by qPCR. In parallel, neurons treated with siRNA targeting Stau2 at 3DIV, were also tested after 3 to 4 days. As a negative control, cells were transfected with either the *pSuperior* vector containing a mismatch in its target sequence (misStau2), with empty *pSuperior* or non-targeting siRNA. The effects of these different treatments on *Stau2* mRNA levels determined by qPCR are shown in **Fig. 3.4a**. 7 individual experiments were performed with the siRNA and 3 with each *pSuperior* plasmid, using partly hippocampal and partly cortical neuron cultures.

Which culture type was used and for how long cells were incubated after transfection – either 3 or 4 days – had no apparent influence on the outcome of these experiments. In all cases certain variations between experiments occurred, most likely due to differences in the success of transfection or slight variations of individual cell cultures. The average quantity of *Stau2* mRNA in treated neurons was compared to untreated neurons (**Fig. 3.4a**, light blue bars), or neurons transfected with a mismatch plasmid or a non-targeting siRNA (blue bars). In the case of the plasmid siStau2-2, results were compared to the mismatch plasmid or to the empty *pSuperior* (purple bar). The amount of *Stau2* mRNA changed only slightly, ranging from a reduction to 33% by *Accell*® oligos to 45% by the shStau2 plasmid with the same sequence, in comparison to the control. These differences may be caused by varying transfection efficacies. However, the difference between cells transfected with the control plasmids/siRNA (in relation to untransfected cells, green bars) and the knockdown plasmids/siRNA are significant (p-value < 0.05), thereby proving that both systems lead to efficient Stau2 downregulation. The significance was determined by student's t-test.

Similar experiments were performed using the plasmid and siRNA targeting ZBP1. Neurons treated with siZBP1 showed a decrease of *ZBP1* mRNA down to 43% of the non-targeting siRNA treated cells (**Fig. 3.4b**, red bar). An experiment using a *pSuperior* plasmid with the same target sequence, however, did not lead to a significant knockdown of ZBP1, which corresponds to previous failed attempts to downregulate ZBP1 with the use of short hairpin vectors. While the outcome achieved with siZBP1 seemed rather promising according to the qPCR results, reaching stable reductions of protein levels proved to be more challenging.

3.2.2 Comparing the effects of pSuperior and Accell® siRNA on the protein level

To determine the effects of these two different methods of downregulation on the protein levels of Stau2 and ZBP1, protein samples were separated on denaturing gels and probed by Western Blotting. Either total protein was extracted using *Trizol®* – which has the advantage that the RNA can be used for qPCR in parallel, but results in relatively low yields – or whole cell lysates were loaded on SDS gels. **Fig. 3.4c** shows a representative blot, for which neurons (3 DIV) were treated with oligonucleotides targeting Stau2 or ZBP1, or GAPDH as a positive control. Non-targeting siRNA (NT) served once more as negative control. The left half of the membrane was stained with antibodies against Stau2 (anti-Stau2 rabbit serum), while the

right half was stained with ZBP1 antibodies (rabbit serum). The membrane was then decorated with antibodies against GAPDH, β-actin and Tubulin (all mouse monoclonal antibodies). Secondary antibodies from *LI-COR Biosciences,* donkey anti-rabbit 488 (green fluorescence) or anti-mouse Cy3 (red) were used. After scanning the membrane using the Odyssey Infrared Imaging System®, the intensities of relevant bands were measured and normalized to the intensities of the Tubulin band of the same lane (at 55 kDa), Tubulin being used as a loading control. Tubulin antibodies were not isoform-specific. The intensities of GAPDH bands (found at 36kDa) are reduced in the protein extract from neurons treated with siRNA targeting GAPDH, whereas they are not significantly decreased in any other sample. Against our expectations after real-time PCR results, the ZBP1 band (68 kDa) does not differ between the siZBP1 treated and the control samples. However, downregulation of Stau2 by *Accell®* siRNA on the protein level was successful. The quantification of the 3 major isoforms of Stau2 at the size of 52kDa, 59kDa and 62kDa, is depicted in **Fig. 3.4d**. The intensities of the different Stau2 bands were normalized to Tubulin and set in relation to non-targeting siRNA transfected cells: the respective band intensities from the control were therefore set to 100%. The neurons treated with siStau2 (blue bars) contained significantly less of all Stau2 isoforms, whereas siGAPDH treated cells (light blue bars) showed only minor variations. Yet the isoforms are not present at equal amounts after down-regulation. The reduction varies considerably, and the strongest decrease to 29% of the control is seen in the 59 kDa isoform, while the 52 kDa isoform is least affected, with 55% of the control remaining.

Corresponding experiments with neurons transfected with sh-plasmids yielded comparable results, as can be seen in **Fig**. **3.4e**. The amount of Stau2 protein was decreased by nucleofection at DIV 0 with the *pSuperior* plasmids siStau2-2 and shStau2 in comparison to the controls, the mismatch plasmid (Stau2mis) and empty *pSuperior*. Tubulin was again used as a loading control. Downregulation of ZBP1 was also tested once more with the use of the *pSuperior* plasmid shZBP1, as well as with a different sh-plasmid (generously provided by Stefan Hüttelmaier) based on the *psiSTRIKE™ U6 Hairpin Cloning System* (*Promega*), named shIMP1 (after the human homologue of ZBP1). The controls used were the empty *pSuperior* vector and a mismatch plasmid to shIMP1. However, no decreased intensity of the ZBP1 bands could be observed in either case (**Fig. 3.4e**, right side).

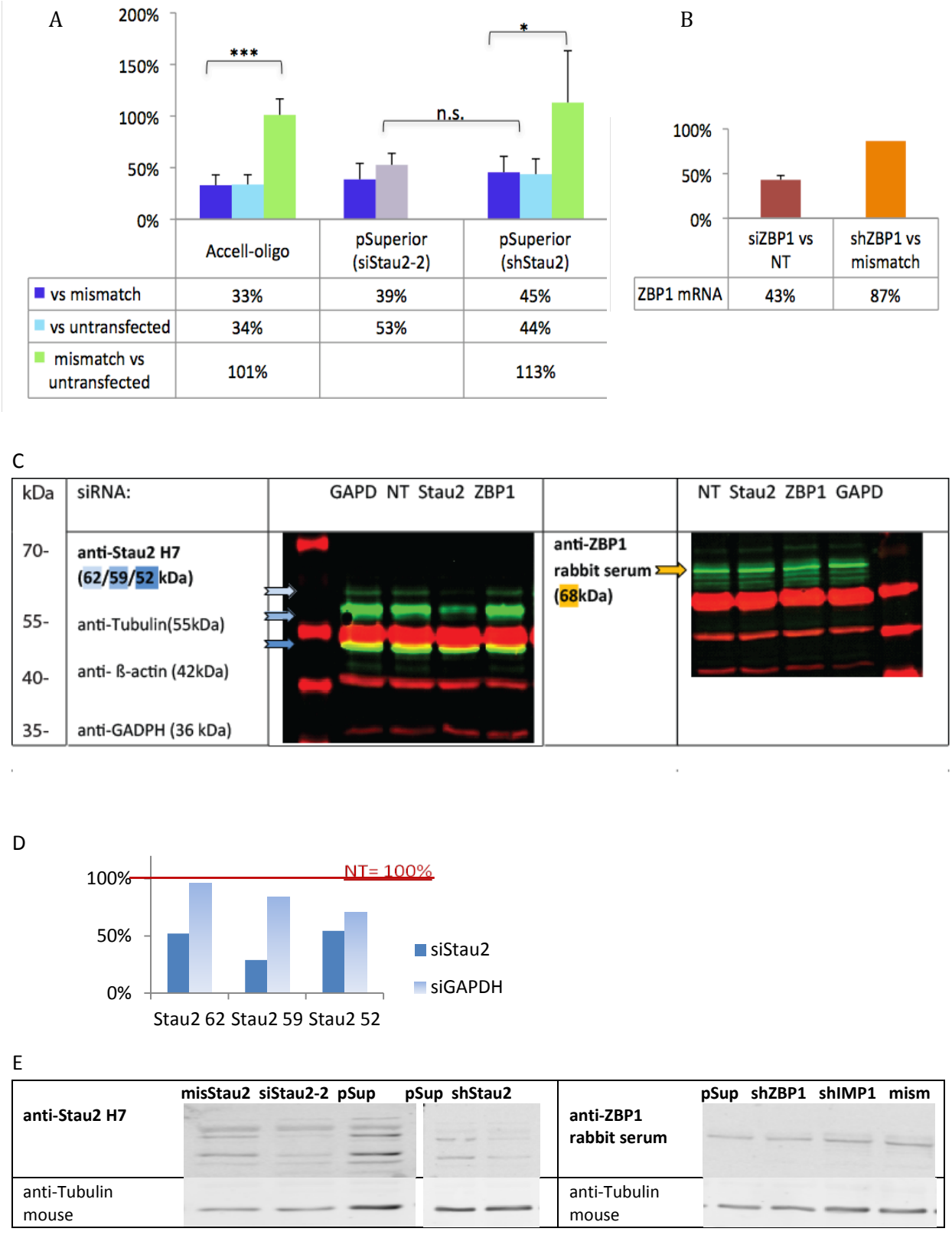

Figure 3.4 – Knockdown efficiency of short hairpin vectors (*Amaxa*® nucleofection) compared to *Accell*® siRNA

(**A**) Comparison of *Stau2* mRNA levels by qPCR. Neurons were transfected either with *Accell*® siRNA targeting Stau2 or with one of two different shStau2 *pSuperior* plasmids by *Amaxa*® nucleofection: siStau2-2 (middle), a plasmid that had been previously established in the lab, and a new *pSuperior* plasmid (right), with a matching target sequence to the *Accell*® siRNA. 7 individual experiments were performed with the siRNA (n=7), and 3 with each *pSuperior* plasmid (n=3); results are given in percentage of *Stau2* mRNA from transfected cells,

compared to either untransfected cells or to neurons transfected with control plasmids (containing a mismatch). Green bars depict RNA levels in mismatch-transfected compared to untransfected cells. Asterisks indicate significance by *student's t-test* [p >0.05- not significant; p <0.05- *; p<0.01- **;p<0,001- ***].
(**B**) *ZBP1* mRNA levels determined by qPCR. Neurons were transfected with shZBP1 pSuperior plasmids (n=1) containing the same target sequence as the respective *Accell®* oligo (n=2).
(**C-E**) Assessing downregulation of Stau2 and ZBP1 at the protein level by Western Blot. (**C**) *Accell* siRNA targeting Stau2 and ZBP1, as well as GAPDH, as a positive control for down-regulation: A representative Western blot is shown (anti-Stau2 rabbit H7 1:500, 3 bands of 62, 59 and 52 kDa; anti-ZBP1 rabbit serum 1:600, 68 kDa; anti-GAPDH mouse mAb 1:1500, 37kDa), Tubulin (mouse anti-Tubulin 1:5,000, 55kDa) was used as loading control. See quantification of the intensities of the 3 Stau2 bands (indicated by arrows) below (**D**). Intensities of cells transfected with siNon-targeting are set to 100%, and siStau2 transfected cells (blue bars) are compared to siGAPDH transfected cells (light blue). (**E**) Nucleofection with plasmids for the down-regulation of Stau2 (siStau2-2, Stau2 mismatch, empty pSuperior, and shStau2) or ZBP1 (the *pSuperior* based construct shZBP1, and the psiSTRIKE vectors shIMP1 and shIMP1 mismatch).

3.3 Consequences of decreased amounts of cellular Staufen2 on β-actin

3.3.1 Effects of Staufen2 knockdown on β-actin mRNA

The next steps concerned the investigation of the influence of *trans*-acting factors on β-actin in young neurons. This actin isoform is enriched in dynamic structures like growth cones or filopodia, where cytoskeletal rearrangements take place Stau2 has been shown to affect both β-actin localization and the morphogenesis of dendritic spines in mature neurons (Goetze et al., 2006). During the development of young neurons, a role of Stau2 in the regulation of β-actin levels and axonal outgrowth has been suggested (Y. Xie, P. Macchi and M. Kiebler, unpublished results). Another protein involved in the transport of *β-actin* mRNA is ZBP1, which binds to a sequence known as "zipcode" in the *β-actin* 3'-UTR (Ross et al., 1997). As a result of the insufficient knockdown of ZBP1, however, I decided to concentrate on unraveling the role of Stau2 in this process by downregulating Stau2 in primary neurons.
First, *β-actin* mRNA levels were analyzed by qPCR. Initially, the chosen reference genes caused problems, since the housekeeping genes GAPDH and Tubulin, which are supposed to remain constant throughout treatments, were also affected by Stau2 knockdown. Thus, a set of several typical reference genes was used from there on for internal cross-normalization (Weidensdorfer et al., 2009) to balance out the deviations of individual genes, including cyclophilin A, vinculin, 18S ribosomal RNA, γ-actin and septin7. New real-time primers for these reference genes were designed by A. Konecna or by adapting sequences from S. Hüttelmaier (pers. communication), and all were confirmed by standard curve assays. Only primers working in a linear range and with efficiency close to 100% were used. Amongst the aforementioned reference genes, however, 18S rRNA was least suitable. The ribosomal RNA is extremely abundant. Therefore, cDNA samples always had to be diluted more than samples used with other real-time PCR primers, usually 1:100 instead of 1:10. Septin7, on the other hand, which was suggested to be especially unaffected by Stau2 (M. Mikl, diploma thesis), is present at very low cellular levels and thus was also not an ideal reference for the highly abundant β-actin.

For Stau2 knockdown, hippocampal or cortical neuron cultures were treated with *Accell®* siRNA at 3 DIV and analyzed after 72 hours of incubation in several individual experiments.

Fig. 3.5a shows a quantification of *β-actin* mRNA from these cultures in relation to siNT treated (blue bar) or untransfected neurons (green bar). In both cases, the β-actin level appeared to be unaffected by a reduction of Stau2, which was also confirmed during each qPCR experiment. The transfection with *pSuperior* plasmids yielded quite different results (see **Fig. 3.5b**), with clear reductions of *β-actin* mRNA quantities compared to cells transfected with the corresponding mismatch plasmid or empty *pSuperior* (set to 100%, indicated by the red line). During one experiment (data not shown), where transfection had apparently been insufficient and *Stau2* mRNA was still present at 76% of the control, practically no reduction of *β-actin* mRNA was observed (96% of the control), thereby representing another indication for a direct relationship between *Stau2* and *β-actin* levels.
A slightly stronger effect than with shStau2 was observed with the plasmid siStau2-2, which reduced the *β-actin* mRNA level by almost 40%. However, as the plasmid shStau2, which shares its target sequence with the *Accell®* oligo siStau2, also leads to a *β-actin* downregulation, the disparity in effect does not seem to be strictly sequence specific. In the case of nucleofection with plasmids, neurons were treated before plating and analyzed after 4 DIV. To examine whether Stau2 downregulation at an earlier stage would cause *β-actin* changes, experiments with *Accell®* siRNA were also performed at 0 DIV and analyzed after 4 days, while otherwise the oligonucleotides had not been added before cell adherence. Of two individual experiments, one had to be excluded due to very atypical qPCR results, the other one is shown in **Fig. 3.5a** on the right. While the *Stau2* levels were reduced in the usual range upon siRNA treatment, a clear decrease of the *β-actin* mRNA level to approximately half of the level compared to untransfected cells could be observed. NT siRNA had no significant effect, as would be expected.

3.3.2 Evaluating β-actin protein levels after up- or downregulation of trans-acting factors

To validate the effect seen at the mRNA level, the cellular protein contents were analyzed using the Western Blot technique. Blots were stained with antibodies against β-actin and Tubulin as loading control (both are mouse monoclonal Antibodies from *Sigma*, their specificity had been previously tested in the lab). A representative blot from cortical neurons transfected at 3 DIV with *Accell®* siRNA targeting Stau2, ZBP1 and GAPDH, as well as with

non-targeting siRNA, is shown in **Fig. 3.6a**. Tubulin (55 kDa) and β-actin bands (42 kDa) are presented together with a prestained protein marker. The intensities of β-actin bands were measured and normalized to Tubulin intensities; the values below the bands represent the percentage of β-actin levels relative to the respective control, which is indicated by green numbers. Analogous to the mRNA quantities determined by qPCR, no obvious changes of β-actin on the protein level could be observed. The diagram on the right visualizes these results. As before, these experiments were repeated using the plasmids shStau2 and siStau2-2 for the downregulation of Stau2 and the empty vector as a control. Cortical neurons were analyzed 4 days after nucleofection; an example of the resulting Western blots is depicted in **Fig**. **3.6**. To test whether opposing effects of overexpression and downregulation of Stau2 on the expression of β-actin would be detectable, neurons were transfected simultaneously with an overexpression construct of Stau2 fused to EGFP, as well as with the empty pEGFP plasmid, and analyzed after 1 DIV. The successful overexpression is visualized by Stau2 antibody staining; pEGFP-Stau2 is detected at approximately 95kDa (see **Fig. 3.6b**, left). Yet, neither overexpression nor downregulation of Stau2 caused significant changes in the intensities of β-actin bands.

Additionally, a putative effect of ZBP1 was also examined by transfection with the plasmids shZBP1 and shIMP1. As a significant and reproducible decrease of ZBP1 protein levels in primary neurons using these constructs was not possible (**Fig. 3.6c**), it is not surprising that – in spite of certain variations – stable changes in β-actin intensities did not occur in relation to transfections with empty *pSuperior* or ZBP1 mismatch (see **Fig. 3.6c**). Overexpression of ZBP1, on the other hand, worked well, the 95kDa band of pEGFP-ZBP1 being clearly visible by staining with anti-ZBP1 antibodies, yet again without any significant effect on the β-actin staining. To ensure that the rabbit serum antibody against ZBP1 was definitely specific, it was compared to the mouse monoclonal antibody (gift from S. Hüttelmaier) on a test blot with 10µg brain lysate. Though the staining with the mouse antibody was very weak, at least the band it stained proved to be identical to the main band stained by the much stronger rabbit antibody (**Fig. 3.6c**, right side).

A

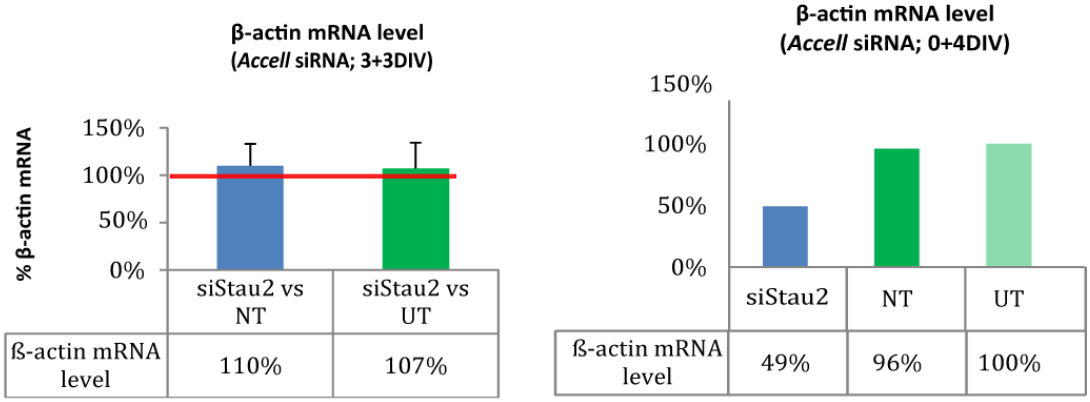

B

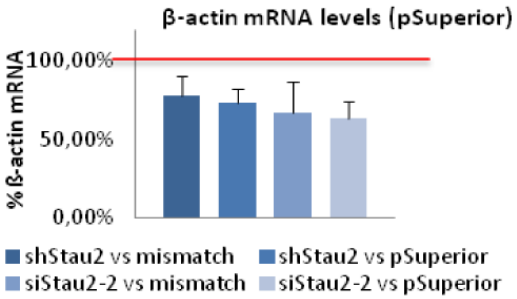

3.5 - Changes in *ß-actin* mRNA levels after Stau2 knockdown

(**A**) The amount of *ß-actin* mRNA after knockdown of Stau2 with *Accell* siRNA was measured by qPCR. Cultures of hippocampal or cortical neurons were usually transfected at day 3 and analyzed after 72 hours (left side; 6 individual experiments). Once the siRNA was added at day 0 and cells were analyzed after 4 days, which yielded differing result (right side). All results stand in relation to either cells transfected with non-targeting siRNA (NT) or to untransfected neurons (UT).

(**B**) Quantification of *ß-actin* mRNA by qPCR after downregulation of Stau2 with two different *pSuperior* constructs, siStau2-2 (pre-existing plasmid) and shStau2 (plasmid with a target sequence corresponding to the *Accell®* oligo siStau2). *ß-actin* levels of transfected cells are shown relative to those of cells transfected with either a mismatch sh-plasmid or empty *pSuperior* (which were thus set to 100%, indicated by the red line). Cortical neurons were transfected before plating and used for assays after 4 days (2 experiments).

A

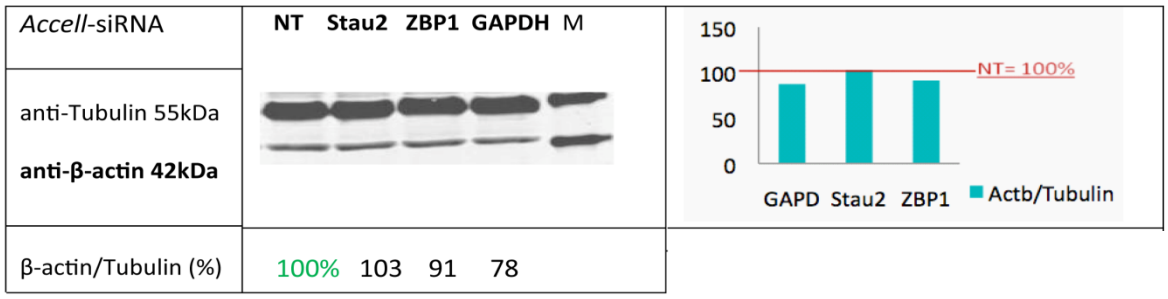

B

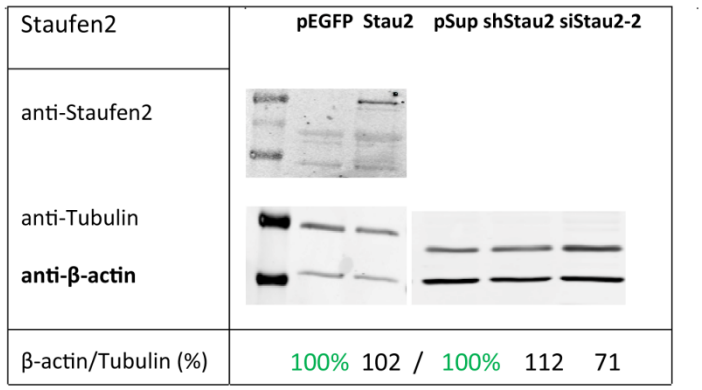

C

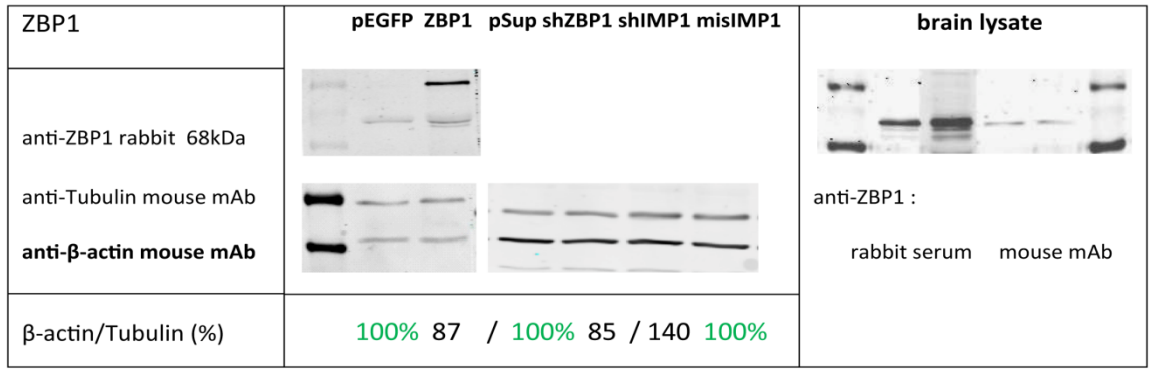

3.6 - Changes in *β-actin* protein levels after Stau2 knockdown

(**A-C**) Western Blots to determine changes in β-actin protein levels. Blots were stained with β-actin antibodies (mouse, 1:2,500; 42 kDa band) and Tubulin antibodies (mouse, 1:5,000; 55 kDa band). The intensities of bands were quantified using the Odyssey® Application Software. Intensities of β-actin bands were normalized to Tubulin; the numbers are given below every band, in percentage of the respective control (the controls are therefore set to 100%, green numbers). (**A**) A representative blot from cortical neurons transfected with *Accell* siRNA (3+3 DIV) targeting Stau2 and ZBP1. A graph (right side) represents the intensities of β-actin bands normalized to Tubulin and compared to the siNT transfected cells. siGAPDH and siNon-targeting were used as controls. (**B**) Cortical neurons were nucleofected with pEGFP-Stau2 and analyzed after 1DIV or alternatively, with one of two *pSuperior* plasmids to knockdown Stau2 (shStau2 and siStau2-2) and analyzed after 4 days. Transfection with the respective empty vectors served as a control. Stau2 antibodies (rabbit H4, 1:500) visualize overexpression of Stau2 (pEGFP-Stau2 band at 95kDa). (**C**) A blot from cortical neurons transfected with pEGFP-ZBP1 and lysed after 1 DIV, the expression of the construct was confirmed by antibodies against ZBP1 (rabbit, 1:600; pEGFP-ZBP1 band at 95kDa). Another blot shows transfection with ZBP1 knockdown plasmids (shZBP1, a *pSuperior* vector, and shIMP1, a *psiSTRIKE* vector), and with empty *pSuperior* or a mismatch vector (of shIMP1). On the right: a test blot with 10 µg brain lysate for two different ZBP1-antibodies (anti-ZBP1 rabbit serum, 1:600 and anti-ZBP1 mouse mAb, 1:250).

3.3.3 Analysis of the effects of Staufen2 downregulation on the actin cytoskeleton

To test whether an overall effect on the actin cytoskeleton would occur after the downregulation of Stau2 (which was suggested by previous work in the Kiebler lab), transfected cells were fixed and stained with phalloidin coupled to *Alexa* fluorophore (*Invitrogen*). Phalloidin is a toxin, derived from the death cap *Amanita phalloides*, which binds specifically to filamentous actin (Löw & Wieland, 1974) and, by stabilizing the junctions between actin subunits, inhibits the depolymerization of F-actin (Barden et al., 1987).

Therefore, coverslips with hippocampal neurons (3 DIV) were either treated with *Accell®* siRNA or transfected by Calcium-Phosphate precipitation (Goetze et al., 2004) Usually after 3 days, neurons were fixed using PFA and incubated with phalloidin or with antibodies against Stau2 or ZBP1 to check for successful down-regulation in treated cells. Additionally, nuclear staining with DAPI was performed, and phase contrast pictures were taken to monitor the state of the cells. A reduction of signal detected by Stau2 antibodies in siStau2-treated neurons is demonstrated in **Fig**. **3.7a**. There was no significant difference in the amount of Stau2 between untreated and control cells. Yet, the knockdown of Stau2 did not have any obvious effects on the actin staining, neither in cell bodies nor growth cones. The latter ones, however, were not examined individually, while the average intensities from the cell bodies of a few randomly chosen neurons were measured using the *Metamorph* software. A comparison of the intensities of phalloidin staining from neurons treated with siRNA targeting Stau2, ZBP1 or both (in which case equal amounts of each siRNA were used as in single transfections), relative to the control revealed no significant differences of F-actin levels. Subtle cytoskeletal changes might still have occurred, but their detection would take further intensive investigation and the assessment of larger cell numbers or local structures, such as protrusions or growth cones.

Correspondingly, these experiments were also performed in cells transfected at 0 DIV, yet the resulting cells looked too damaged for any further evaluation. Mature neurons (up to 18 DIV) were also transfected. Phalloidin levels in older neurons were similar in treated and untreated cells, yet the assessment of individual cells was complicated by an increased presence of glia cells, which contain large amounts of actin and are therefore stained very brightly by phalloidin (for an example, see **Fig. 3.7c**). Staining hippocampal neurons

transfected with the plasmids siStau2-2 or mismatchStau2 showed that GFP expressing cells (marked by arrows) contained in some cases lower actin levels (**Fig. 3.7e**, middle images), while very often no significant changes were seen (top images) relative to the control. As these nucleofected cells did not appear to be in ideal condition, any observed changes might not necessarily be physiological.

Since the knockdown of ZBP1 did not work well using siRNA or *pSuperior*, it is not surprising that actin levels were unaffected. Transfections with shIMP1, the aforementioned *psiSTRIKE*-plasmid targeting ZBP1, were also tested. Although immunostaining with ZBP1 antibodies (mouse anti-ZBP1) was reduced in most transfected cells, they appeared also to be more damaged then their untransfected neighbors, thus successful knockdown with this plasmid in primary neurons could not yet be proved (data not shown).

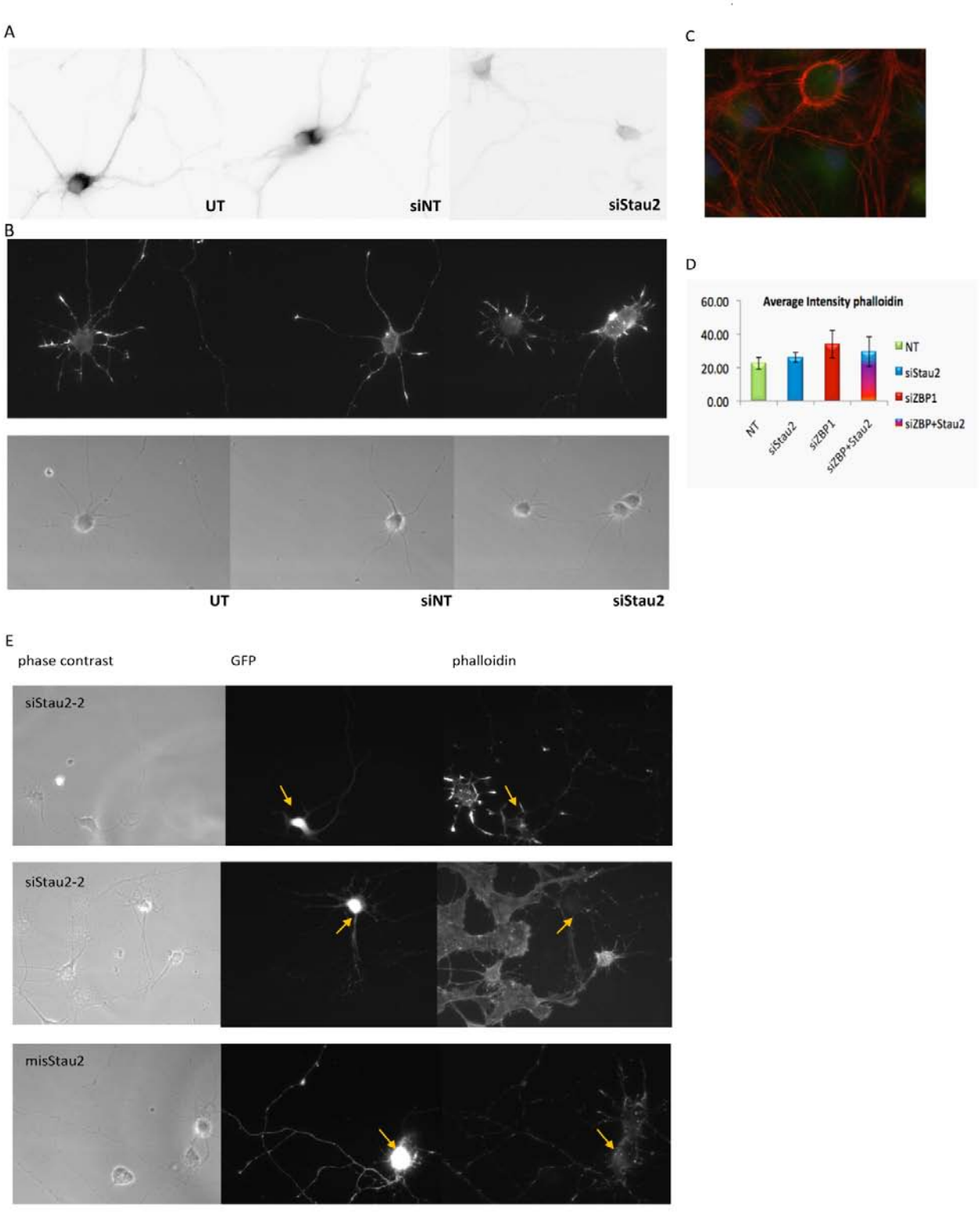

3.7 – The actin cytoskeleton after Stau2 downregulation

3-day-old hippocampal rat neurons were treated with siRNA or transfected with plasmids by Calcium-Phosphate precipitation. After 3 to 4 days, cells were fixed with PFA and stained with the respective antibodies or chemicals. (**A**) Cells that were either untreated (UT), treated with Non-targeting siRNA (siNT) or with siStau2 were incubated with rabbit anti-Stau2 (1:300, for 2 hours at RT) followed by secondary antibodies (donkey anti-rabbit Cy3, 1:2,000). Fluorescent images are depicted in reversed colors. (**B**) Fluorescent and phase contrast images of siRNA- treated or untreated hippocampal neurons (6DIV) after staining with phalloidin (1:500). (**C**) Example of phalloidin staining (red) of glial cells, combined with Stau2 immunostaining (green) and DAPI (blue).

(**D**) Diagram representing mean average intensities (arbitrary units) of phalloidin, measured (using *Metamorph*) from 10 random cell bodies after treatment with siStau2, siZBP1 or both, or with siNT. (**E**) Hippocampal neurons (7DIV) transfected with siStau2-2 (top and middle) or mismatchStau2 (bottom). Transfected cells expressing GFP are indicated by orange arrows. Images on the right show the phalloidin staining of these cells.

3.4 The influence of Staufen2 on the stability of β-actin mRNA

As, at least in some cases, a certain decrease of *β-actin* mRNA could be seen after downregulation of Stau2. Therefore, the question arose, whether this effect would be caused by a stabilizing influence of Stau2 on the *β*-actin message. To assess the stability of mRNA, RNA decay assays were performed – a schematic overview on this assay's principle is given in **Fig**. **3.8a**. In this example, Accell oligonucleotides were added at 3 DIV and neurons were analyzed 3 days later. When overexpression contructs were used, the assay was essentially done in the same way, except that cells were transfected at 0 DIV and analyzed 24 hours later. The procedure was based on the inhibition of RNA synthesis by adding 5µM of Actinomycin D (95%, dissolved in DMSO, Sigma-Aldrich). This toxic compound is an antibiotic derived from *Streptomyces* species, which blocks DNA-primed RNA synthesis by forming stable complexes with double-stranded DNA. At the same time as Actinomycin D was added (time point 0), total RNA was isolated using *Trizol*®, and again after 3 hours and 6 hours. Successively, the *β*-actin mRNA content of these 3 samples was quantified by qPCR. Thus, the degree of mRNA degradation during 6 hours can be monitored and differences between treated and untreated or control samples can be compared.

In any experiment where RNA is quantified, the intactness of the isolated RNA is critical, and an RNase-free handling of samples has to be ensured. As a confirmation of the quality of RNA samples used for cDNA synthesis and ultimately real-time PCR, a set of 13 randomly chosen RNA samples, which were used for these experiments, was tested by RNA gel electrophoresis. After running 1 µg of each sample on a 1.5% agarose gel and staining with SYBR® gold, two bands became clearly visible (**Fig. 3.8b**). A DNA marker (M) was used as an indicator and RNA extracted from brain lysate (lane 14) was used as a positive control. The presence of distinct 28S and 18S rRNA bands at a ratio of approximately a 2:1, as well as the absence of smear proved that none of the tested samples showed signs of degradation.

Fig. 3.9a shows the decay curve of *β-actin* mRNA after Stau2 knockdown by siRNA in cortical neurons. All *β*-actin amounts were quantified in relation to a set of several reference genes,

and the relative *β*-actin mRNA quantity at the beginning of the decay curve was set to 100%. Values from samples treated with siStau2 were compared to those from cells treated with non-targeting siRNA and showed a significant decrease after 6 hours, of almost 40% ($p < 0.05$ by student's t-test, indicated by an asterisk). A slight effect in the opposite direction was observed when neurons had been transfected with pEGFP-Stau2 (**Fig. 3.9b**). Neurons overexpressing Stau2 showed a moderate 1.24-fold increase of *β*-actin mRNA after inhibiting transcription for 6 hours compared to cells transfected with pEGFP, and a 1.78-fold increase compared to untransfected neurons ($p < 0.05$). Thus, it seems that pEGFP alone causes minor alterations, which does, however, not exclude a small effect of the overexpression of Stau2 itself on β-actin stability.

The importance of using several different reference genes for the quantification by qPCR using theΔΔCt -method has been mentioned before and weighs even more as soon as varying decay kinetics of reference genes come into play. The graph in **Fig. 3.9c** shows an example of the variations of *β-actin* mRNA levels relative to each of four selected reference genes - Tubulin, Vinculin, GAPDH and Peptidylprolyl Isomerase A (Cyclophilin A) - in untransfected cortical neurons at 1 DIV. Only when the quantities of several genes are averaged (black line) during cross-normalization can the differences between the decay of β-actin and of the reference genes be considered insignificant.

A

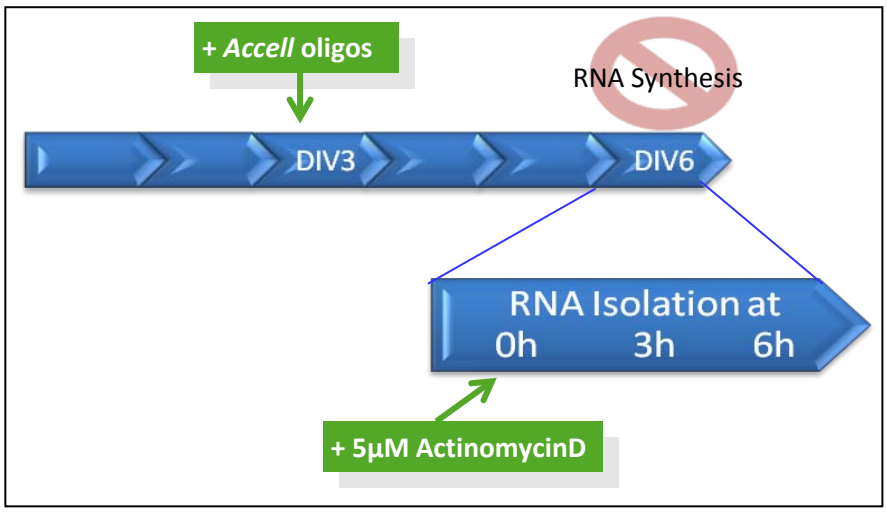

B

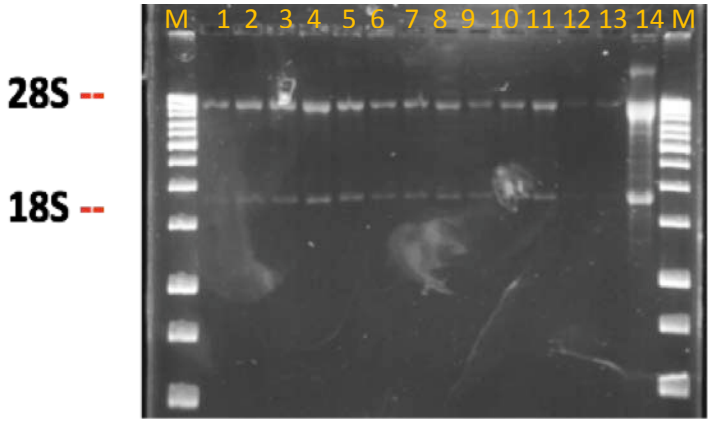

3.8 – RNA decay assay

(**A**) Schematic depiction of the RNA decay assay method. 3 days after transfection, the RNA synthesis was inhibited by addition of Actinomycin D, and then total RNA was isolated at time points 0, 3 and 6 hours. RNA levels were then determined by qPCR.

(**B**) Verifying the quality of several random RNA samples from various experiments by RNA gel electrophoresis (on a 1.5% agarose gel, stained with SYBR® gold). Intact RNA was defined by two prominent bands, the *28S* rRNA and the *18S* rRNA, while degraded RNA would show as a smear. M= 1Kb DNA ladder; lanes 1-13= various RNA samples; lane 14= RNA extract from brain lysate (positive control)

A

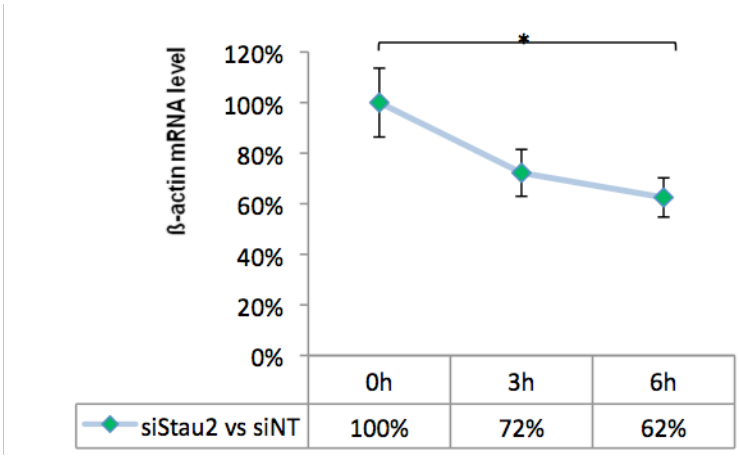

B

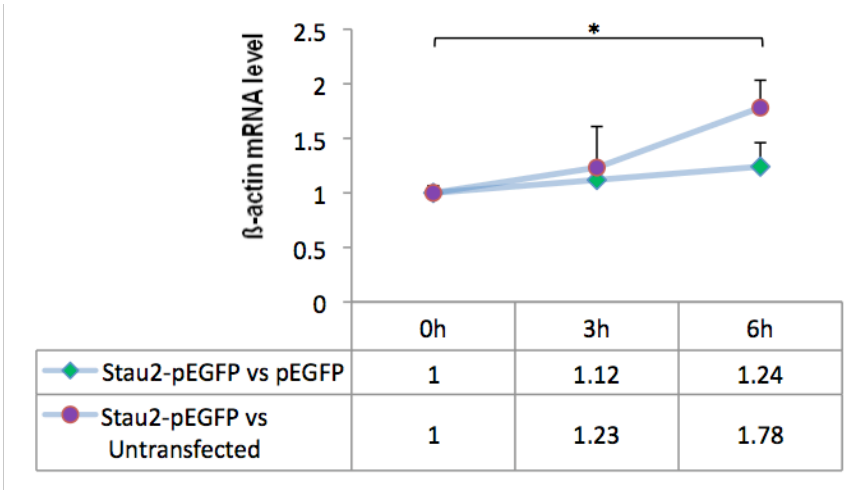

C

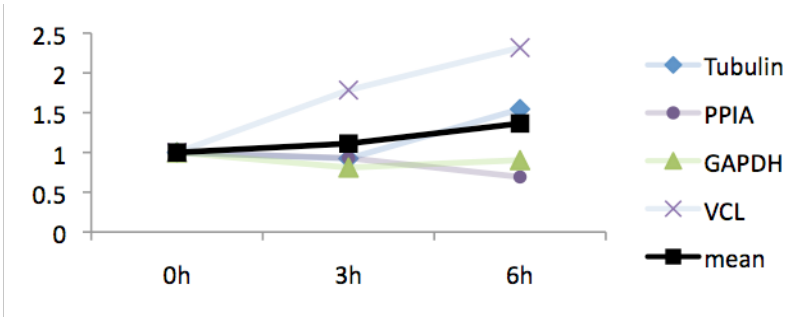

3. 9 - Decay kinetics of *ß-actin* mRNA

Graphs show *ß-actin* mRNA levels from samples collected at different time points after RNA synthesis inhibition were analyzed using qPCR. The relative amount of *ß-actin* at the start of the decay experiment (t=0h) was arbitrarily set to 100%. Error bars indicate the standard deviation of 3 individual experiments. Assays were performed after (**A**) Stau2 knockdown by siRNA in cortical neurons (3+3 DIV), using Non-targeting siRNA as control or (**B**) Stau2 overexpression by transfection of cortical neurons with Stau2-pEGFP (0+1 DIV), using empty pEGFP as control. In the latter case, *ß-actin* levels of transfected cells were set into relation with those of untransfected cells (purple dots) and of cells transfected with pEGFP alone (green dots). (**C**) Graph showing the differing decay kinetics of four selected reference genes used for quantification by qPCR, namely Tubulin, GAPDH, Vinculin (VCL) and Peptidylprolyl isomerase A (cyclophilin A) – as well as their average (black line). All relative *ß-actin* levels were set to 1 at t=0. The RNA from 1 day-old untransfected cortical neurons was used.

3.5 A comparison of Staufen2 and ZBP1 as regulators of translation

While mRNA stability seemed to be affected by Stau2, it had yet remained unresolved whether Stau2 could also act as a translational regulator. ZBP1 on the other hand had already been shown to be involved in translation repression by binding to the "zipcode" in the *β-actin* 3'-UTR (Hüttelmaier et al., 2005). As testing the total protein content by Western Blot did not lead to significant results, we looked for a more sensitive method to detect possible changes of translation activity and started with luciferase assays (these assays were performed in cooperation with L. Schoderböck in the lab). Therefore, 3 different parts of the human β-actin sequence had previously been cloned by L. Schoderböck into psiCHECK™-2 (*Promega*), a plasmid carrying genes for both renilla and firefly luciferase. These sequences included either the coding region and the zipcode (1388 bp) or the full length 3'-UTR (607 bp), or the zipcode by itself (268 bp), and were cloned into the multiple cloning site between the renilla luciferase gene and a synthetic polyA stretch (**Fig. 3.10a**). The *Dual-Luciferase® Reporter System* (Promega) was used to measure the activities of both firefly and renilla luciferase from the same sample by successive addition of their respective substrates (Beetle Luciferin and Coelenterazine). As one plasmid carried both enzyme genes, the activities of the renilla enzyme, the transcripts of which contained the sequences of interest, could be easily normalized to the firefly activities, excluding different transfection efficiencies. Cells were cotransfected with either *pSuperior* or siRNA for downregulation or with pEGFP plasmids for overexpression (for a schematic drawing see **Fig. 3.10b**). In accordance with the results of titration experiments (performed in parallel by L. Schoderböck), a 1:4- ratio of reporter and effector plasmids was further used.

First, assays were performed in HeLa cells, transfected with each of the 3 reporter constructs together with either pEGFP-Stau2 (the long isoform of 62 kDa) or pEGFP-ZBP1 using *FuGENE*™ reagent (Roche) for lipofection. As a control, cells were also transfected with empty psiCHECK™-2 or pEGFP vectors. After normalization to empty psiCHECK™-2, only a slight decrease in activity of the reporter with *β-actin* 3'-UTR or zipcode remained when Stau2 or ZBP1 was overexpressed, compared to cells transfected with pEGFP alone (see **Fig. 3.11a**). When these experiments were repeated with primary neurons, however, the outcome was noticeably different. Thus, we decided not to continue using HeLa cells for our experiments.

Cortical and hippocampal neurons were nucleofected at 0 DIV with one reporter and one overexpression (or control) plasmid each and lysed after 24 hours. The measured luminescence from the reaction catalyzed by renilla luciferase was normalized to the luminescence from firefly luciferase, and then all results were normalized to the activities from cells transfected with empty psiCHECK™-2 and cells transfected with pEGFP. As shown in Fig. **3.11b**, there were no significant differences between cortical (green bars) and hippocampal neurons (blue bars). Surprisingly, only the reporter containing the β-actin coding sequence and zipcode was regulated differentially by the overexpression of ZBP1 and Stau2 to a significant extent ($p < 0.05$). Compared to pEGFP alone, pEGFP-Stau2 expression caused a 2-fold increase in luciferase activity, with a slightly bigger increase in hippocampal neurons. pEGFP-ZBP1 overexpression led to a similar effect. The expression of the renilla luciferase genes with a *β-actin* 3'-UTR or zipcode was not significantly affected by Stau2 or ZBP1, although there might be a trend towards a minor repressive effect.

Luciferase assays were also performed after knockdown of Stau2 with *Accell®* siRNA or with the *pSuperior* plasmid siStau2-2. Cortical neurons were transfected at 0 DIV and lysed after 4 days. In relation to siNT treated neurons, siStau2-treated cells seem to lead to a minor repression of the expression of reporters with the *β-actin* 3'-UTR (**Fig. 3.11c**, blue bar). Treatment with siZBP1 should not show any effect, as it did not lead to sufficient down-regulation of ZBP1 protein. Interestingly, there was a small effect in the opposite direction for Stau2 (red bar). Although these results would principally be in agreement with my expectations, both effects are probably negligible. Contrary to the results obtained with siRNA, identical experiments using the plasmid siStau2-2 (and Stau2 mismatch as a control) led to somewhat elevated activities of luciferase with the *β-actin* 3'-UTR (**Fig. 3.11c**, right diagram). For one experiment, the reporter containing the coding sequence was also used. Stau2 downregulation caused reduced activities of this reporter, which would correspond to Stau2 overexpression leading to increased activities. Certainly, these experiments need to be repeated to obtain robust and reliable results. However, by plating triplicates of every sample relatively large amounts of cells were needed. Considering that not every cell culture or transfection was usable, achieving a high enough number of independent experiments was not within the reach of this diploma thesis.

As we could not exclude that small differences between human and rat β-actin sequences would possibly influence the results of experiments performed in rat neurons, identical

psiCHECK™-2 constructs were cloned with sequences from *rattus norvegicus*, yet preliminary tests did not hint at any species-specific divergence (L. Schoderböck, personal communication).

A

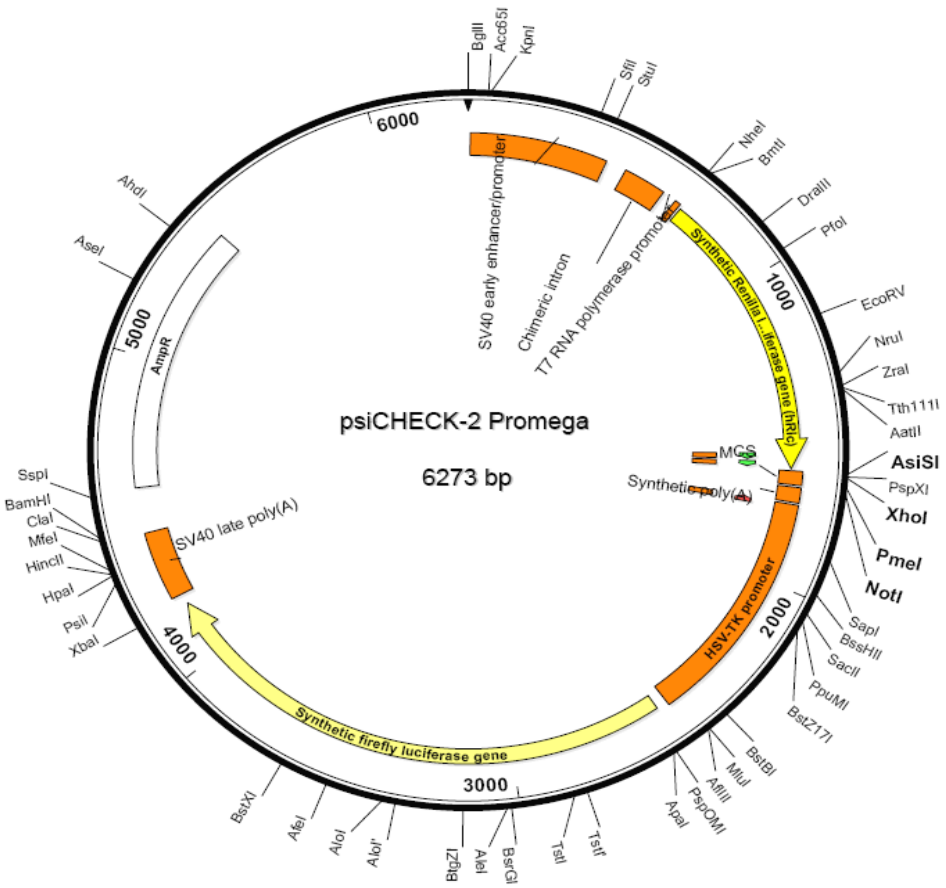

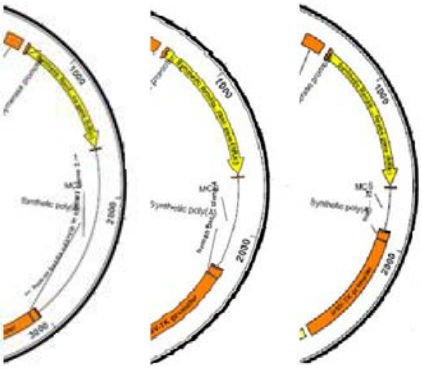

	vector size
psiCHECK-2 human β-actin coding region +zipcode	(7630 bp)
psiCHECK-2 human β-actin 3‘-UTR	(6849 bp)
psiCHECK-2 human β-actin zipcode	(6510 bp)

B

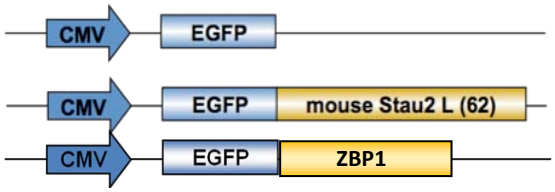

3.10 - **Luciferase assay**

(**A**) Plasmid map of PsiCHECK™-2 (Promega) which carries genes for both renilla and firefly luciferase. 3 stretches of various lengths of the human β-actin sequence (ranging from 273bp to 1357bp) were cloned into the MCS at the end of the renilla gene: the zipcode, the whole 3’-UTR, and the zipcode with the coding region (designed by L. Schoderböck)

(**B**) Schematic drawing of the pEGFP-vector and the pEGFP-Stau2 and pEGFP-ZBP1 overexpression constructs.

A

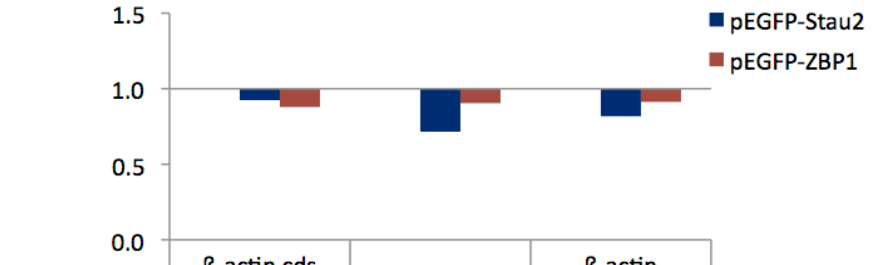

	ß-actin cds +zipcode	ß-actin 3'UTR	ß-actin zipcode
pEGFP	1.00	1.00	1.00
pEGFP-Stau2	0.92	0.72	0.82
pEGFP-ZBP1	0.88	0.90	0.91

B

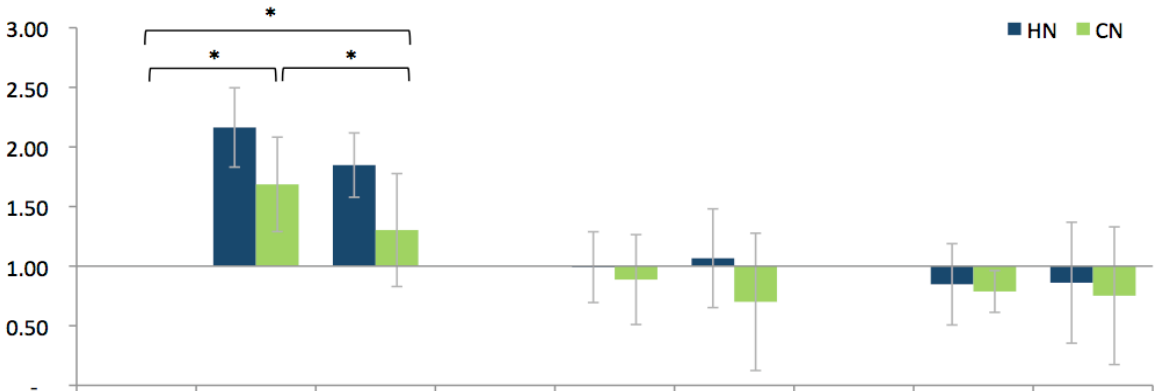

	β-act cds +zipcode +EGFP	β-act cds +zipcode + EGFP-Stau2	β-act cds +zipcode + EGFP-ZBP1	β-act 3'UTR + EGFP	β-act 3'UTR + EGFP-Stau2	β-act 3'UTR + EGFP-ZBP1	β-act zipcode + EGFP	β-act zipcode + EGFP-Stau2	β-act zipcode + EGFP-ZBP1
HN	1.00	2.16	1.85	1.00	0.99	1.07	1.00	0.85	0.86
CN	1.00	1.69	1.30	1.00	0.89	0.70	1.00	0.79	0.75

C

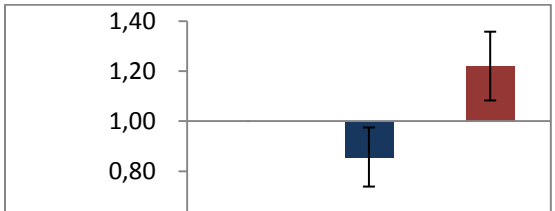

	β-actin 3'UTR + siNT	β-actin 3'UTR + siStau2	β-actin 3'UTR + siZBP1
to psiCheck2 +NT	1,00	0,86	1,22

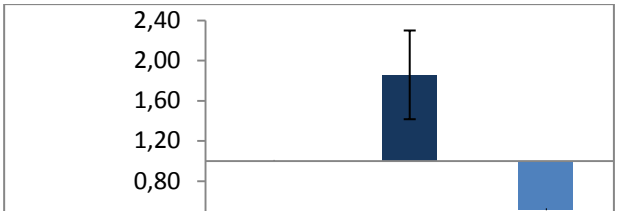

	β-actin 3'UTR+ misStau2	β-actin 3'UTR+ siStau2-2	β-actin cds+zip + siStau2-2
to psiCheck2 + mismatch	1,00	1,86	0,52

3.11 - Regulatory activity of Staufen2 on luciferase reporters containing different β-actin sequence fragments

(**A**) Luciferase assays in HeLa cells, 1 day after lipofection with pEGFP, pEGFP-Stau2 (blue bars) or pEGFP-ZBP1 (red bars). All luciferase activities were normalized to those of cells transfected with empty psiCHECK2-vector, and to cells transfected with pEGFP.

(**B**) Luciferase assays in cortical (green bars) and hippocampal neurons (blue bars) after overexpression of Stau2 or ZBP1 (0+1 DIV; 3 individual experiments with hippocampal and 3 with cortical neurons). Luciferase activities were normalized as before. Error bars indicate standard deviation, asterisks indicate significance (* $p < 0.05$) according to student's t-test.
(**C**) Luciferase assays in cortical neurons after 4 DIV of knockdown with siRNA targeting Stau2 and ZBP1. Only psiCHECK2 vectors with the β-actin 3'-UTR were used for transfections, 2 experiments were performed. Luciferase activities were normalized to transfections with psiCHECK2 and Non-targeting siRNA (left table). After downregulation of Stau2 with the *pSuperior* plasmid siStau2-2 (2 experiments with the β-actin 3'-UTR construct, 1 with the β-actin coding region+zicode construct), results were normalized to the activities of Stau2 mismatch (right table).

3.6 Lim kinase1, another candidate for the regulation by Staufen2?

To examine how a different mRNA than *β-actin* would behave during the same experiments, another available psiCHECK™-2 construct (cloned by L. Schoderböck) was included in some luciferase assays, containing the 3'-UTR of Lim kinase 1 (LimK1). It codes for a serine/threonine kinase that is involved in brain development (Goda et al., 2002) phosphorylating actin binding proteins thereby inducing cytoskeletal reorganization (Yang et al, 1998). It is regulated by different signaling pathways and was also identified as a target of the brain-specific microRNA miR-134, which binds in the 3'-untranslated region of *LimK1* (Schratt et al, 2006). Stau2 knockdown using siStau2-2 had an effect on the LimK1 reporter similar to its effect on the β-actin reporter – the luciferase activity was again upregulated, which could mean that this effect was not necessarily specific (**Fig. 3.12a**). An experiment using siRNA targeting Stau2 showed only very small change of activity when compared to non-targeting siRNA treated or samples without any effector (named "untransfected" in Fig. 3.12a). Regarding β-actin, the effect caused by knockdown with siRNA had also been smaller; but in the case of LimK1, the trend of the effect was the same as when using the plasmid. As seen in **Fig. 3.12b**, overexpression of Stau2 had the opposite effect, namely a reduction of reporter activity, which was, however, too small to be significant. Overexpression of ZBP1 led to an equally small increase of activity.

A quantification of *LimK1* mRNA levels by qPCR in parallel with *β-actin* supported the luciferase assay results. Although changes were not big, ranging from a 55% increase of *LimK1* mRNA quantities in siStau2-treated neurons to a 30% decrease in neurons expressing Stau2-pEGFP, the reaction of *LimK1* mRNA was significantly different between Stau2 up- and

downregulation. Since the behavior of *LimK1* was not identical with that of β-actin, this indicated that the results presented so far were not due to unspecific effects. While this preliminary outcome does not allow for safe conclusions regarding a regulatory influence of Stau2 on *LimK1* expression, I nevertheless regard it as an interesting potential candidate for future investigations.

A

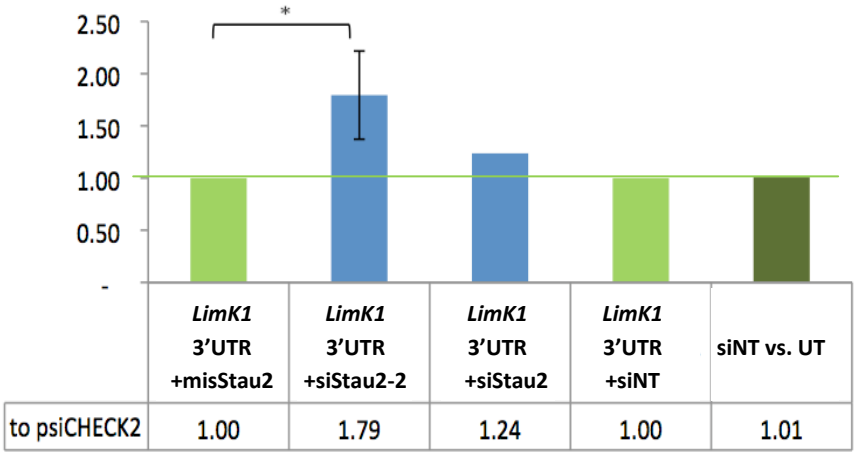

	LimK1 3'UTR +misStau2	*LimK1* 3'UTR +siStau2-2	*LimK1* 3'UTR +siStau2	*LimK1* 3'UTR +siNT	siNT vs. UT
to psiCHECK2	1.00	1.79	1.24	1.00	1.01

B

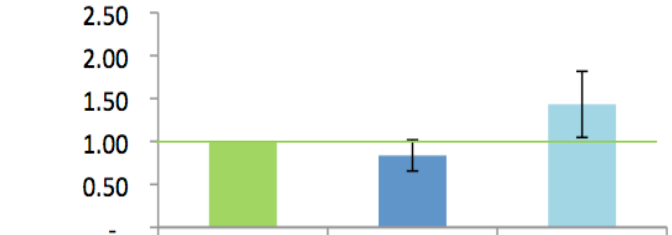

	LimK1 3'UTR	*LimK1* 3'UTR +pEGFP-Stau2	*LimK1* 3'UTR +pEGFP-ZBP1
to psiCHECK2	1.00	0.84	1.43

C

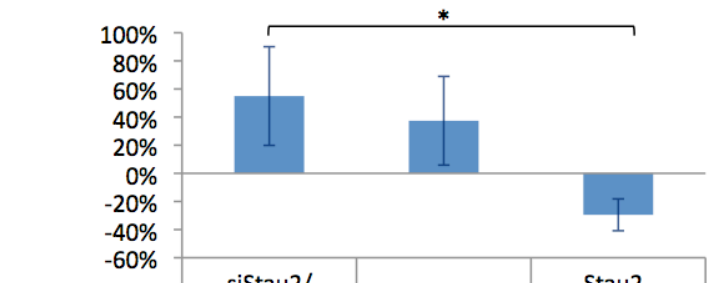

	siStau2/ Non-targeting	shStau2/ mismatch	Stau2-pEGFP/ pEGFP
LimK1 mRNA	55%	37%	-30%

3.12 – Influence of Stau2 on *LimK1* expression

(**A**) Expression of psiCHECK2 luciferase reporters with the *LimK1* 3'-UTR after Stau2 knockdown with the *pSuperior* plasmid siStau2-2 (2 experiments) or with the *Accell®* oligo siStau2 (1 experiment) for 4 days (blue bars). Luciferase activities were normalized to psiCHECK2, as well as to either the Stau2 mismatch plasmid or to Non-targeting siRNA (green bars). The activity of cells transfected with Non-targeting siRNA compared to untransfected cells is shown by the dark green bar.
(**B**) Luciferase reporters with *LimK1* 3'-UTR after Stau2 overexpression for 1 day (2 experiments). Activities are normalized to psiCHECK2 and pEGFP. (**C**) Quantification of *LimK1* mRNA levels by qPCR after Stau2 knockdown with siRNA (3+3 DIV) or the plasmid siStau2-2 (0+4 DIV) and after Stau2 overexpression (2 individual experiments for each condition).

IV Discussion

4.1 Establishing knockdown of Staufen2 and ZBP1 by siRNAs

The aim of this project was to investigate the actions of RNA-binding proteins, such as Stau2 or ZBP1, on localized mRNA in neurons. Therefore, the first step was to establish successful knockdown of these proteins in primary hippocampal neurons. In particular the downregulation of ZBP1 was problematic, which works well in several cell lines (Hüttelmaier et al., 2005), but did not yet work in primary neurons. Cell lines, however, may not reflect the best model for the physiologic state of a neuron. Although primary dissociated cultures are not perfect either - for example naturally neurons are surrounded by a different micro-environment within their tissue and exposed to growth factors, different oxygen levels, etc. - it can be assumed that they mimic real conditions closer than cell lines.

To achieve downregulation, the method of RNA interference was used, where target mRNAs are recognized by siRNA, consisting of symmetrical duplexes of 19-21 bps with 3‘-overhangs. This method can induce efficient and durable gene silencing through post-transcriptional mRNA cleavage, although it may also cause side effects, such as the overloading of microRNA processing machinery or the activation of protein kinase R (Sledz et al., 2003). Off-target effects can be caused by the incorporation of the sense strand into RISC, which sometimes leads to unspecific alterations of gene expression (Jackson et al., 2003). Additionally, the transfection procedure itself can be stressful for cultured neurons. Thus, a specially modified siRNA provided by *Accell®* was tested, which can enter the cell without any additional transfection procedure (**Fig. 3.1**). Viability and transfection efficiencies were higher than with conventional siRNA delivery approaches and treatment with siRNA targeting GAPDH led to a strong knockdown of *GAPDH* mRNA levels, as assessed by quantitative real-time PCR, in comparison to untreated cells. To exclude unspecific changes caused by the siRNA reagent, non-targeting (NT) siRNA was used as a negative control for further experiments, which did not cause significant changes in mRNA levels (**Fig. 3.2**). Thus, after modifications of the protocol provided from the company, *Accell®* siRNAs presented a suitable method for the downregulation of expression in hippocampal neurons. As the efficiency of knockdown by siRNA is also dependent on the specific sequence of the oligonucleotide, four different siRNAs targeting either Stau2 or ZBP1 were tested. *Stau2* and

ZBP1 mRNA levels after transfection were determined by qPCR and only the siRNAs leading to the strongest knockdown were chosen for the following experiments. In particular, the effects of the four different oligonucleotides targeting ZBP1 varied considerably (**Fig. 3.3**).

As a significant reduction of not only mRNA, but also protein levels would be essential for further experiments, the effects of siRNA on Stau2 and ZBP1 protein levels were tested performing Western blot experiments with protein extracted from siRNA treated and untreated neurons at 3+4 DIV. Stau2 oligonucleotides successfully reduced Stau2 protein levels down to 29% when compared to controls, either NT oligonucleotides or siRNA targeting GAPDH. Interestingly, the different isoforms of Stau2 were observed to be affected to a varying extent, with the 59 kDa isoform being most severely reduced and the smallest isoform (52 kDa) only being knocked down to 55% of the control (**Fig. 3.4d**).

Unfortunately, the knockdown of ZBP1 protein was less promising, as there was no significant reduction seen after treatment with either siRNA or different sh-plasmids. Even the reduction of *ZBP1* mRNA to roughly 33% of control mRNA levels was variable and not always achieved. Thus, the change may have been too small to translate into detectable protein level changes, or alternatively, ZBP1 protein was too stable to be affected by RNA interference after 3 to 4 days. Importantly, ZBP1 protein levels were also not affected by knockdown of Stau2, suggesting there is no direct influence of Stau2 on ZBP1 levels (**Fig. 3.4c**).

4.2. The effects of Staufen2 on β -actin

4.2.1 Staufen2 affects β -actin mRNA levels dependent on conditions

A potential target of these RBPs is *β-actin,* an actin isoform responsible for dynamic cytoskeletal structures that are needed during axonal growth or spine formation in neurons. The *β-actin* transcript was shown to be regulated both by ZBP1 (Ross et al., 1997) and Stau2 and localizes together with Stau2 in dendrites of mature neurons (Goetze et al., 2006). To investigate the effects of Stau2 on β-actin in developing neurons, *β-actin* mRNA levels after Stau2 knockdown were assessed by qPCR.

While treatment with Stau2 siRNA led to a robust decrease of Stau2, *β-actin* mRNA levels were not significantly altered (**Fig. 3.5a**) in young hippocampal neurons, as would have been expected from previous unpublished results in the lab. One potential reason why smaller changes in transcript levels may have been difficult to detect could be that *β -actin* is very abundant in the cell in comparison to other RNAs, and the analysis of obtained qPCR results relied on the normalization to reference gene levels.

In preceding studies in the lab, the knockdown of Stau2 had led to a reduction of *β-actin* mRNA levels. Thus, a comparison of the novel siRNAs to the knockdown using short hairpin plasmids, which had been shown to have an effect (siStau2-2, Goetze et al., 2006) was carried out, to rule out that a difference of transfection method was responsible for the divergent results. *Amaxa*® nucleofection with *pSuperior* plasmids targeting Stau2 yielded comparable knockdown levels of *Stau2* mRNA, although they appeared to be slightly weaker (**Fig. 3.4a**). To compare both methods for knockdown more accurately, *pSuperior* plasmids were designed carrying the exact same sequences as the corresponding *Accell®* siRNAs. The short hairpin-plasmid targeting Stau2 (shStau2) led to a reduction of *Stau2* mRNA, but to a lesser extent. The fact that the knockdown in *Accell®* siRNA treated cells was roughly 10% more potent indicates that the targeting sequence itself is no sufficient explanation for a difference between these two methods. Knockdown of *ZBP1* mRNA levels with shZBP1 could not be achieved to significant levels. As far as protein levels are concerned, both siRNA and *pSuperior* transfection led to very similar results, also shStau2 and siStau2-2 reduced the middle isoform of 59 kDa most efficiently. Thus, differential expression of Stau2 isoforms does not seem to be a reason for conflicting effects on β-actin levels.

Another difference between the short hairpin and *Accell®* knockdown method lies in the age of the transfected cells. While neurons were transfected with plasmids before plating and usually analyzed after 4 DIV, siRNAs were added after adherence of the cells at 3 DIV. Therefore, Stau2 siRNA treatment before plating was attempted, which indeed led to a knockdown of *β-actin* levels to roughly 50% (**Fig. 3.5**). Unfortunately, these results were obtained only from one successful experiment and would need to be confirmed. Even though Stau2 is equally downregulated in both cases, *β-actin* mRNA levels seemingly change when neurons are transfected with Stau2 knockdown plasmids before plating, but not when

treated with siRNA against Stau2 at later stages. This would suggest that the influence of the *trans*-acting factor on *β-actin* messages is more severe at an early developmental stage.

4.2.2 Staufen2 downregulation and the actin cytoskeleton

The effect of Stau2 on β-actin protein levels was assessed by immunohistochemistry or by Western blot. Amounts of total β-actin protein on Western blots (stained with monoclonal β-actin antibodies) seemed unaffected by both overexpression of Stau2 and ZBP1 and knockdown of Stau2 with different methods. Yet measuring the intensities of antibody labeled protein bands is not a very sensitive method, as it requires consistent antibody quality and errors may occur due to normalization to the loading control. Thus very small changes might easily have been missed. Importantly, even with reasonably good transfection efficiencies a proportion of cells will remain untransfected, so that a putative effect is likely to be attenuated.

Transfected hippocampal neurons on coverslips were also stained with fluorophore-coupled phalloidin, which binds F-actin. After knockdown of Stau2, some cells appeared to contain lower F-actin levels, although the variation between individual cells on a coverslip or between cell cultures was too big to detect clear differences between treated and untreated or control cells (**Fig. 3.7a**). Staining with Stau2 antibodies revealed that Stau2 knockdown with siRNA was successful in reducing Stau2 levels in most cells. As transfected cells could not be easily discerned using unlabeled siRNAs, cotransfection with siStau2 and non-targeting siRNA labeled with a fluorophore (which had initially been used to determine transfection efficiencies) was tested once to identify transfected cells. Unfortunately the fluorophore may have been bleached during the fixation and staining procedure and the signal was very weak in the obtained images.

In neurons transfected with sh-plasmids by Calcium-Phosphate precipitation, a lack of F-actin staining could be observed in some transfected cells (**Fig. 3.7e**, middle panel), while in other transfected cells there was no visible change. Transfection before plating (with nucleoporation at 0 DIV) unfortunately produced rather unhealthy looking neurons. Cells responded rather severely to these treatments at this stage and were not considered for further analysis.

It should be remembered that phalloidin does not discriminate between the actin isoforms, and changes in *β-actin* mRNA level, for example, have not been observed. Also, the phalloidin intensities were measured only in cell bodies, maybe distant processes such as growth cones would need to be measured separately to reveal local differences in the actin cytoskeleton. Closer investigation and assessment of higher cell numbers would be necessary to detect subtle effects of Stau2 on the actin cytoskeleton.

4.3 Translation control of β-actin

To examine whether Stau2 would control translation of β-actin similarly to ZBP1 (Hüttelmaier et al., 2005), a more sensitive assay was needed than assessing total protein levels by Western blot or phalloidin staining. Therefore, different luciferase reporters were created which contained the firefly luciferase gene with either the 3´-UTR of the human β-actin sequence, just the "zipcode", or the "zipcode" with part of the coding region (designed by L. Schoderböck) (**Fig. 3.10**). Neurons were cotransfected with these reporter plasmids and sh-plasmids or siRNA for downregulation or plasmids overexpressing GFP fusions of Stau2.

Overexpression of Stau2 led to significant changes of luciferase activity only in one case, when the reporter was fused to the zipcode and part of the coding region (**Fig. 3.11**). This suggests that presence of the zipcode, the localization element of the *β-actin* mRNA (Kislaukis et al., 1994), by itself is not sufficient to elicit an effect mediated by Stau2 in primary neurons. There is a reported case of an association of an RNA-binding protein with a sequence within the coding region, the CRD (coding region instability determinant), namely ZBP1 in complex with other proteins acting on the CRD within *c-myc* mRNA to promote stabilization and hinder endonucleolytic cleavage (Weidensdorfer et al., 2009). As the exact binding sites of Stau2 on *β-actin* mRNA have not yet been determined, the existence of a comparable region in the coding sequence of *β-actin* mRNA is probable.

Overexpression of ZBP1, which is known to repress the translation of mRNA with a zipcode, had a similar effect on luciferase activity as Stau2, which may indicate that the observed effect is unspecific. Yet ZBP1 is suspected to have a general stimulating effect on translation, which makes it difficult to obtain interpretable results and knockdown of ZBP1, which should be more informative, was unfortunately not successful.

While overexpression of Stau2 caused an increase of luciferase activity from the reporter containing the coding region, Stau2 knockdown caused a decrease of its activity in a first experiment. The effect of Stau2 knockdown on the *β-actin* 3´-UTR reporter yielded ambiguous results, transfection with the sh-plasmid leading to an increase of translation. Since neurons were transfected before plating with nucleofection, the achieved knockdown was potentially insufficient. Transfecting with effector and reporter at the same time is not ideal for knockdown, as there may be too much protein left at the time of the assay. Thus, a better approach might be to knockdown Stau2 some days before transfection with the reporter. This would be possible with different transfection methods, for example lipofection for cell lines, which is actually very difficult for primary neurons.

All results were normalized to the luciferase activity of cells transfected with psiCHECK-2 (without the β-actin sequences) and of cells transfected with pEGFP or mismatch siRNA as controls. As transfection with the pEGFP plasmid had a considerable effect on luciferase activity on its own, this may have masked some subtle effects after normalization.

Beside hippocampal neurons, also cortical neurons were used for practical reasons, as they can be harvested in much higher cell numbers. That only small differences were observed between luciferase activities in these two cell types suggests that Stau2 would have similar effects on β-actin in all brain cells. As overexpression of Stau2 in HeLa cells did not cause any significant changes, it is conceivable that interaction with other neuronally expressed proteins is necessary for the effect of Stau2 on β-actin.

Whether transcription or translation is regulated cannot be determined by luciferase assays alone, as higher efficiency of transcription or greater stability of the transcripts would also lead to an increased protein expression. Combining luciferase assays with qPCR would be ideal to test whether effects on luciferase activities are transcription- or translation-dependent. The relative amount of renilla to firefly luciferase mRNA could have been tested with the appropriate primers after isolation of total RNA, yet a problem was encountered: although levels of residual genomic DNA within the samples were always very low, there was high contamination by plasmid DNA even after prolonged DNase I-treatment, which made analysis of these samples by quantitative real-time PCR impossible.

4.4 Staufen2 delays mRNA decay

To investigate a putative role of Stau2 in the stabilization of *β-actin* mRNA, RNA decay assays were performed. After knockdown of Stau2 with siRNA, the RNA synthesis inhibitor Actinomycin was added to hippocampal neurons at 6 DIV. The levels of *β-actin* mRNA at 3 time points after blocking transcription were quantified by quantitative real-time PCR. As relative RNA amounts were determined, selecting suitable reference genes for normalization was of high importance. The decay kinetics of different reference genes can vary considerably even in untreated cells (**Fig. 3.9c**), thus using a set of several genes for cross-normalization is necessary to balance this variation.

6 hours after adding Actinomycin, the levels of *β-actin* mRNA had decreased approximately by 40%, when comparing neurons treated with siStau2 to neurons treated with non-targeting siRNA. Thus, in the absence of normal amounts of Stau2 in the cell, the *β-actin* transcript seems to be destabilized and to be degraded faster.

In agreement with these results, the overexpression of Stau2 led to a slightly enhanced stability of the *β-actin* transcript. It has to be considered, however, that the transfection procedure and age of these neurons was different, as neurons were transfected with Stau2-pEGFP at 0 DIV and analyzed at 1 DIV, and transfection with the empty pEGFP vector by itself also had a mild effect.

4.5 Staufen2 and LimK1

The dynamics of the actin cytoskeleton depends on the presence of β-actin, but is also regulated by a broad variety of factors, LimK1 (Lim domain-containing protein kinase 1) being one of them. LimK1 stabilizes actin filaments through the inhibition of ADF (actin binding depolymerizing factor)/cofilin and thereby controls dendritic spine width. It is developmentally regulated and inhibited by a brain-specific microRNA, which binds to a target sequence in the *LimK1* 3´-UTR.

To investigate whether Stau2 would also influence LimK1 and whether it was affected in a similar manner as β-actin, *LimK1* mRNA levels were measured by qPCR in parallel to *β-actin* after knockdown or overexpression of Stau2. In contrast to *β-actin* levels, which were slightly

reduced after transfection with *pSuperior* plasmids, and mostly unaffected by knockdown with *Accell* siRNA, *LimK1* mRNA levels increased in neurons transfected with shStau2 compared to mismatch transfected cells after 4DIV, even more so at 6DIV after knockdown with *Accell* siRNA. Overexpression of Stau2, on the other hand, led to a small reduction of *LimK1* mRNA (**Fig. 3.12c**). Correspondingly, knockdown of Stau2 in young neurons led to a significant increase of luciferase activity of reporters containing the *LimK1* 3´-UTR, and Stau2 overexpression caused a minor decrease of activity.

Further experiments with *LimK1* mRNA were not performed due to time constraints, although it might be interesting to see how *LimK1* behaves in mRNA decay assays. *In situ* hybridization or immunoprecipitation experiments might give more insight into whether *LimK1* mRNA is actually present in Stau2 containing granules. The observed negative regulation of Stau2 on LimK1 does not necessarily require any direct molecular interaction; another possible explanation would be that LimK1 is influenced by proteins which are regulated by Stau2. Maybe Stau2 RNPs could enhance the binding of microRNAs to LimK1, as overexpression of miR-134 was shown to decrease the activity of *LimK1* 3´-UTR containing luciferase reporters (Schratt et al., 2006).

4.6 Conclusions

The goal of my diploma thesis was to show the effects of the RBP Stau2 on localized mRNAs in developing rat hippocampal neurons. After knockdown of Stau2 in primary neuronal cell culture, the degradation of the *β-actin* transcript was accelerated. The finding that Stau2 promotes mRNA stabilization, however, does not exclude additional regulatory mechanisms for Stau2. Even based on the results obtained from luciferase assays, it is impossible to discriminate between enhanced stability and translation. If Stau2 stabilizes *β-actin* mRNA, interaction of Stau2 and *β-actin* mRNA should increase luciferase reporter activity, while translational repression would be expected to counteract this effect. In principle, it is even conceivable that both effects occur simultaneously, thus in combination leading to the relatively small effects observed in luciferase experiments.

Possibly changes of total protein levels were not detectable due to incomplete knockdown of Stau2 and consequently a decrease of *β-actin* mRNA levels which was too subtle. Also, β-actin protein might be too stable for altered mRNA levels to show severe effects on global

protein levels. Hence, it can be speculated that Stau2 stabilizes the message RNA during transport to a specific dendritic (or axonal) site where it could be translated if needed. This in turn would lead to predominantly local changes in β-actin protein concentration.

Cytoskeletal remodeling at the growth cone or dendritic spine is likely to depend on other factors as well. One of the many proteins interacting with the actin cytoskeleton is LimK1, which is important in the phase of dendritic spine maturation. With the experiments I have described, I was able to show that *LimK1* mRNA levels were negatively regulated by Stau2 in developing neurons, which makes LimK1 an interesting candidate for further exploration. If the observed effects turned out to be specific for young neurons, it could be speculated that Stau2 – directly or indirectly – represses LimK1 selectively during early neuronal development.

In summary, the depicted results suggest that localized RNAs, such as *β-actin* mRNA, are regulated by different RNA-binding proteins and that this regulation could be dependent on the stage of development. Stau2 and ZBP1 seem to exert diverse actions on their target transcript. Yet it remains to be revealed whether their functions are also partly overlapping and whether they interact within the same particles, maybe binding different *cis*-acting elements in their target mRNAs. The intricate network of posttranscriptional regulation of localized RNAs plays an essential role in neuronal plasticity or development and still holds many interesting questions for future investigations.

V References

Anderson K, Morin MA, Beckel-Mitchener A, et al. Overexpression of HuD, but Not of Its Truncated Form HuD I+II, Promotes GAP-43 Gene Expression and Neurite Outgrowth in PC12 Cells in the Absence of Nerve Growth Factor. *J. Neurochem.;* 2000:75**,** 1103–1114.

Anderson P and Kedersha N. RNA granules. *J Cell Biol*; 2006;172:803-808.

Barden JA, Miki M, Hambly BD, et al. Localization of the phalloidin and nucleotide-binding sites on actin. *Eur J Biochem*. 1987;2;162(3):583-8.

Barzilai A, Kennedy TE, Sweatt JD, Kandel ER. 5-HT modulates protein synthesis and the expression of specific proteins during long-term facilitation in aplysia sensory neurons. *Neuron*. 1989; 6(2):1577-1586.

Bassell GJ, Warren ST. Review Fragile X Syndrome: Loss of Local mRNA Regulation Alters Synaptic Development and Function. *Neuron*. 2008;60(2):201-214.

Bassell GJ, Zhang H, Byrd AL, et al. Sorting of beta-actin mRNA and protein to neurites and growth cones in culture. *J. Neurosci.* 1998;18(1):251-265.

Bestman JE, Cline HT. The RNA binding protein CPEB regulates dendrite morphogenesis and neuronal circuit assembly in vivo. *PNAS.* 2008;105(51): 20494–20499.

Bolognani F, Perrone-Bizzozero NI. RNA–Protein Interactions and Control of mRNA Stability in Neurons. *Journal of Neuroscience Research*. 2008;489:481-489.

Brightwell JJ, Smith CA, Neve RL & Colombo PJ. Long-term memory for place learning is facilitated by expression of cAMP response element-binding protein in the dorsal hippocampus. *Learning & Memory*. 2007;14:195–199.

Broadus J, Fuerstenberg S, Doe CQ. Staufen-dependent localization of prospero mRNA contributes to neuroblast daughter-cell fate. *Nature*. 1998;391:792–795.

Brownawell, AM and Macara, IG. Exportin-5, a novel karyopherin, mediates nuclear export of double-stranded RNA binding proteins. *J. Cell Biol.* 2002;156: 53–64.

Brummelkamp TR, Bernards R, Agami R. A system for stable ex- pression of short interfering RNAs in mammalian cells. *Science.* 2002;296:550–553.

Cao Q, Richter JD. Dissolution of the maskin- eIF4E complex by cytoplasmic polyadenylation and poly(A)-binding protein controls cyclin B1 mRNA translation and oocyte maturation. *EMBO Journal*. 2002;21(14): 3852 – 3862.

Chang YF, Saadi Imam J, Wilkinson MF. The Nonsense-Mediated Decay RNA Surveillance Pathway. *Annual Review of Biochemistry*. 2007;76: 51-74.

Chen C, Gherzi R, Ong S, et al. AU Binding Proteins Recruit the Exosome to Degrade ARE-Containing mRNAs. *Cell.* 2001;107:451-464.

Chen CA, Shyu A. AU-rich elements: characterization and importance in mRNA degradation. *Science*. 1995**.** 20(11):465-70.

Condeelis J, Singer RH. How and why does b-actin mRNA target. *Biol. Cell*. 2005;97:97-110.

Dahm R, Macchi P. Human pathologies associated with defective RNA transport and localization in the nervous system Biology of the Cell. *Cell*. 2007;99:649-661.

Dahm R, Kiebler M. Silenced RNA on the move. *Nature*. 2005;438:432-434.

Dahm R, Kiebler M, Macchi P. RNA localisation in the nervous system. *Semin. Cell Dev. Biol.* 2007;18:216-223.

Dugré-Brisson S, Elvira G, Boulay K et al. Interaction of Staufen1 with the 5' end of mRNA facilitates translation of these RNAs. *Nucleic Acids Res*. 2005;33(15):4797-812.

Eom T, Antar LN, Singer RH, Bassell GJ. Localization of a β -Actin Messenger Ribonucleoprotein Complex with Zipcode-Binding Protein Modulates the Density of Dendritic Filopodia and Filopodial Synapses. *J. of Neurosci.* 2003;23(32):10433-10444.

Ephrussi A., Dickinson L. K. and Lehmann R. Oskar organizes the germ plasm and directs localization of the posterior determinant nanos. *Cell.* 1991;66, 37–50.

Eulalio A, Behm-Ansmant I, Izaurralde E. P-bodies: at the crossroads of post-transcriptional pathways. *Nature*. 2007;8(January):9-22.

Giorgi C, Yeo GW, Stone ME, et al. The EJC factor eIF4AIII modulates synaptic strength and neuronal protein expression. *Cell*. 2007;130:179-191.

Goda Y, Street G, Kingdom U. Head, Neck, and Spines: A Role for LIMK-1 in the Hippocampus. *Neuron*. 2002;1:3-5.

Goetze B, Grunewald B, Baldassa S, Kiebler M. Chemically controlled formation of a DNA/calcium phosphate coprecipitate: application for transfection of mature hippocampal neurons. *J Neurobiol.* 2004;60:517–525.

Goetze B, Tuebing F, Xie Y, et al. The brain-specifi c double-stranded RNA-binding protein Staufen2 is required for dendritic spine morphogenesis. *Cell*. 2006;172(2):221-231.

Gong C, Maquat LE. lncRNAs transactivate STAU1-mediated mRNA decay by duplexing with 3′ UTRs via Alu elements. *Nature*. 2011;470(7333):284-288.

Hengst UH, Jaffrey SR. Regulation of mRNA translation during axonal development, *Semin. Cell & Dev. Biol*. 2007;18:209-15.

Huang Y, Carson JH, Barbarese E, Richter JD. Facilitation of dendritic mRNA transport by CPEB. *Genes & Development*. 2003;17:638-653.

Hüttelmaier S, Zenklusen D, Lederer M, et al. Spatial regulation of beta-actin translation by Src-dependent phosphorylation of ZBP1. *Nature*. 2005;438:512–515.

Jackson, A. L., S. R. Bartz, et al. Expression profiling reveals off-target gene regulation by RNAi. *Nat Biotech.* 2003; 21(6): 635-637.

Jeong JH, Nam YJ, Kim SY, et al. The transport of Staufen2-containing ribonucleoprotein complexes involves kinesin motor protein and is modulated by mitogen-activated protein kinase pathway. *J. Neurochem.* 2007;102:-2084.

Jurado S, Rodríguez-Pascual F, Sánchez-Prieto J et al. NMDA induces post-transcriptional regulation of α_2-guanylyl-cyclase-subunit expression in cerebellar granule cells *J Cell Sci.* 2006; 119:1622-1631

Kanai Y, Dohmae N, Hirokawa N. Kinesin transports RNA: isolation and characterization of an RNA-transporting granule. *Neuron.* 2004;43:513–525.

Keene, J.D. Why is Hu where? Shuttling of early-response-gene messenger RNA subsets. *Proc. Natl. Acad. Sci. USA* 1999;96:5–7.

Keene JD, Tenenbaum SA. Eukaryotic mRNPs May Represent Posttranscriptional Operons. *Cell*. 2002;9:1161-1167.

Kelleher RJ, Govindarajan A, Jung HY et al. Translational control by MAPK signaling in long-term synaptic plasticity and memory. *Cell.* 2004;116:467–479.

Kiebler MA, Bassell GJ. Neuronal RNA granules: movers and makers. *Neuron*. 2006;51:685-690.

Kiebler MA, Desgroseillers L. Molecular insights into mRNA transport and local translation in the mammalian nervous system. *Neuron*. 2000;25:19-28.

Kiebler MA, Hemraj I, Verkade P et al. The mammalian Staufen protein localizes to the somatodendritic domain of cultured hippocampal neurons: implications for its involvement in mRNA transport. *J. Neurosci.* 1999;19, 288–297.

Kiebler MA, Jansen RP, Dahm R et al. A putative nuclear function for mammalian Staufen. *Trends Biochem Sci*. 2005;30(5):228-31.

Kim YK, Furic L, Parisien M, et al. Staufen1 regulates diverse classes of mammalian transcripts. *EMBO J.* 2007;26:2670-2681.

Kislauskis EH, Zhu X, Singer RH. Sequences Responsible for Intracellular Localization of β-Actin Messenger RNA Also Affect Cell Phenotype. *Journal of Cell Biol.* 1994;127(2):441-451.

Kislauskis EH, Zhu X, Singer RH. β -Actin Messenger RNA Localization and Protein Synthesis Augment Cell Motility. *Cell*. 1997;136(6):1263-1270.

Klann E, Sweatt JD. Altered protein synthesis is a trigger for long-term memory formation. *Neurobiology of Learning and Memory*. 2008;89:247-259.

Lebeau G, Miller LC, Tartas M, et al. Staufen 2 regulates mGluR long-term depression and Map1b mRNA distribution in hippocampal neurons. *Learning & Memory*. 2011;18:314-326.

Leung K, Horck FP, Lin AC, Allison R, Holt CE. Asymmetrical β-actin mRNA translation in growth cones mediates attractive turning to netrin-1. *Nat. Neurosci*. 2006;9(10):1247-1256.

Löw I, Wieland T. The interaction of phalloidin. Some of its derivatives, and of other cyclic peptides with muscle actin as studied by viscosimetry. *FEBS Lett.* 1974;30;44(3):340-3.

Macchi P, Brownawell AM, Grunewald B, et al. The Brain-specific Double-stranded RNA-binding Protein Staufen2. *Biochemistry*. 2004;279(30):31440 -31444.

Marion RM, Fortes P, Beloso A et al. A human sequence homologue of Staufen is an RNA-binding protein that is associated with polysomes and localizes to the rough endoplasmic reticulum. *Mol Cell Biol.* 1999;19, 2212-2219.

Martin KC, Ephrussi A. Gene Expression in the Spatial Dimension. *Cell*. 2009;136(4):719-730.

Martin KC, Zukin RS. RNA trafficking and local protein synthesis in dendrites: an overview. *Journal of Neurosci.* 2006;26:7131-7134.

Mendez R, Hake LE, Andresson T, et al. Phosphorylation of CPE binding factor by Eg2 regulates translation of c-mos mRNA. *Nature*. 2000;404:302-307.

Miki T and Yoneda Y. Alternative splicing of Staufen2 creates the nuclear export signal for CRM1 (Exportin 1). *J. Biol. Chem.* 2004;279:47473–47479.

Napoli I, Mercaldo V, Boyl PP, et al. The Fragile X Syndrome Protein Represses Activity-Dependent Translation through CYFIP1, a New 4E-BP. *Molecular Biology*. 2008:1042-1054.

Oleynikov Y, Singer RH, York N. Real-Time Visualization of ZBP1 Association with β -Actin mRNA during Transcription and Localization. *Current Biology*. 2003;13(03):199-207.

Pan F, Huttelmaier S, Singer RH, Gu W. ZBP2 facilitates binding of ZBP1 to beta-actin mRNA during transcription. *Mol Cell Biol*. 2007;27:8340-8351.

Panja D, Dagyte G, Bidinosti M, et al. Novel Translational Control in Arc-dependent Long Term Potentiation Consolidation in Vivo. *Journal of Biological Chemistry*. 2009;284(46):31498 -31511.

Paquin N, Chartrand P. Local regulation of mRNA translation: new insights from the bud. *Trends Cell Biol.* 2008;18:105–111.

Pastalkova E, Serrano P, Pinkhasova D et al. Storage of spatial information by the maintenance mechanism of LTP. *Science*. 2006; 313:1141–1144.

Quattrone A, Pascale A, Nogues X, et al. Posttranscriptional regulation of gene expression in learning by the neuronal ELAV-like mRNA-stabilizing proteins. *PNAS*. 2001;28:11668–11673.

Richter JD. CPEB: a life in translation. *Trends in biochemical sciences*. 2007;32(6): 279-285.

Roegiers F and Jan Y N. Staufen: a common component of mRNA transport in oocytes and neurons? *Trends Cell Biol.* 2000;10:220–224.

Ross AF, Oleynikov Y, Kislauskis EH, Taneja KL, Singer RH. Characterization of a β-Actin mRNA Zipcode-Binding Protein. *Microbiology*. 1997;17(4):2158-2165.

Rubeis SD, Bagni C. Fragile X mental retardation protein control of neuronal mRNA metabolism: Insights into mRNA stability. *Molecular and Cellular Neuroscience*. 2010;43(1):43-50.

Schmittgen TD, Livak KJ. Analyzing real-time PCR data by the comparative C(T) method. *Nat. Protoc*. 2008;3(6):1101-1108.

Schratt G. Fine-tuning neural gene expression with microRNAs. *Current Opinion in Neurobiology*. 2009; 19:1–7.

Schratt GM, Tuebing F, Nigh EA, et al. A brain-specific microRNA regulates dendritic spine development. *Nature*. 2006;439(January):283-289.

Sekino Y, Kojima N, Shirao T. Role of actin cytoskeleton in dendritic spine morphogenesis. *Neurochem. In*. 2007;51:92-104.

Sledz CA, Holko M, de Veer MJ et al. Activation of the interferon system by short-interfering RNAs. *Nat Cell Biol*. 2003;5(9):834-9.

St Johnston DS, Brown NH, Gallt JG, Jantscht M. A conserved double-stranded RNA-binding domain. *Biochemistry*. 1992;89(November):10979-10983.

Stöhr N, Lederer M, Reinke C, et al. ZBP1 regulates mRNA stability during cellular stress. *J. Cell Biol.* 2006;175:527-534.

Tiruchinapalli DM, Oleynikov Y, C SK, et al. Activity-dependent trafficking and dynamic localization of zipcode binding protein 1 and β-actin mRNA in dendrites and spines of hippocampal neurons. *J. Neurosci.* 2003;23:3251-3261.

Vessey JP, Macchi P, Stein JM, et al. A loss of function allele for murine Staufen1 leads to impairment of dendritic Staufen1-RNP delivery and dendritic spine morphogenesis. *Proc. Natl. Acad. Sci. USA.* 2008;105:16374-16379.

Wickham, L, Duchaîne T, Luo M et al. Mammalian staufen is a double-stranded- RNA- and tubulin-binding protein which localizes to the rough endoplasmic reticulum. *Mol. Cell. Biol.* 1999;19, 2220–2230.

Weidensdorfer D, Stöhr N, Baude A, et al. Control of c-myc mRNA stability by IGF2BP1-associated cytoplasmic RNPs. *RNA*. 2009;15:104-115.

Yang N, Higuchi O, Ohashi K et al. Cofilin phosphorylation by LIM-kinase 1 and its role in Rac-mediated actin reorganization. *Nature*. 1998;393(6687):809-12.

Yao J, Sasaki Y, Wen Z et al. An essential role for beta-actin mRNA localization and translation in Ca^{2+} -dependent growth cone guidance. *Nat. Neurosci.* 2006;9:1265-1273.

Yisraeli JK. VICKZ proteins: a multi-talented family of regulatory RNA-binding proteins. *Biol. Cell*. 2005;97:87-96.

Yoon YJ, Mowry KL. Xenopus Staufen is a component of a ribonucleoprotein complex containing Vg1 RNA and kinesin. *Development*. 2004;131:3035-3045.

Zeitelhofer M, Karra D, Vessey JP, et al. High-Efficiency Transfection of Short Hairpin RNAs-Encoding Plasmids Into Primary Hippocampal Neurons. *Journal of Neuroscience Research*. 2009;300:289-300.

Zeitelhofer M, Vessey JP, Xie Y. High-efficiency transfection of mammalian neurons via nucleofection. *Nature Protoc.* 2007;2: 1692 - 1704

Zha X, Costa V, Harding AM, et al. ASIC2 Subunits Target Acid-Sensing Ion Channels to the Synapse via an Association with PSD-95. *Ion Channels*. 2010;29(26):8438-8446.

Zhang HL, Eom T, Oleynikov Y, et al. Neurotrophin-induced transport of a beta-actin mRNP complex increases beta-actin levels and stimulates growth cone motility. *Neuron*. 2001;31:261-275.

Internet references

www.dharmacon.com
www.fermentas.com
www.oligoengine.com
www.promega.com

Textbooks

Kandel ER, Schwartz JH and Jessell TM (editors). Principles of Neural Science. 2000 (Mc Graw Hill, 4th edition)

Acknowledgements

First I want to thank Prof. Michael Kiebler for giving me the opportunity to do my diploma thesis in his lab, and for providing advice, encouragement and critical comments all the way through my project.

Special thanks go to Dr. Lucia Schoderböck for her great support and advice and for critical reading of the thesis- and to Dr. Krzysztof Wieczorek for his help in getting the project started. Both were always helpful and open for questions and discussions, for which I am truly grateful.

Furthermore I would like to thank all my colleagues at the Kiebler lab for their unique and invaluable contributions, be it practical assistance, scientific exchange - or simply friendship and sharing many good laughs.

Last but not least, I want to thank my mother for always supporting me in every imaginable way.

Curriculum Vitae

Personal Information:

Name:	Daniela Bibiana Lenek
Date of birth:	13.08.1982
Place of birth:	Vienna
Nationality:	Austrian

Education:

06/2000 – graduation with distinction from high school “Maria Regina”, 1190 Wien
10/2000 – start of the undergraduate course “Biology” (A437) at the University of Vienna
03/2003 – specialization “Genetics & Microbiology” (A441), major subject: Molecular Genetics and Pathology
01/2004 to
06/2004 – studies abroad at Université Montpellier 2, France
10/2006 to
03/2008 – undergraduate course “French language studies” at the University of Vienna
07/2008 to
10/2009 –diploma thesis at the Center for Brain Research (Medical University of Vienna)

Work experience:

Tutoring in the subjects English, French and Biology, privately and from 02/2008 to 06/2008 at the private lesson agency „Lernquadrat“

Zusammenfassung

Viele zelluläre Prozesse erfordern den Transport spezifischer RNAs in bestimmte Kompartimente, wo sie translatiert oder bis zu ihrer Aktivierung gespeichert werden. RNAs werden in RNPs (Ribonukleoproteine) verpackt, die in Dendriten in die Nähe von Synpasen transportiert werden können. Defekte in der RNA-Lokalisierung werden mit schweren neurologischen Störungen in Verbindung gebracht, wie dem Fragiles-X-Syndrom. Ein bekanntes Beispiel für lokalisierte RNA in Neuronen ist *β-Aktin* mRNA, deren Lokalisation in axonalen Wachstumskegeln oder Neuriten morphologische Veränderungen des Zytoskeletts bewirkt, die während der neuronalen Entwicklung und der synaptischen Plastizität auftreten. Zwei Proteine sind bekanntermaßen an diesem Prozess beteiligt: (i) ZBP1 (zipcode-binding protein 1), welches an ein 54-nt Lokalisationselement in der *β-Aktin* 3´-UTR (den sogenannten „Zipcode“) bindet und die Proteinsynthese während des Transportes supprimiert; und (ii) das doppelsträngige RNA-bindende Protein Staufen2 (Stau2), von dem angenommen wird, für die Lokalisation von β-Aktin in Dendriten notwendig zu sein, sowie für die Bildung dendritischer Spines in reifen Neuronen. Jedoch ist- im Gegensatz zu ZBP1- für Stau2 noch kein bestimmter Aktionsmechanismus beschrieben worden. Das Ziel meiner Diplomarbeit war, die Rolle von Stau2 in der Regulierung von β-Aktin in sich entwickelnden Neuronen zu untersuchen.

Dazu wurde die Expressionsstärke von β-Aktin nach dem Knockdown von Stau2 in jungen Neuronen quantitifiziert. Während die Menge an *β-Aktin* mRNA sich etwas reduzierte, blieben die Proteinmengen unverändert. Um Herauszufinden, ob Stau2 ähnlich wie ZBP1 die Translation von β-Aktin reguliert, wurden Luciferase-Experimente durchgeführt. Während ein Knockdown von Stau2 keinen Effekt hatte, führte die Überexpression von Stau2, wie auch ZBP1, zu erhöhter Luciferaseaktivität, wenn das Luciferase-Plasmid den β-Aktin Zipcode und einen Teil der kodierenden Region von β-Aktin enthielt. Da dieser Assay keine eindeutige Unterscheidung zwischen erhöhter Translation und Stabilität zulässt, wurden RNA-Zerfallstests durchgeführt. Die Menge der verbleibenden *β-Aktin* mRNA zu unterschiedlichen Zeitpunkten nach Inhibierung der RNA-Synthese wurde mit quantitativer real-time PCR bestimmt. Der Zerfall der *β-Aktin* mRNA war in Neuronen mit reduzierten Stau2 Levels beschleunigt. Demgegenüber hatte die Überexpression von Stau2 nur einen geringfügig stabilisierenden Effekt.

Zusammengenommen zeigen meine Ergebnisse, dass das RNA-bindende Protein Stau2 die Stabilität von *β-Aktin mRNA* in sich entwickelnden Neuronen erhöht, ohne seine Translation zu beeinflussen. Da die Gesamtmenge an β-Aktin Protein gleich blieb, ist es denkbar, dass Stau2 die Stabilisierung nur vorübergehend während des Transportes fördert, in vergleichbarer Weise wie ZBP1 eine vorzeitige Translation für die Dauer des *β-Aktin* Transportes hemmt. Ob *β-Aktin* mRNA direkt an Stau2 bindet, möglicherweise über eine Sequenz innerhalb der kodierenden Region, und ob es in gemeinsamen RNPs mit ZBP1 interagiert, könnte ein interessantes Thema für zukünftige Untersuchungen sein. Um die Rolle von Stau2-RNPs letztendlich aufzuklären, ist es notwendig, die Identität der RNA-Targets und der Proteininteraktionen von Stau2 zu klären und die Funktionsweise von Stau2 während des Transportes bzw. in Spines oder Wachstumkegeln im Detail zu beschreiben.